ADVISORY COMMITTEE

EDITORIAL BOARD

[1] The Faculty of Civil Engineering, Wrocław University of Technology
Wybrzeże Wyspiańskiego 27, 50-370 Wrocław, Poland
Tel. +48 71 320 41 35, Fax. +48 71 320 41 05, E-mail: jan.kmita@pwr.wroc.pl

[2] The Faculty of Mechanical Engineering, Wrocław University of Technology
ul. Łukasiewicza 5, 50-371 Wrocław, Poland
Tel. +48 71 320 21 73, Fax. +48 71 320 34 22, E-mail: matalplast@pwr.wroc.pl

POLISH ACADEMY OF SCIENCES – WROCŁAW BRANCH
WROCŁAW UNIVERSITY OF TECHNOLOGY

ARCHIVES OF CIVIL AND MECHANICAL ENGINEERING

Quarterly
Vol. VIII, No. 1

WROCŁAW 2008

EDITOR IN CHIEF

ZBIGNIEW GRONOSTAJSKI

EDITORIAL LAYOUT AND PROOF-READING

WIOLETTA GÓRALCZYK

TYPESETTING

SEBASTIAN ŁAWRUSEWICZ

SECRETARY

WIOLETTA GÓRALCZYK

Publisher: Committee of Civil and Mechanical Engineering
of Polish Academy of Sciences – Wrocław Branch,
Faculty of Civil Engineering and Faculty of Mechanical Engineering
of Wrocław University of Technology

OFICYNA WYDAWNICZA POLITECHNIKI WROCŁAWSKIEJ
Wybrzeże Wyspiańskiego 27, 50-370 Wrocław
http://www.oficyna.pwr.wroc.pl
e-mail: oficwyd@pwr.wroc.pl

ISSN 1644-9665

Drukarnia Oficyny Wydawniczej Politechniki Wrocławskiej. Zam. nr 117/2008.

Contents

Obituary of Professor Jerzy Gronostajski 5

T. WACŁAWCZYK, T. KORONOWICZ, Remarks on prediction of wave drag using VOF method with interface capturing approach 7
P. DYMARSKI, Computations of the propeller open water characteristics using the SOLAGA computer program. Predictions of the cavitation phenomenon 17
J. JACHOWSKI, Assessment of ship squat in shallow water using CFD 29
L. KOBYLIŃSKI, Stability of ships: risk assessment due hazards created by forces of the sea 39
T. KORONOWICZ, J. SZANTYR, P. CHAJA, A computer system for the complete design of ship propellers 49
J. MATUSIAK, T. MIKKOLA, Recent developments in the field of ship hydrodynamics at the ship laboratory of Helsinki University of Technology 61
J. SZANTYR, The crucial contemporary problems of the computational methods for ship propulsor hydrodynamics 71
T. TABACZEK, Computation of flow around inland waterway vessel in shallow water 99
B. GRONOSTAJSKA, The affect of human feelings on creation of housing 109
Information about PhDs and habilitations 121

Spis treści

Wspomnienie o Profesorze Jerzym Gronostajskim 5

T. WACŁAWCZYK, T. KORONOWICZ, Uwagi na temat wyznaczania oporu falowego w oparciu o metodę VOF oraz schematy o wysokiej rozdzielczości 7
P. DYMARSKI, Obliczenia charakterystyk śrub swobodnych przy użyciu programu komputerowego SOLAGA. Prognozowanie zjawiska kawitacji 17
J. JACHOWSKI, Ocena siadania statku na wodzie płytkiej przy użyciu metod numerycznej mechaniki płynów 29
L. KOBYLIŃSKI, Stateczność statku: ocena ryzyka w stosunku do zagrożeń spowodowanych siłami morza 39
T. KORONOWICZ, J. SZANTYR, P. CHAJA, System komputerowy do kompleksowego projektowania śrub okrętowych 49
J. MATUSIAK, T. MIKKOLA, Najnowsze prace badawcze z dziedziny hydrodynamiki okrętu w Laboratorium Okrętowym w Helsinki University of Technology 61
J. SZANTYR, Kluczowe współczesne problemy metod obliczeniowych hydrodynamiki pędników okrętowych 71
T. TABACZEK, Obliczanie przepływu wokół statku śródlądowego na wodzie płytkiej 99
B. GRONOSTAJSKA, Wpływ ludzkich uczuć na kreowanie budownictwa 109
Informacja o pracach doktorskich i habilitacyjnych 121

Obituary of
Professor Jerzy Gronostajski

28.10.1933–14.11.2007

Professor Jerzy Gronostajski, Editor in Chief of "Archives of Civil and Mechanical Engineering" journal, died on November 14th, 2007.

Professor Jerzy Gronostajski was born on October 28th 1933 in Chełm. His whole adult life was bonded with Wrocław University of Technology, beginning in the 1951 as a student of Mechanical Engineering Faculty. The professional career he started in 1955 and then after PhD exam in 1963 he became a lecturer. In 1965, he was nominated for the Head of Metal Forming Processes Division that he held until 2004. In 1967, after defence of postdoctoral thesis he got the position of Reader. In 1967, he became Professor extraordinarius, and in 1987 he was made Professor ordinarius. In 2001 he was awarded an honorary doctorate by the University of Bacau (Romania). To the very last moment of his life The Professor worked in his beloved University. Before he died, the Vol. VII, No. 4 of 2007 issue of "Archives of Civil and Mechanical Engineering" has been published as the last under his editing.

Prof. Jerzy Gronostajski is a creator of Scientific School which is going about the research and design of forming processes, metal science and mechanics of metal forming processes. He is regarded as one of the most outstanding scientist in Poland. The achieve results he put forward in 13 books, monographs and course books; 50 publications in journals being on the ISI Master Journal List and over 300 other publications. Professor Jerzy Gronostajski attended over 100 symposiums and conferences. His speeches were always very popular and received wide recognition.

Professor Jerzy Gronostajski was outstanding tutor of the research personnel. He promoted 23 doctors. Fife from his research workers have got the post-doctoral degree and four out of them – professor.

He was the member of editorial committee of "Archives of Metallurgy" being on the ISI Master Journal List and the member of journal "Metallurgy and Foundry Engineering" and "Machine Engineering" editorial committee.

He was a chair of the Civil and Mechanical Engineering of the Polish Academy of Sciences – Wrocław Branch, the member of Boards of Directors – of The International Scientific Society ESAFORM, the member of Metallurgy Committee of Polish Academy of Science since 1966, The Committee of Metal Science, The Committee of Machine Building, International Deep Drawing Research Group, International Culture and Philosophy Society, the chair of the Scientific Council of the Military Institute of Technical Engineering. His service for the country was rewarded with many state decorations.

Professor Jerzy Gronostajski was buried on September 23rd, 2007 in Wrocław, on the Parish Cemetery belonging to the church dedicated to Holy Family.

He will always remain in our memory as the eminent scientist and great man of exceptional intelligence and brilliant mind. He had considerable standing and was held in high esteem by everyone.

Jan Kmita
Eugeniusz Rusiński

ARCHIVES OF CIVIL AND MECHANICAL ENGINEERING

Vol. VIII 2008 No. 1

Remarks on prediction of wave drag using VOF method with interface capturing approach

T. WACŁAWCZYK, T. KORONOWICZ
The Szewalski Institute of Fluid Flow Machinery, Polish Academy of Sciences, ul. J. Fiszera 14, 80-952 Gdańsk

This paper concerns modeling of the free surface flow using Volume of Fluid (VOF) method with interface capturing approach. Equation for transport of the volume fraction is discretized using three high-resolution schemes. We show that artificial dependence of the high-resolution scheme on the Courant number and switching to first order upwind differencing scheme introduces numerical diffusion that affects solution. Moreover, dynamic character of the scheme can cause artificial interface deformation influencing final wave profile and thus wave drag prediction. Additionally some results connected with modeling of the flow around free surface piercing body are presented.

Keywords: *volume of fluid method, high resolution schemes, wave drag prediction*

1. Introduction

Wave drag of the ship is essential component of the total force acting on the hull. Accurate estimation of this component is necessary condition for correct assignment of the engine room power. This far wave drag was estimated using approximate formulas for certain hull type or potential methods when deformation of the free surface could be assumed linear. Recently, rapid development of the industrial Computational Fluid Dynamics (CFD) allows for simulation of the viscous, turbulent flows including effects of the hull interaction with free surface also with trim effects [1–2]. In most of the cases, commercial tools give satisfactory approximation of the desired quantities [3]. However, one needs to notice that physical models and numerical approximations used for the discretization of the conservation equations, introduce some restrictions, that limit range of the applicability of the methods used.

This paper deals with effects, introduced by application of different high-resolution schemes for discretization of the convective term in the equation for transport of the volume fraction [4–6]. We consider dynamics of the two-fluid system consisting of viscous immiscible on the molecular level fluids with high density and viscosity ratio. Comparison of High Resolution Interface Capturing scheme (HRIC) [7] with Interface Capturing Scheme for Arbitrary Meshes (CICSAM) [8] and its modified version M-CICSAM allow us to discuss influence of the discretization of non-linear convective term on the solution and access its impact on the wave drag.

1.1. One Fluid Formulation

In this paper the so called one-fluid formulation is used i.e. the whole system of immiscible fluids is treated as a single continuum medium. This assumption leads to the sharing of the same velocity in one control volume, between all fluids that are modelled and thus enforces continuity of the pressure and velocity field. Using this model dynamics of the system of incompressible, viscous and immiscible fluids is described by the Navier–Stokes Equation (1) and continuity equation Equation (2):

$$\frac{\partial(\rho u_i)}{\partial t} + \frac{\partial(\rho u_j u_i)}{\partial x_j} = -\frac{\partial p}{\partial x_i} + \frac{\partial}{\partial x_j}\left(\mu\left(\frac{\partial u_i}{\partial x_j} + \frac{\partial u_j}{\partial x_i}\right)\right) + \rho g_i + \sigma\kappa n_i, \tag{1}$$

$$\frac{\partial u_i}{\partial x_i} = 0. \tag{2}$$

Additional term that appears in Equation (1) is inherited from one fluid formulation and describes influence of the surface tension. When surface tension coefficient σ is constant the resulting force acts in the direction n_i normal to the interface. κ denotes mean Gaussian curvature. In this paper we will neglect effects of surface tension.

To introduce material properties of the fluids that built aforementioned system, one needs to consider additional constitutive relations. In the case of the set of two fluids: water and air, it is enough to choose one fluid as the background (water) and to consider only its volume fraction ϕ:

$$\rho = \phi\rho_1 + (1-\phi)\rho_2, \tag{3}$$

$$\mu = \phi\mu_1 + (1-\phi)\mu_2, \tag{4}$$

where:

ρ_j, μ_j denotes density and dynamic viscosity of the j-th fluid respectively. Using assumption about incompressible character of the considered fluids one can notice that substitution of the Equation (3) to the conservative form of the continuity equation leads to the equation for transport of the volume fraction:

$$\frac{\partial\phi}{\partial t} + u_j\frac{\partial\phi}{\partial x_j} = 0, \tag{5}$$

where, as mentioned before, ϕ denotes volume fraction of the background fluid. In the case of the VOF framework, value of the volume fraction ϕ in the control volume

indicates its presence $\phi = 1$ or absence $\phi = 0$. When $0 < \phi < 1$ volume fraction distribution carries information about position of the interface. The crucial issue for the modelling of the multiphase flow is a proper solution of Equation (5), i.e., discretization of time derivative and nonlinear convective term. The discretization has to avoid smearing of the step interface profile and has to assure that the boundedness criterion is satisfied. Here, Equation (5) is discretized using finite volume method, employing Crank-Nicholson scheme for integration in time, this procedure results in the implicit, unsplit time discretization scheme, cf. Equation (9).

2. High-resolution schemes

Among different approaches to the discretization of the non-linear convective term in the framework of the VOF method, Equation (5), the most effective one is connected with high-resolution schemes. The main idea of high-resolution schemes employed in this paper is connected with the Normalized Variable Diagram (NVD), that allows to derive a numerical scheme with desirable properties, see Figure 1.

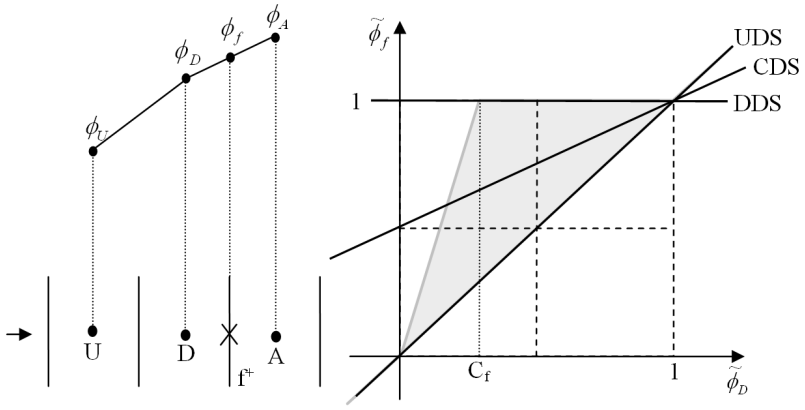

Fig. 1. a) Boundedness criterion, b) Normalized Variable Diagram (NVD) with upwind (UDS), downwind (DDS) and central (CDS) differencing schemes

Its origin comes from convective boundedness criterion (CBC) which allows introducing normalized variables in donor cell *D* and on the control volume face *f*, assuring smooth distribution of the volume fraction in computational domain:

$$\tilde{\phi}_D = \frac{\phi_D - \phi_U}{\phi_A - \phi_U}, \qquad \tilde{\phi}_f = \frac{\phi_f - \phi_U}{\phi_A - \phi_U}, \tag{6}$$

where ϕ_D, ϕ_A and ϕ_U are the volume fractions in the donor, acceptor and upwind cells, respectively. One can notice that Equations (6) can be used to find the volume fraction at the face ϕ_f in terms of normalized variables:

$$\phi_f = \left(1 - \tilde{\beta}_f\right)\phi_D + \tilde{\beta}_f \phi_A , \tag{7}$$

$$\tilde{\beta}_f = \frac{\tilde{\phi}_f - \tilde{\phi}_D}{1 - \phi_D} . \tag{8}$$

Equation (7) is used for calculation of the cell face values at the walls of the control volumes in discretized Equation (5):

$$\frac{V_P}{\Delta t}\phi_P^{t+\Delta t} + \frac{1}{2}\sum_{f=1}^{n}\phi_f^{t+\Delta t} S_{i,f} u_{i,f}^t = \frac{V_P}{\Delta t}\phi_P^t - \frac{1}{2}\sum_{f=1}^{n}\phi_f^t S_{i,f} u_{i,f}^t . \tag{9}$$

In this paper we discuss modification of the HRIC [7] and CICSAM [8] to the M-CICSAM high-resolution scheme. Proposed formulation combines advantages of both high-resolution schemes i.e. sharp interface reconstruction (CICSAM) and low numerical diffusion (HRIC) [5]. Firstly we derive Courant number independent formulation, which satisfies total variation diminishing (TVD) criterion [9]. Thereafter we show that dependence of the scheme on Courant number deteriorates its shape preserving properties. Secondly we notice, that in general case both component schemes of the high-resolution formulation are responsible for the advection when the interface moves perpendicular to the flow direction. For this reason we replace bounded ULTIMATE-QUICKEST with more compressive bounded linear FROMM scheme [9].

2.1. CICSAM

In the case of the CICSAM assumption about dependence of the region where the CBC is satisfied on the local Courant number $C_f = U\Delta t S_f / V_D$ is used [10]. Combining the donor-acceptor scheme [11] with NVD formulation dependent on the local Courant number results in the compressive HYPER-C scheme:

$$\tilde{\phi}_{f_{CBC}} = \begin{cases} \tilde{\phi}_D & : \; 0 < \tilde{\phi}_D, \tilde{\phi}_D > 1 \\ \min\left\{1, \dfrac{\tilde{\phi}_D}{C_f}\right\} & : \; 0 \le \tilde{\phi}_D \le 1 \end{cases} . \tag{10}$$

Because it was found that when interface is tangential to the direction of the flow downwind differencing scheme (DDS) tends to wrinkle its shape. To improve shape preserving properties of this scheme ULTIMATE-QUICKEST scheme (UQS) is used:

$$\widetilde{\phi}_{f_{UQ}} = \begin{cases} \widetilde{\phi}_D & : \ 0 < \widetilde{\phi}_D, \widetilde{\phi}_D > 1 \\ \min\left\{ \dfrac{8C_f\widetilde{\phi}_D + (1-C_f)(6\widetilde{\phi}_D + 3)}{8}, \widetilde{\phi}_{f_{CBC}} \right\} & : \ 0 \le \widetilde{\phi}_D \le 1 \end{cases}. \tag{11}$$

To switch smoothly between schemes decision factor $0 \le \gamma_f \le 1$ is introduced, cf. Equation (14), which depends on the angle θ_f, cf. Equation (13), between unit vector normal to the interface $\nabla\phi_D / |\nabla\phi_D|$ and unit vector parallel to the line between centers of donor and acceptor cells $\bar{d} / |\bar{d}|$. When interface position is normal to the direction of flow $\gamma_f = 1$ and the scheme based on CBC criterion Equation (10) is used. In the case of tangential position of the interface $\gamma_f = 0$ and UQS is employed, see Equation (11):

$$\widetilde{\phi}_f = \gamma_f \widetilde{\phi}_{f_{CBC}} + (1-\gamma_f)\widetilde{\phi}_{f_{UQ}}, \qquad 0 \le \gamma_f \le 1, \tag{12}$$

$$\theta_f = \arccos\left| \frac{\nabla\phi_D \bar{d}}{|\nabla\phi_D||\bar{d}|} \right|, \tag{13}$$

$$\gamma_f = \min\left\{ \frac{1+\cos 2\theta_f}{2}, 1 \right\} \tag{14}$$

Normalized value at the face of the control volume $\widetilde{\phi}_f$ is used for calculation of ϕ_f, see Equation 7, and than in Equation (9) for calculation of the convective term. When aforementioned procedure is applied in multiple dimensions the local Courant number C_f is replaced by its cell definition C_D [8].

2.2. HRIC

To simplify above procedure and get rid of the explicit dependence on the local Courant number the HRIC scheme was introduced. As it was mentioned this scheme also relies on the NVD and normalized variables. Application of the HRIC scheme can be divided in to three steps. Firstly, normalized cell face value will be estimated from a scheme that continuously connects upwind and downwind on the NVD diagram:

$$\widetilde{\phi}_f = \begin{cases} \widetilde{\phi}_D & : \ 0 < \widetilde{\phi}_D, \widetilde{\phi}_D > 1 \\ 2\widetilde{\phi}_D & : \ 0 \le \widetilde{\phi}_D < 0.5 \\ 1 & : \ 0 \le \widetilde{\phi}_D \le 1 \end{cases}. \tag{15}$$

Secondly, since DDS can cause alignment of the interface with the mesh and its artificial deformation (as in the case of the HYPER-C scheme) one needs other scheme that satisfies the CBC. In the case of the HRIC, as the most straightforward choice is UDS scheme. Again the blending factor γ_f connected with angle θ_f is introduced, see Equation (16), to switch smoothly between schemes, cf. Equation (17).

$$\gamma_f = \sqrt{\left|\cos\theta_f\right|}\,, \tag{16}$$

$$\widetilde{\phi}_f^{*} = \gamma_f \widetilde{\phi}_f + (1-\gamma_f)\widetilde{\phi}_D, \quad 0 \le \gamma_f \le 1\,. \tag{17}$$

According to [7], blending of the UDS and the DDS schemes is dynamic and takes into account local distribution of the volume fraction. In the case when the local value of the Courant number is larger than 1 and the CFL condition is not satisfied the dynamic character of the HRIC can cause stability problems. Therefore, $\widetilde{\phi}_f^{*}$, see Equation (17), is corrected with respect to the local Courant number C_f:

$$\widetilde{\phi}_f = \begin{cases} \widetilde{\phi}_f^{*} & : \; C_f < 0.3 \\ \widetilde{\phi}_D & : \; C_f > 0.7 \\ \widetilde{\phi}_D + \left(\widetilde{\phi}_f^{*} - \widetilde{\phi}_D\right)\dfrac{0.7 - C_f}{0.7 - 0.3} & : \; 0.3 \le C_f \le 0.7 \end{cases}. \tag{18}$$

2.3. M-CICSAM

Using our experience about the properties of the CICSAM and HRIC high resolution schemes [5–6] we noticed that the first aforementioned scheme posses very good shape preserving properties while the latter is less dependant on the Courant number distribution. This two features can be combined in the single formulation, derived using two principles: remove dependence on the Courant number and thus switching to the UDS, retain high accuracy of the UQ scheme. Using this two constrains we can write compressive part of the M-CICSAM, similarly to HRIC:

$$\widetilde{\phi}_{f_{CBC}} = \begin{cases} \widetilde{\phi}_D & : \; 0 < \widetilde{\phi}_D, \widetilde{\phi}_D > 1 \\ \min\left(1, 2\widetilde{\phi}_D\right) & : \; 0 \le \widetilde{\phi}_D \le 1 \end{cases}. \tag{19}$$

Blending with respect to the interface orientation employs both schemes for the calculation of the cell face value, see Equations (12), (17). For this reason higher-order scheme used when interface is parallel to the flow direction should also be as com-

pressive as possible. For M-CICSAM a second order accurate bounded linear FROMM scheme is used, since it posses better compressive and dispersion properties [9] than UQ used in CICSAM:

$$\widetilde{\phi}_{f_{Fr}} = \begin{cases} \widetilde{\phi}_D & : \ 0 \ < \ \widetilde{\phi}_D, \widetilde{\phi}_D \ > \ 1 \\ \min\left(\dfrac{1}{4} + \widetilde{\phi}_D, \widetilde{\phi}_{CBC}\right) & : \ 0 \ \le \ \widetilde{\phi}_D \ \le \ 1 \end{cases}. \tag{20}$$

Finally blending factor γ_f that depends on the interface orientation and value of the normalized variable on the face of the control volume are calculated from the following expressions:

$$\gamma_f = \left|\cos\theta_f\right|^{1/4}, \tag{21}$$

$$\widetilde{\phi}_f = \gamma_f \widetilde{\phi}_{f_{CBC}} + (1-\gamma_f)\widetilde{\phi}_{f_{Fr}}, \quad 0 \le \gamma_f \le 1, \tag{22}$$

where θ_f is calculated using Equation (13). Since in the case of M-CICSAM we use more compressive FROMM scheme it was found that it is necessary to increase switching rate between compressive steady HYPER-C and higher order FROMM scheme, (compare Equation (21) and Equation (16)).

3. Comparison of the schemes properties

To check shape preserving properties of the considered schemes and asses influence of the non-uniform Courant number distribution, clockwise rotation of the solid body with a slot is considered. In this test we use single grid with 128×128 control volumes and two maximal Courant numbers $C_D^{\max} = 0.32$, 1.28. Results obtained in this test case are presented on Figure 2. In the upper and bottom rows, final distributions of the volume fraction after one revolution for smaller Courant number and after four revolutions for larger Courant number are given. When $C_D^{\max} \approx 0.32$ the sharpest interface profile is reconstructed with CICSAM scheme, while shape obtained with M-CICSAM is comparable to the reconstruction obtained with HRIC.

Superiority of the CICSAM is explained by using of the more compressive dynamic HYPER-C scheme. On contrary, when $C_D^{\max} \approx 1.28$ both CICSAM and HRIC suffer from artificial interface deformation, while M-CICSAM reconstructs interface profile almost without noticeable influence of the non-uniform distribution of the Courant number. The shape deformation in the case of CICSAM and HRIC is connected with switching to UDS when C_D tends to 1, see Equations (11), (18). From this test case we can conclude that any dependence of the high-resolution scheme on the Courant number will cause artificial deformation of the interface shape.

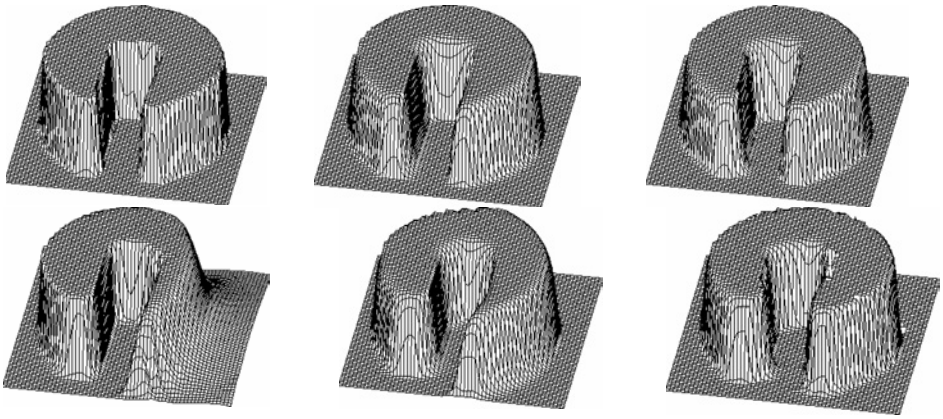

Fig. 2. Comparison of the deformation during the rotation of the solid body in circular velocity field, first column CICSAM, second column HRIC, third column M-CICSAM. First row max. Courant number 0.32, second row max. Courant number 1.28

4. Flow around surface piercing airfoil

To check if we are able to calculate flow in complex geometries as a first test we chose flow around free surface piercing foil placed in a towing tank. More details about experimental set up can be found in [12]. This simulation was carried on using

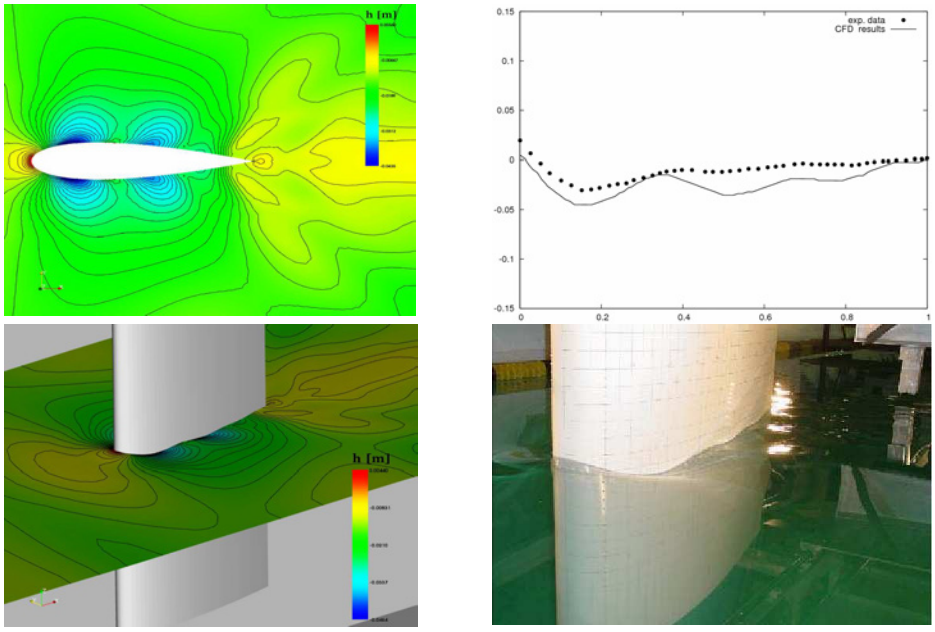

Fig. 3. Wave elevation for the flow around surface piercing foil $Fr = 0.2$, $Re = 8.2 \times 10^5$

FASTEST code with VOF method and high-resolution schemes implemented by authors (cooperation with TU Darmstadt, FNB department). Computational domain was discretized using ICEM-Hexa mesh generator; block structured grid consists of about 125000 control volumes. Figures 3, 4 present results obtained using M-CICSAM scheme compared with experimental data: mean wave profile on a foil and pictures taken in a towing tank. We notice that in the case of the Fr = 0.2, obtained solution only qualitatively reconstructs wave elevation. The explanation of this fact might be connected with comparison of instantaneous wave profile with time averaged wave elevations from [12], additionally mesh may be not fine enough in the boundary layer region. Despite this fact, a comparison with pictures is reliable, similarly to results obtained in the case of the Fr = 0.37 closer to the experimental data.

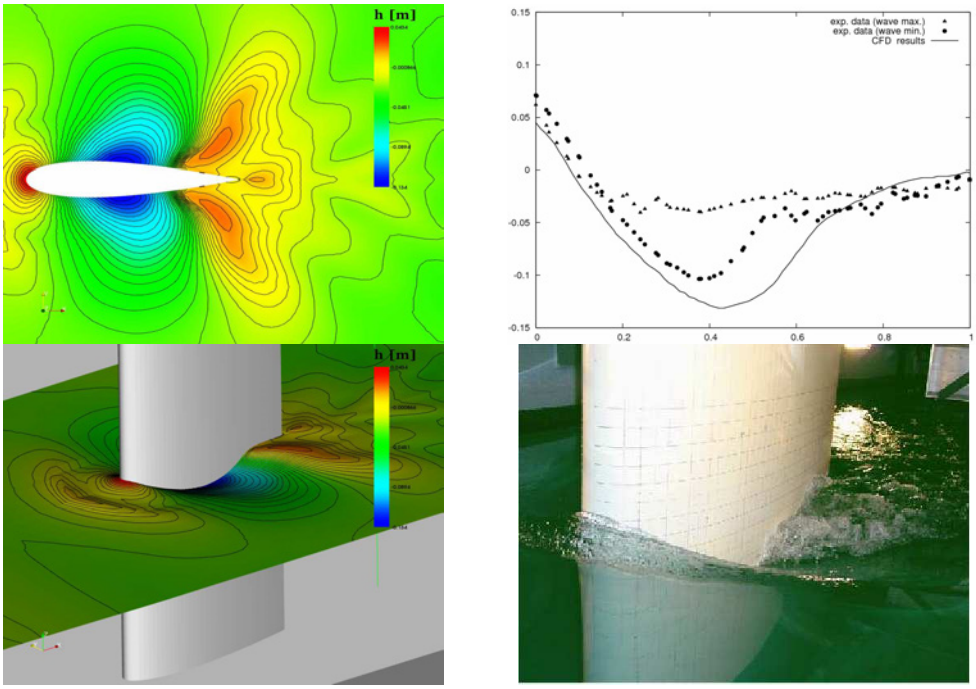

Fig. 4. Wave elevation for the flow around surface piercing foil Fr = 0.37, Re = 1.52 × 10^6

References

[1] Wilson R. V., Carrica P. M., Stern F.: *Unsteady RANS method for ship motions with application to roll for a surface combatant*, Comp. & Fluids, Vol. 35, 2006, pp. 501–524.

[2] Azcueta R., Caponnetto M., Schoeding H.: *Planning Boats in Waves*, Gdańsk HYDRONAV, 2003.

[3] Wacławczyk T., Palm M.: *Numerical prediction of ferry resistance with RANS turbulence model and the Volume of Fluid method for the free surface flow*, Gdańsk HYDRONAV, 2003.
[4] Wacławczyk T., Koronowicz T.: *Modeling of the flow in systems of immiscible fluids using volume of fluid method with CICSAM scheme*, Turbulence, Vol. 11, 2005, pp. 267–276.
[5] Wacławczyk T., Koronowicz T.: *Modelling of the wave breaking with CICSAM and HRIC highresolution schemes*, ECCOMAS for CFD, 2006.
[6] Wacławczyk T., Koronowicz T.: *Modelling of the free surface flows with high resolution schemes*, Chem. Proc. Eng., Vol. 27 3/1, 2006, pp. 783–802.
[7] Muzaferija S., Peric M., Sames P., Schelin T.: *A twofluid Navier-Stokes solver to simulate water entry*, Twenty Second Symposium on Naval Hydrodynamics, 1998.
[8] Ubbink O., Issa R.I.: *Method for Capturing Sharp Fluid Interfaces on Arbitrary Meshes*, J. Comp. Phys., Vol. 153, 1999, pp. 2650.
[9] Wesseling P.: *Principles of Computational Fluid Dynamics*, Springer-Verlag Berlin Heidelberg New York, 2000.
[10] B.P. Leonard.: *The ULTIMATE conservative difference scheme applied to unsteady one-dimensional advection*, Comp. Met. App. Mech. Eng., Vol. 88, 1991.
[11] Hirt C.W., Nicholls B.D.: *Volume of fluid method for dynamics of free boundaries*, J. Comp. Phys., Volume 39, 1981, pp. 201–221.
[12] Metcalf B., Longo J., Ghosh S., Stern F.: *Unsteady free-surface wave-induced boundary layer separation for a surface piercing NACA 0024 foil. Towing tank experiments*, J. Fluids Struct., Vol. 22, 2006, pp. 77–98.

Uwagi na temat wyznaczania oporu falowego w oparciu o metodę VOF oraz schematy o wysokiej rozdzielczości

W artykule przedstawiono model jednopłynowy stosowany w metodzie VOF oraz przedyskutowano i porównano właściwości trzech schematów o wysokiej rozdzielczości. Zależności schematu o wysokiej rozdzielczości od liczby Couranta, schematy CICSAM [8], HRIC [7], prowadzi do występowania sztucznej dyfuzji w wyniku przełączania do schematu różnicowego pierwszego rzędu tzw. pod-prąd (UDS), zobacz Rysunek 2. Zaproponowana modyfikacja, schemat M-CICSAM, pozwala na uniknięcie tego efektu, zapewniając jednocześnie poprawną rekonstrukcję powierzchni rozdziału. W drugiej części artykułu przedstawiono pierwsze wyniki obliczeń stosując zaproponowany schemat M-CICSAM, w trójwymiarowej przestrzeni obliczeniowej. Wyniki zostały otrzymane za pomocą akademickiego kodu FASTEST wraz z zaimplementowaną przez autorów metodą VOF ze schematami o wysokiej rozdzielczości (współpraca z TU Darmstadt FNB). Otrzymane wyniki obliczeń porównano z profilami fali otrzymanymi eksperymentalnie [12], otrzymując jakościową zgodność. Dalsze prace będą polegały na uwzględnieniu w obliczeniach modelu turbulencji oraz przeprowadzeniu wyznaczania oporu dla rzeczywistych kadłubów statków.

ARCHIVES OF CIVIL AND MECHANICAL ENGINEERING

Vol. VIII 2008 No. 1

Computations of the propeller open water characteristics using the SOLAGA computer program. Predictions of the cavitation phenomenon

PAWEŁ DYMARSKI
Ship Design and Research Centre S.A. (CTO SA) – Ship Hydromechanics Division, 65, Szczecińska St., 80-392 Gdańsk

This paper presents the theoretical model and numerical methods which are applied in computer program SOLAGA for computations of viscous flow around ship propeller as well as for modelling of cavitation phenomenon. The model presented in the article is based on mass conservation equation and Reynolds averaged Navier-Stokes equation, the turbulent viscosity is approximated with the use of Spalart-Allmaras turbulent model. The numerical model used for solving the system of main equations is based on Finite Volume Method. The procedures for cavitation predictions applied in the SOLAGA program are based on travelling bubble model. This paper presents the results of computations of K_T, K_Q characteristics for conventional and skewed propeller. The results are compared with the data obtained from experiment. The results of computation of cavitation for the skewed propeller are presented as well.

Keywords: *propeller, viscous flow, CFD, cavitation, turbulence*

1. Introduction

The main target of the paper is to show state of development of computer program SOLAGA, especially its ability to solve problems connected with viscous flow around ship propeller with the use of periodic boundary conditions as well as to present the results of computations of cavitation. Program SOLAGA has been developed in the framework of research project supported by Polish Committee of Science. It has been also the main subject of the author's PhD thesis.

2. Governing Equations

The closed system of motion equations, derived for incompressible fluid, is based on the momentum and mass conservation laws. An integral form of mass conservation equation formulated for control volume Ω with a surface S reads

$$\int_S \rho \mathbf{v} \cdot \mathbf{n} \mathrm{d}S = 0, \tag{1}$$

and the conservation equation of i-th momentum component has the following form:

$$\frac{\partial}{\partial t}\int_{\Omega}\rho u_i \mathrm{d}\Omega + \int_{S}\rho u_i \mathbf{v}\cdot\mathbf{n}\mathrm{d}S = \int_{S}\left(\tau_{ij}\mathbf{i}_j - p\mathbf{i}_i\right)\cdot\mathbf{n}\mathrm{d}S\,, \tag{2}$$

where:

v is velocity vector,

u_i – i-th velocity component,

p – pressure,

ρ – density,

n – unit vector normal to S surface,

i_i – i-th component of Cartesian unit vector,

τ_{ij} is a viscous stress tensor.

When the flow is turbulent, **v** and u_i refer to mean velocity vector and mean i-th velocity component, p is a mean value of pressure. The word "mean" denotes average in a time period, which is long compared to the period of turbulent oscillations [5].

The viscous stress tensor τ_{ij} is specified by Boussinesq approximation [1], [5]:

$$\tau_{ij} = 2(\mu + \mu_t)S_{ij}, \tag{3}$$

where:

μ is a molecular viscosity,

μ_t is the turbulent viscosity,

S_{ij} is the mean strain-rate tensor.

The turbulent viscosity is calculated with the use of Spalart-Allmaras turbulence model [1], [5].

3. Cavitation

The cavitation model is based on travelling bubble method [4]. It is assumed in the model, that a large number of micro gas nuclei is present in the liquid. When pressure value decreases below a specified critical level, the radius of nucleus starts to grow rapidly and – according to the model – this is the inception of cavitation.

To determine behaviour of a single bubble the pressure field, velocity field (or bubble trajectory) and initial size of nucleus have to be given.

The single bubble dynamic is described by Rayleigh-Plasset equation:

$$R\frac{\mathrm{d}^2R}{\mathrm{d}t^2} + \frac{3}{2}\left(\frac{\mathrm{d}R}{\mathrm{d}t}\right)^2 + \frac{\mu}{\rho R}\frac{\mathrm{d}R}{\mathrm{d}t} = \frac{-p + \dfrac{2\mathrm{A}}{R} - p_v - p_g}{\rho}\,, \tag{4}$$

where:

R is a radius of the bubble,

t is time,

p is pressure far from the bubble,
p_v – vapour pressure,
p_g – pressure of the gas in the bubble,
A – denotes the surface tension coefficient.

When spectrum of nuclei at inflow is given (i.e. number of nuclei in a given range of radius) one can calculate nuclei distribution in every point inside the domain. Probability of cavitation phenomenon can be approximated by the following simplified formula:

$$P_{CAV} = \mathrm{cut}\left(\sum_i \frac{4}{3} \pi R_i^3 n_i \right), \tag{5}$$

where:

n_i is the number of nuclei of size R_i inside the unit volume and function cut(x) is defined as:

$$\mathrm{cut}(x) = \{x \text{ for } x \le 1; 1 \text{ for } x > 1\}. \tag{6}$$

4. Numerical Methods

The solution algorithm for solving the viscous flow is based on Finite Volume Method. The Finite Volume Method is based on integral form of conservation equations. The solution domain is subdivided into a finite number of control volumes, and the conservation equations are applied to each of them. The computational node at which the values of field functions are to be calculated lies at the centroid of each control volume (CV).

To express the value of each field quantity on CV surface S, suitable interpolation methods are used. In the presented program two methods are applied: upwind UDS (first order) and linear interpolation CDS (second order). Surface and volume integrals are approximated using midpoint quadrature [3]. As a result of FV discretization approach, one obtains an algebraic equation for each CV. The system of equations (after linearization) is solved using an iterative method. Two algorithms for solving the systems of algebraic equations are used: ICCG for symmetric systems and Bi-CGSTAB for non-symmetric systems [3].

When the problem of flow around a propeller is solved with the use of rotating grid, the problem becomes unsteady. The time integral in the Navier-Stokes equation is solved with the use of implicit Euler method.

a. Rotating grid

Computation of flow around ship propeller requires the use of rotating grid or rotating coordinate system. In the first method, the conservations equations have to be

modified in order to take into account a relative velocity between grid (control volumes) and coordinate system. The mass conservation of equation for single rotating control volume in integral form reads

$$\int_S \rho(\mathbf{v} - \mathbf{v}_b)\cdot \mathbf{n}\mathrm{d}S\,, \tag{7}$$

where:

$\mathbf{v}_b = \omega \times \mathbf{r}_b$ is a velocity of CV boundary,

ω – rotational velocity of the grid,

$\mathbf{r}_b$ – position vector of a point at S.

The momentum conservation equation for i-th momentum component takes the following form:

$$\frac{\mathrm{d}}{\mathrm{d}t}\int_\Omega \rho u_i \mathrm{d}\Omega + \int_S \rho u_i(\mathbf{v} - \mathbf{v}_b)\cdot \mathbf{n}\mathrm{d}S = \int_S \left(\tau_{ij}\mathbf{i}_j - p\mathbf{i}_i\right)\cdot \mathbf{n}\mathrm{d}S\,. \tag{8}$$

b. Periodic boundary conditions

In case of computation of open water characteristic of a propeller, it is possible to use periodic boundary conditions (Figure 1). This approach reduces the size of domain z – times (where z is a number of blades).

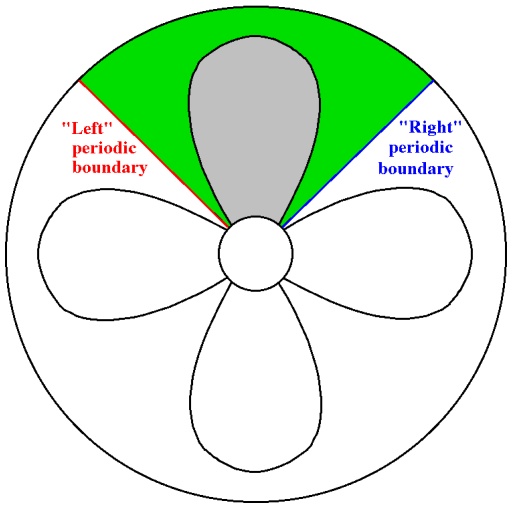

Fig. 1. Periodic subdomain and periodic “left” and “right” boundary conditions. The periodic subdomain covers only a single blade and its size is z times lower than size of whole domain. (z is a number of blades)

At the periodic boundaries we have the following conditions:

$$p_L = p_R, \qquad \varphi_L = \varphi_R, \qquad \mathbf{v}_L = \mathbf{Q}_{RL}\mathbf{v}_R, \tag{9}$$

where:
φ is a scalar quantity (i.e.: turbulent viscosity),
$\mathbf{Q}_{RL}$ is a transformation matrix from "right" R to "left" L periodic boundary:

$$\mathbf{Q}_{RL} = \begin{bmatrix} 1 & 0 & 0 \\ 0 & \cos\alpha & -\sin\alpha \\ 0 & \sin\alpha & \cos\alpha \end{bmatrix}, \tag{10}$$

$\alpha = 2\pi/z$ is an angle between left and right periodic boundary.

Non-matching interfaces

From the numerical point of view periodic boundary condition is an interface between two subdomains (Figure 2a, b). In SOLAGA solver, the grid at periodic interface may be non-matching, it allows to build almost orthogonal grids with better structure than "matching" meshes (Figure 2c, d).

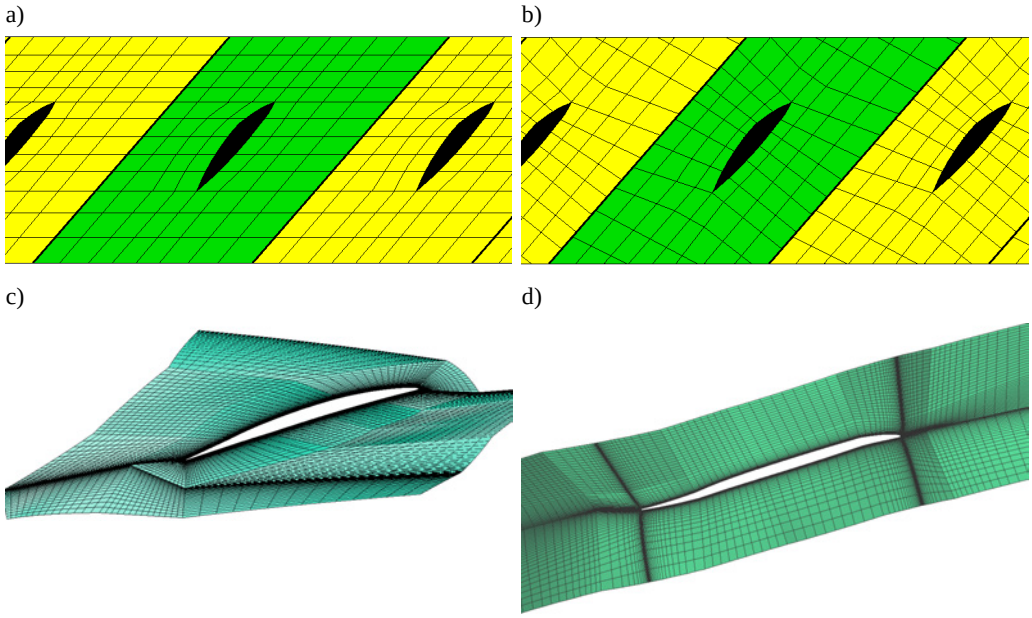

Fig. 2. Scheme of matching (a) and non-matching (b) connections at periodic boundary. Difference between structure of periodic matching (c) and non-matching grid (d) for calculation of flow around propeller blade

5. Computations

Computations were carried out for two propeller models: model A – conventional propeller and model B – skewed propeller. Computations were carried out with rotating grid and with the use of periodic boundary conditions with non-matching interfaces. The details of computational settings are presented in Table 1.

Table 1. Computational settings

Time step	0.0001 s
Number of iterations per time step	3
Interpolation scheme	CDS (blending factor 0.8)
Time integral approximation	Implicit Euler

a. Test case 1 – model A. Flow around conventional propeller

Geometry of the model A. Computational conditions

Table 2. Geometry of propeller model A

Type	Fixed pitch
No of blades	4
Diameter	183.90 mm
Pitch ratio at 0.7 radius	0.7413
Expanded area ratio	0.574
Hub ratio	0.175
Blade width at 0.7 radius	55.79 mm

Table 3. Open water test and computational conditions

	Test conditions	Computational conditions
Propeller revolutions n	28.0 1/s	28.0 1/s
Propeller velocity v_p	0.0–4.2 m/s	1.0; 2.0; 3.0; 4.0 m/s
Advance coefficient J	0.0–0.816	0.194; 0.388; 0.583; 0.777

The domain size and grid structure

Size of the domain: the inlet is located 2.3 D upstream from the propeller, the outlet is 2.2 D downstream, the diameter of the domain is 2.9 D. The boundary faces of the domain are presented in Figure 4a.

The grid was generated with the use of program ANSYS ICEM CFD Hexa. The grid is hexahedral and block-structured, number of CV's (per one blade) is 974 424. The grid structure on blade, hub and periodic surface is shown in Figure 4b.

Results of computations

Pressure distribution over the suction and pressure side of the propeller blade is presented in Figure 5.

a) b)

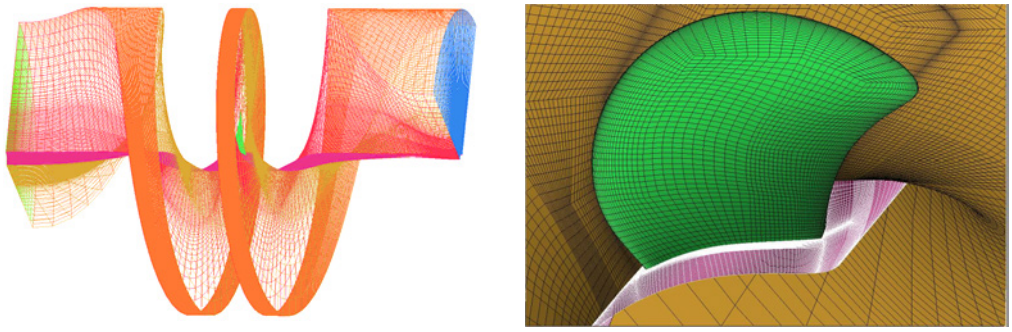

Fig. 4. a) Model A: domain of computations, b) Grid structure on the propeller blade, hub and periodic surface

The comparison of the calculated and experimental values of K_T and K_Q for several values of J is presented in Figure 6a.

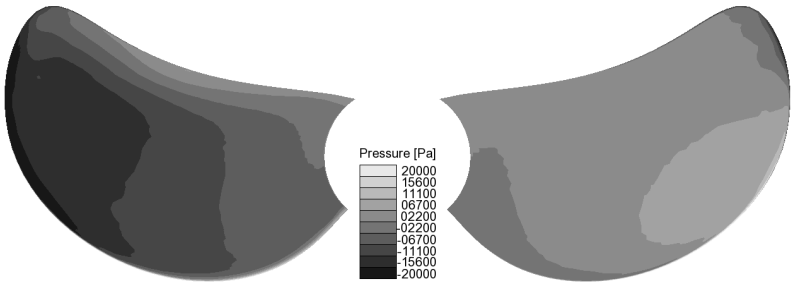

Fig. 5. Pressure distribution over the suction (left) and pressure (right) side of the conventional propeller, J = 0.388

a) b)

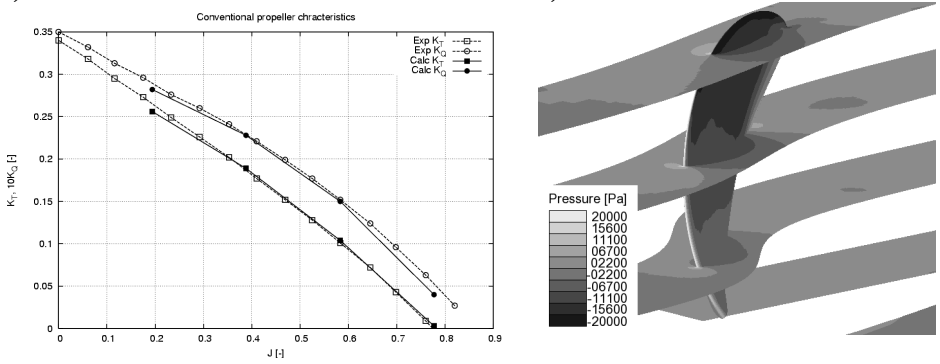

Fig. 6. a) K_T, K_Q characteristics of model A – conventional propeller, b) pressure distribution at the domain intersections, J = 0.388

b. Test case 2 - model B. Flow around skewed propeller

Geometry of the model B. Computational conditions

Table 4. Geometry of Propeller model B:

Type	Controllable pitch
No of blades	5
Diameter	265.73 mm
Pitch ratio at 0.7 radius	1.4281
Expanded area ratio	0.820
Hub ratio	0.3026

Table 5. Test and computational conditions:

	Test conditions:	Computational conditions:
Propeller revolutions n	11.0 1/s	11.0 1/s
Propeller velocity v_p	0.5–4.1 m/s	1.0; 2.0; 3.0; 4.0 m/s
Advance coefficient J	0.171–1.403	0.342; 0.684; 1.026; 1.368

Table 6. Data for computations of cavitation

Propeller velocity v_p	2.0 m/s
Advance coefficient J	0.684
Reference pressure (at inflow) p_0	0.04; 0.06; 0.08; 0.10 bar
Number of nuclei (at inflow) n_0	$0.1 \cdot 10^6$ 1/m^3
Radius of nuclei (at inflow) R_0	$10.0 \cdot 10^{-6}$ m

The domain size and grid structure

Size of the domain: the inlet is located 1.9 D upstream from the propeller, the outlet is 1.9 D downstream, the diameter of the domain is 2.4 D. The boundary faces of the domain are presented in Figure 7a.

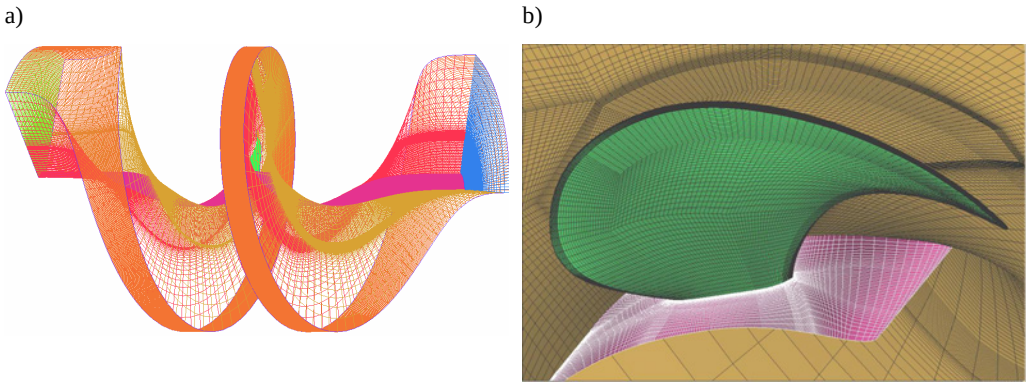

Fig. 7. a) Model B: domain of computations, b) grid structure on the propeller blade, hub and periodic surface

The grid was generated with the use of program ANSYS ICEM CFD Hexa. The grid is hexahedral and block-structured, number of CV's (per one blade) is 1 086 176. The grid structure on blade, hub and periodic surface is shown in Figure 7b.

Results of computations

Pressure distribution over the suction and pressure side of the propeller blade is shown in Figure 8. The comparison of the calculated and experimental values of K_T and K_Q for several J is presented in Figure 9a, however picture 9b shows pressure distribution inside the domain. The low pressure area which is stretched behind a blade tip is caused by a strong vorticity of tip vortex. The tip vortex is visible even far than 180 degrees behind the blade.

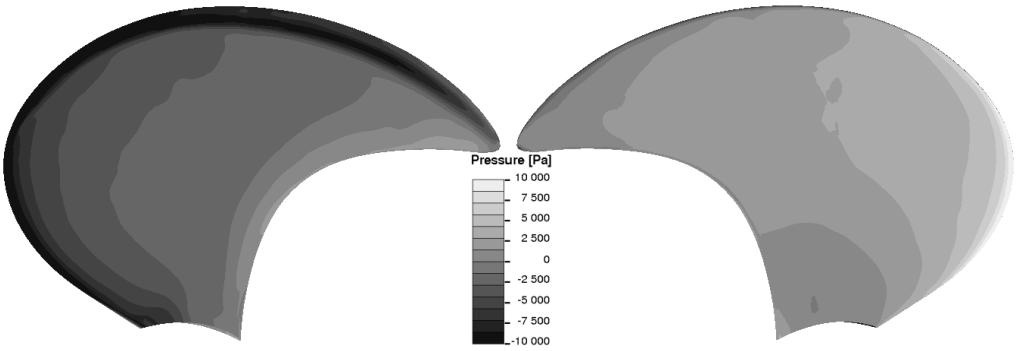

Fig. 8. Pressure distribution over a suction (left) and pressure (right) side of the skewed propeller, J = 0.684

a) b)

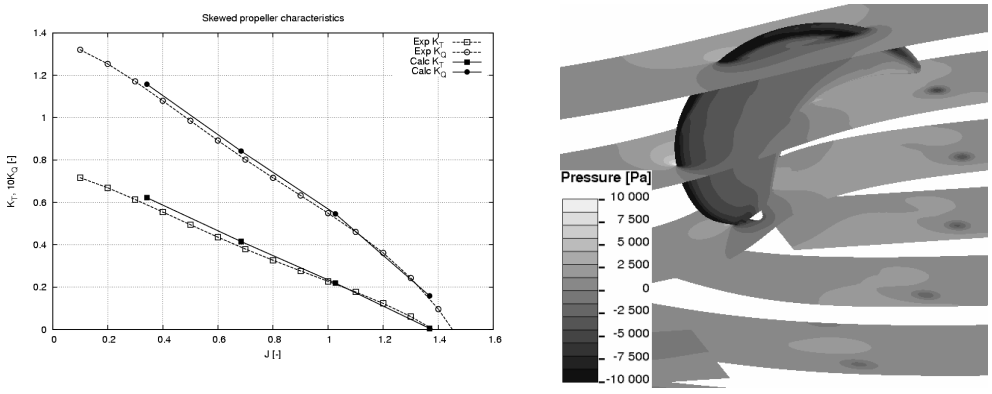

Fig. 9. a) K_T, K_Q characteristics of the skewed propeller (model B), b) pressure distribution at intersections of the domain, J = 0.684

Figure 10 presents distribution of probability of cavitation P_{CAV} at blade surface as well as the shape of isosurface $P_{CAV} = 0.5$ which can be treated as a face of large scale cavitation structures, e.g.: laminar cavitation, tip vortex cavitation or large bubbles. Bubble cavitation can be expected in regions where function of probability takes a value between about 0.1 and 0.5. The presented model does not predict secondary form of cavitation, e.g.: cloud cavitation.

Open water cavitation tests for the propeller are planned to be carried out in the near future. Up to now, the presented cavitation model has been validated on an example of hydrofoil [2].

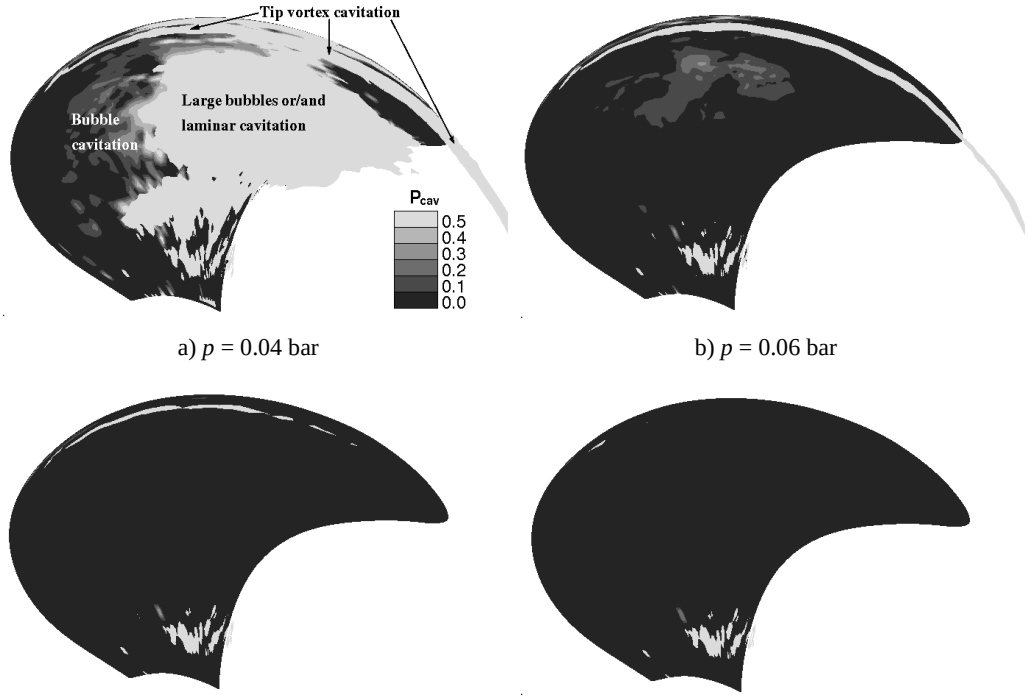

a) p = 0.04 bar b) p = 0.06 bar

c) p = 0.08 bar d) p = 0.10 bar

Fig. 10. Computational predictions of cavitation phenomenon on propeller blade for advance coefficient J = 0.684 and various values of reference pressure. The pictures shows probability of cavitation P_{CAV} on blade surface as well as isosurface $P_{CAV} = 0.5$

6. Conclusions

1. The calculated pressure distribution over the blades of the propellers is smooth, without any numerical oscillations, also there are no pressure oscillations near periodic, non-matching boundaries.

2. The calculated propeller characteristics: thrust K_T, and torque K_Q coefficients are in good agreement with the experimental results for both conventional and skewed propeller.

3. Program SOLAGA can be also a good tool for the tip vortex modelling. The low pressure area caused by vorticity is clearly visible far behind the propeller blade (Figure 9 b). Close examination of his figure shows the core of the vortex created by the next blade.

4. Figure 10, in which the probability of cavitation is presented, shows the structures of cavitation like those observed on similar propeller models in cavitation tunnel. One can distinguish the elongated structure of tip vortex cavitation which spreads from leading edge, through the tip, to the slipstream (Figure 10a–10c). The regions are also visible where bubble cavitation may appear, where P_{CAV} ranges from about 0.1 to 0.5 (Figure 10a, b) as well as large area where laminar or/and developed bubble cavitation can be expected (Figure 10a).

References

[1] Blazek J.: *Computational Fluid Dynamics: Principles and Applications*, ELSEVIER 2001.
[2] Dymarski P.: *Numerical computation of hydrodynamic forces on hydrofoil. Prediction of cavitation phenomenon*, 8th Numerical Towing Tank Symposium, 2–4 Oct., 2005, Varna.
[3] Ferziger J.H, Peric M.: *Computational Methods for Fluid Dynamics*, 2nd ed., Berlin, Springer, 1999.
[4] Lecoffre Y.: *Cavitation. Bubble Trackers*, A. A. Balkema/Rotterdam/Brookfield, 1999.
[5] Wilcox D.C.: *Turbulence Modeling for CFD*, DCW Industries, 2002.

Obliczenia charakterystyk śrub swobodnych przy użyciu programu komputerowego SOLAGA. Prognozowanie zjawiska kawitacji

Niniejszy referat prezentuje pokrótce model teoretyczny oraz metody obliczeniowe zastosowane w programie komputerowym SOLAGA służącym do obliczeń opływu lepkiego śruby okrętowej oraz do wykonywania obliczeniowych prognoz występowania zjawiska kawitacji. W pracy zastosowano model cieczy lepkiej oparty na równaniu zachowania masy oraz równaniu zachowania pędu (rów. Naviera-Stokesa) w formie uśrednionej Reynoldsa. Lepkość turbulentna aproksymowana jest przy użyciu modelu turbulencji Spalarta-Allmarasa. Model numeryczny zastosowany do rozwiązania głównego układu równań bazuje na metodzie objętości skończonej. Metodę prognozowania zjawiska kawitacji oparto na modelu unoszonego pęcherzyka. W artykule przedstawiono ponadto wyniki obliczeń w formie rozkładu ciśnień oraz charakterystyk K_T, K_Q śruby, które zostały porównane z danymi doświadczalnymi. Przedstawione zostały również wyniki obliczeń kawitacji na skrzydle śruby okrętowej.

ARCHIVES OF CIVIL AND MECHANICAL ENGINEERING

Vol. VIII 2008 No. 1

Assessment of ship squat in shallow water using CFD

JACEK JACHOWSKI
Gdańsk University of Technology, G. Narutowicza 11/12, 80-952 Gdańsk

In the recent years much research effort in ship hydromechanics is devoted to the practical navigation problems in getting larger ships safely into existing harbours or to the appropriate design of expansion of harbours for safe accommodation of larger ships. Both these problems are directly related to the safety of navigation and therefore they receive high attention from ship designers, harbour designers, ship operators and maritime administration. The starting point of any navigational or design analysis lies in the accurate determination of the hydrodynamic forces generated on the ship hull moving in confined waters. The analysis of such ship motion should include the effects of shallow water, horizontal restrictions, asymmetric channels, muddy bottoms, ship squat, ship to ship interactions etc. It is natural to use advanced Computational Fluid Dynamics methods for this purpose. The paper includes a wide introduction into the problems of modelling of the restricted water effects on ship motion using CFD. This presentation is illustrated with the examples of calculations performed using the commercial system Fluent.

Keywords: *shallow water, squat of a ship, CFD*

1. Introduction

The problem of ship squat is one among the crucial factors affecting the navigation of ships in restricted waters. The squat can be estimated using either the empirical or analytical models. It may be evaluated by implementing the real scale tests or CFD technology as well.

The main aim of the current research is to investigate if a commercial CFD code may be useful for assessing the clearance. The results of calculations should be validated with the results obtained using the existing methods of squat identification. From the hydrodynamic phenomena point of view the main attention has been paid to identify the system of waves generated by a ship and hydrodynamic forces affecting the hull in shallow water.

2. Squat phenomenon

During the ship motion in shallow water there is a phenomenon when the clearance may decrease. According to the differences regarding the velocity of flow there is change of water pressure along the hull. In shallow water there is a smaller value of pressure at the midship in comparison with the deep water condition. In the opposite way, there is a bigger value of pressure in the bow and aft parts of the ship. According to the pressure distribution the water level increases in the bow and aft parts of the

ship but at the midship the water level decreases. This phenomenon is the reason of the ship squat in shallow water as presented in Figure 1.

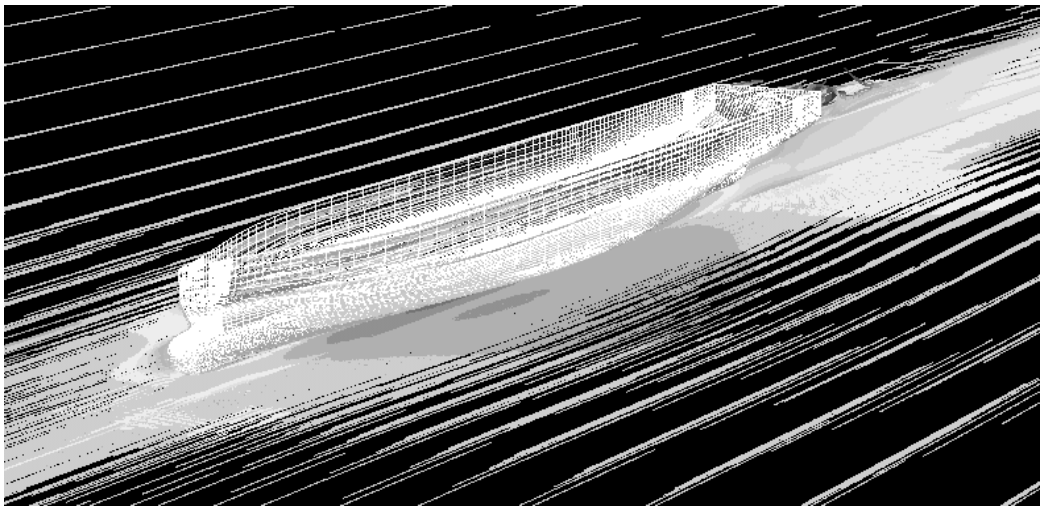

Fig. 1. Change of velocity field and hydrodynamic pressure change along the ship in shallow water at 14 kn; the grey colour under bottom marks increased velocity

All recent research indicates that prediction of squat depends on the following parameters:

- ship speed,
- ship position (proximity to channel bank),
- ship geometry (length, beam, draft, shape, etc.),
- channel geometry (depth, width, area, etc.).

Based on the main parameters, squat can be described by the following function [3]:

$$S_b = f\left(T, \frac{1}{h}, v_s^2, A_s, \frac{1}{A_w}\right), \tag{1}$$

where:

S_b – squat,
h – water depth,
T – ship draft,
v_s – ship speed,
A_s – area of the ship's midship section,
A_w – area of the canal or river cross-section.

3. Computational method

Commercial system Fluent was used for modelling the ship squat in shallow water. Computations were performed for four values of water depth. The following assumptions were used in modelling:

- linear motion with constant speed,
- computation with free surface,
- surface without waves and current,
- water region width equal to four lengths of ship to eliminate wall effect,
- ship is considered without propeller influence,
- flat bottom without natural irregularities,
- no dynamic mesh,
- four values of water depth and speed range from 4 kn to 21.5 kn.

4. Model data and boundary conditions

The basic characteristics of the computational mesh are as follows:

- hexahedral meshes were used. The number of mesh cells was about 700 000. The surface mesh on the hull is shown in Figure 2. The mesh was logarithmic concentrated close to the free surface, hull and bottom.

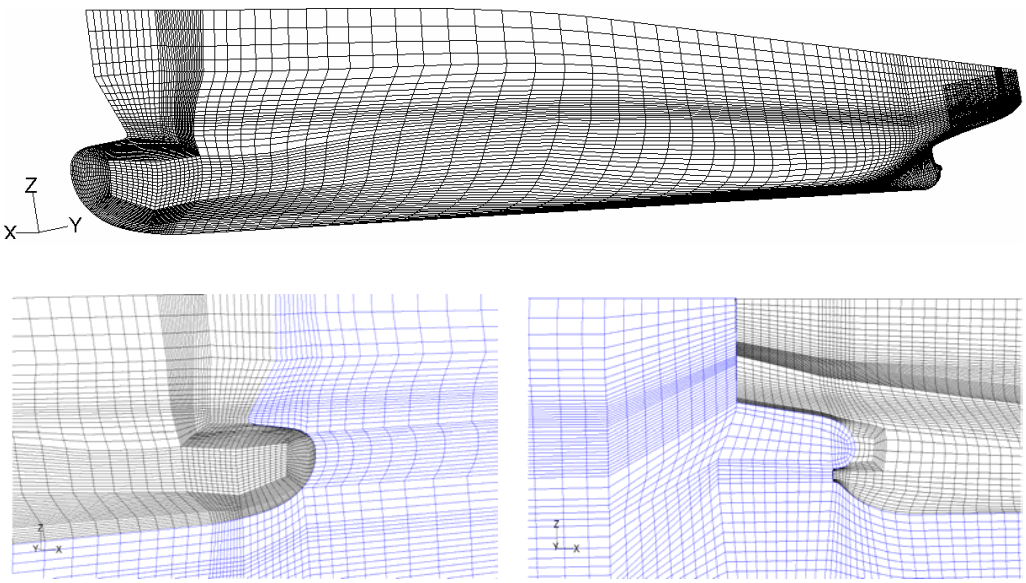

Fig. 2. Surface mesh for KCS hull and regions where difficulties with obtaining a regular mesh were encountered (adapted from [4])

- due to symmetry of the flow the calculations were carried out for half ship.
- computations were performed in model scale for reduction of the computational effort.
- the flow was computed in rectangular domain surrounding the hull – Figure 3.

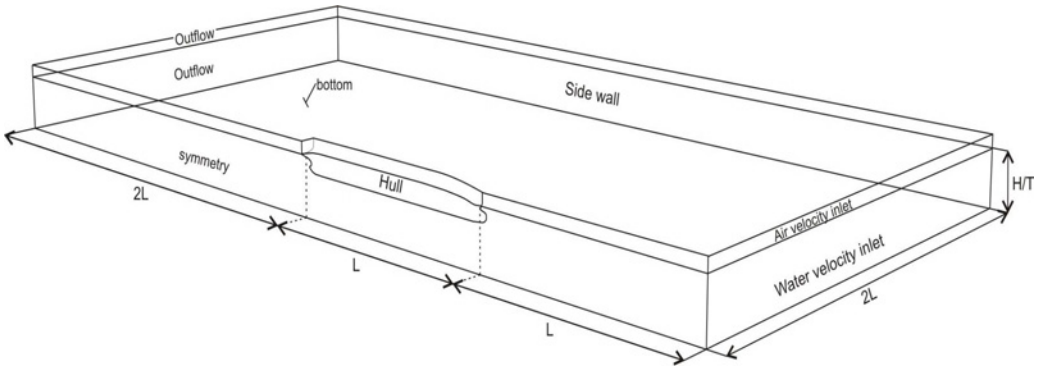

Fig. 3. Domain of the flow – shape and dimensions

3.1. Ship example

The computations were performed for KRISO Container Ship (KCS) in scale 1:25.555.

Table. Main dimensions of the ship and model

Parameters		ship dimensions	model dimensions
Lpp	[m]	184.87	7.2786
B	[m]	25.88	1.0190
T	[m]	8.682	0.3418
Cb	[-]	0.6508	0.6508
Cp	[-]	0.6608	0.6608
Cm	[-]	0.9849	0.9849
V	[m^3]	27531	1.6497
Sw	[m^2]	6203	9.4984

3.2. Shallow water configurations

Water region simulating shallow water for four values of depth (H) to draft (T) ratio is shown in Figure 4.

- H/T = 22.4 – deep water,
- H/T = 2.5 – deep shallow water,
- H/T = 1.2 and H/T = 1.5 – shallow water.

3.3. Boundary conditions

The following boundary conditions were applied in calculations using Fluent [1, 4–6]:

Water inlet	– velocity inlet	– vessel speed
Air inlet	– velocity inlet	– atmospheric pressure
Symmetry plane	– symmetry	– symmetry condition
Waterway bottom	– wall	– moving wall with vessel speed
Side wall	– wall	– stationary wall with zero normal velocity and zero viscous stress
Hull	– wall	– stationary wall
Water outlet	– outflow	– undisturbed outflow
Air outlet	– outflow	– undisturbed outflow
Water surface	– plane of VOF	– atmospheric pressure

Time step of computations = 0 m 001 s.

Initial conditions were set in the whole domain for the velocity, turbulence kinetic energy k and dissipation rate ε. The initial value of k was set based on turbulence intensity of 2%. The initial value of ε was set as 0.07 of hull model length. The computations were performed with one iteration per time step.

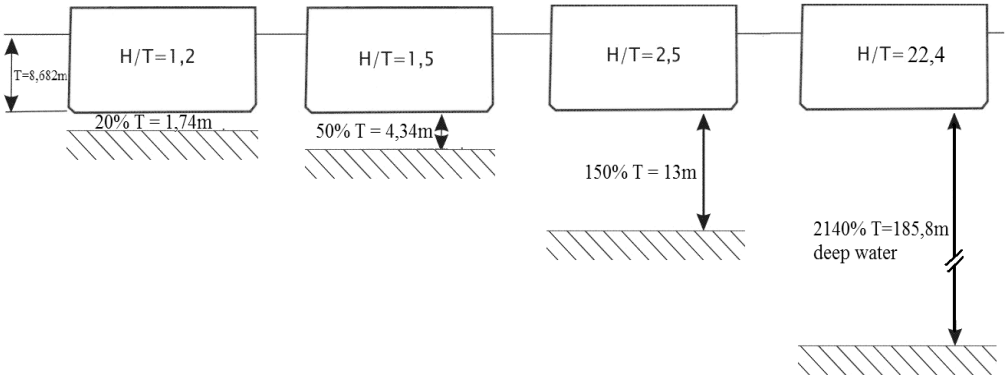

Fig. 4. Shallow water configurations

4. Results of calculations

Vertical hydrodynamic forces calculated by Fluent were taken for squat calculation. These values were treated as total force which is the sum of static and dynamic buoyancy force. Dynamic buoyancy force changes upon hydrodynamic pressure generated on the hull moving over bottom. The values of total buoyancy force are shown in Figure 5.

For depths ratios H/T = 1.2 and 1.5 further investigation was carried out. This investigation included mesh modification, which allowed incorporation of the draught change calculated in the first iteration.

For the purpose of evaluating the reliability of ship squat prediction using Fluent, six of the most common empirical methods for calculation of ship squat in confined waters are compared (Figure 7). The six methods are: Barrass 2, Huuska, Eryuzlu, Eryuzlu & Hausser, Icorels, and Hooft & Turner. These methods were previously compared with full scale test and the comparison showed that the Eryuzlu, Barras 2 and Hooft methods give good results for ships with C_b of around 0.6 [2, 3].

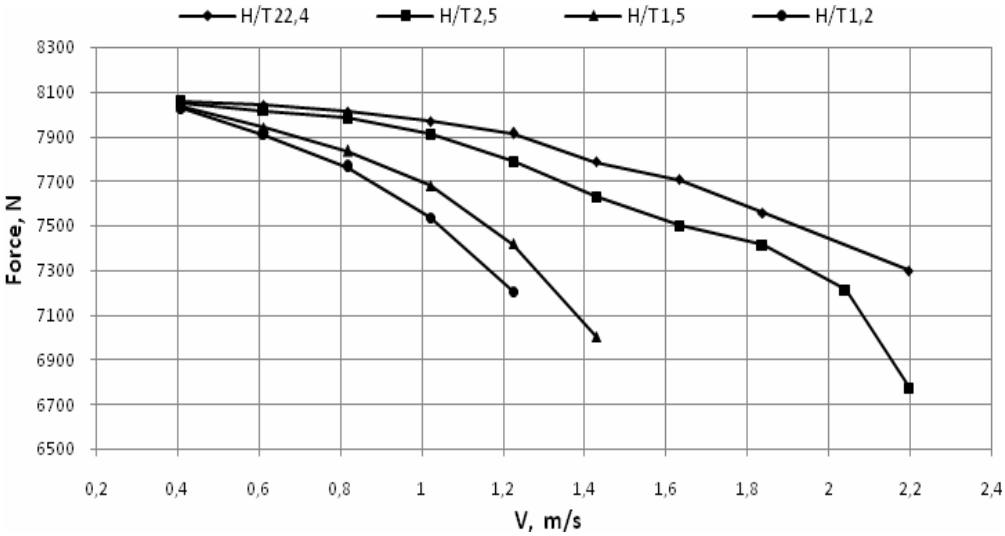

Fig. 5. Fluent calculations of the total buoyancy force for four H/T values in model scale

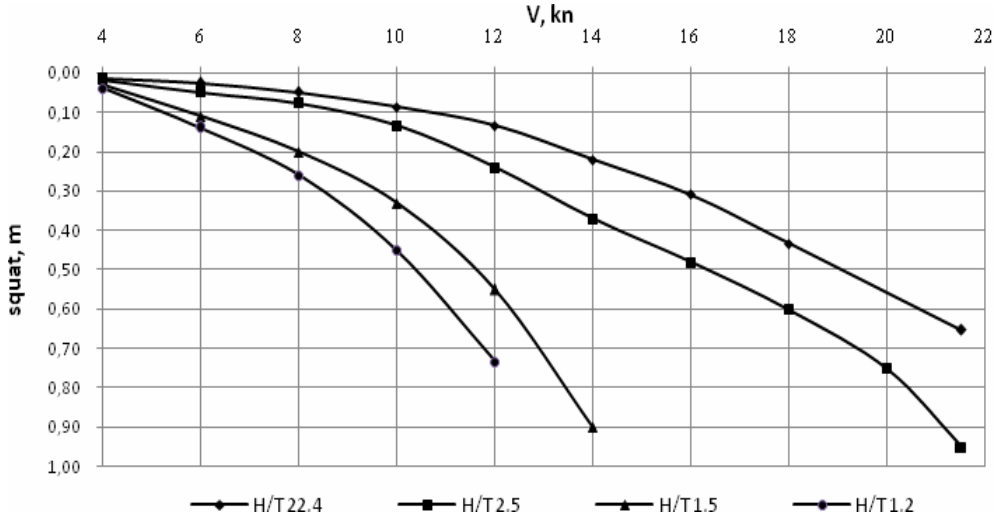

Fig. 6. Ship squat values calculated using Fluent for four H/T values (in full scale)

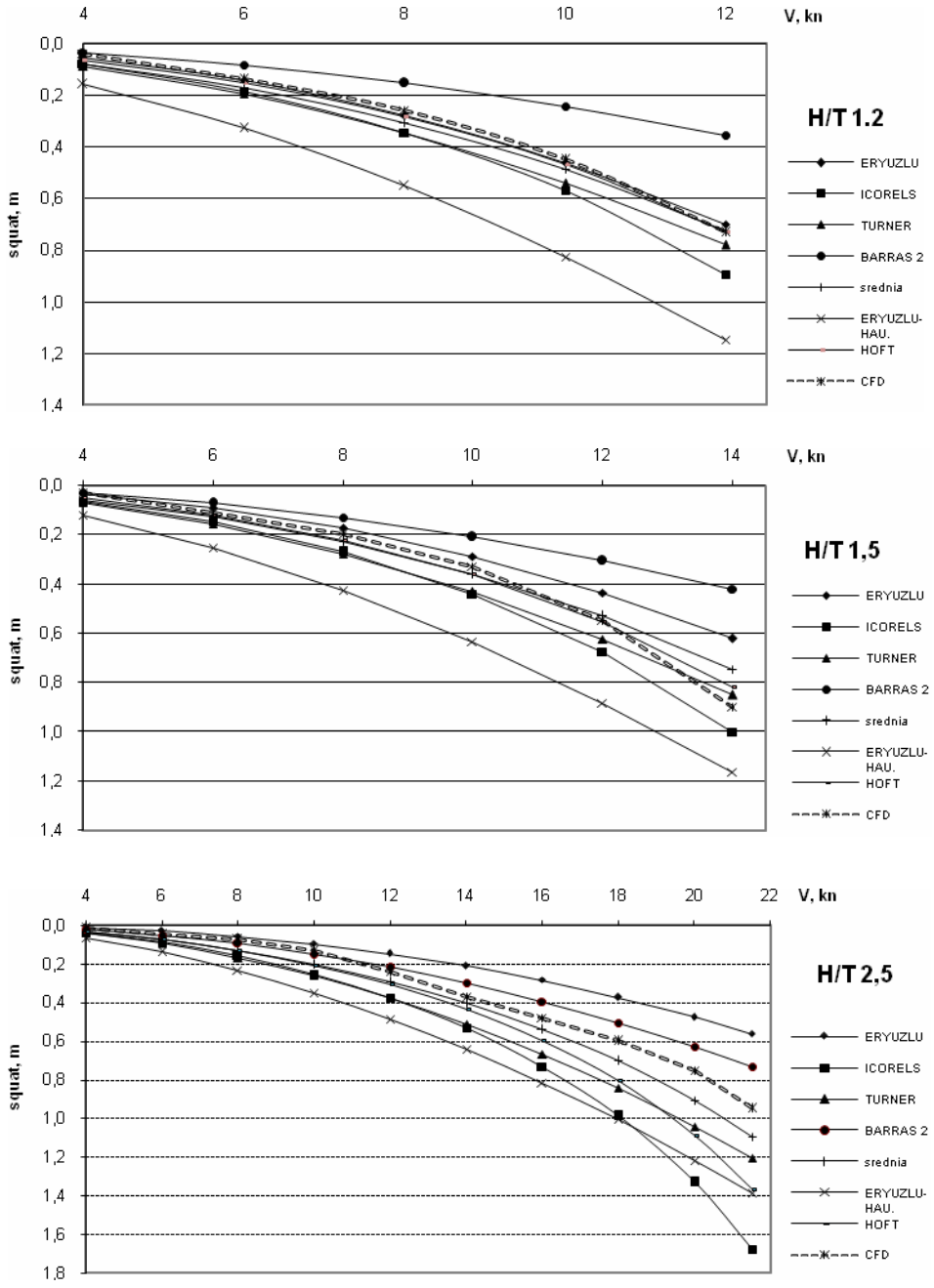

Fig. 7. Comparison of ship squat values calculated using the empirical methods and Fluent for three selected H/T values

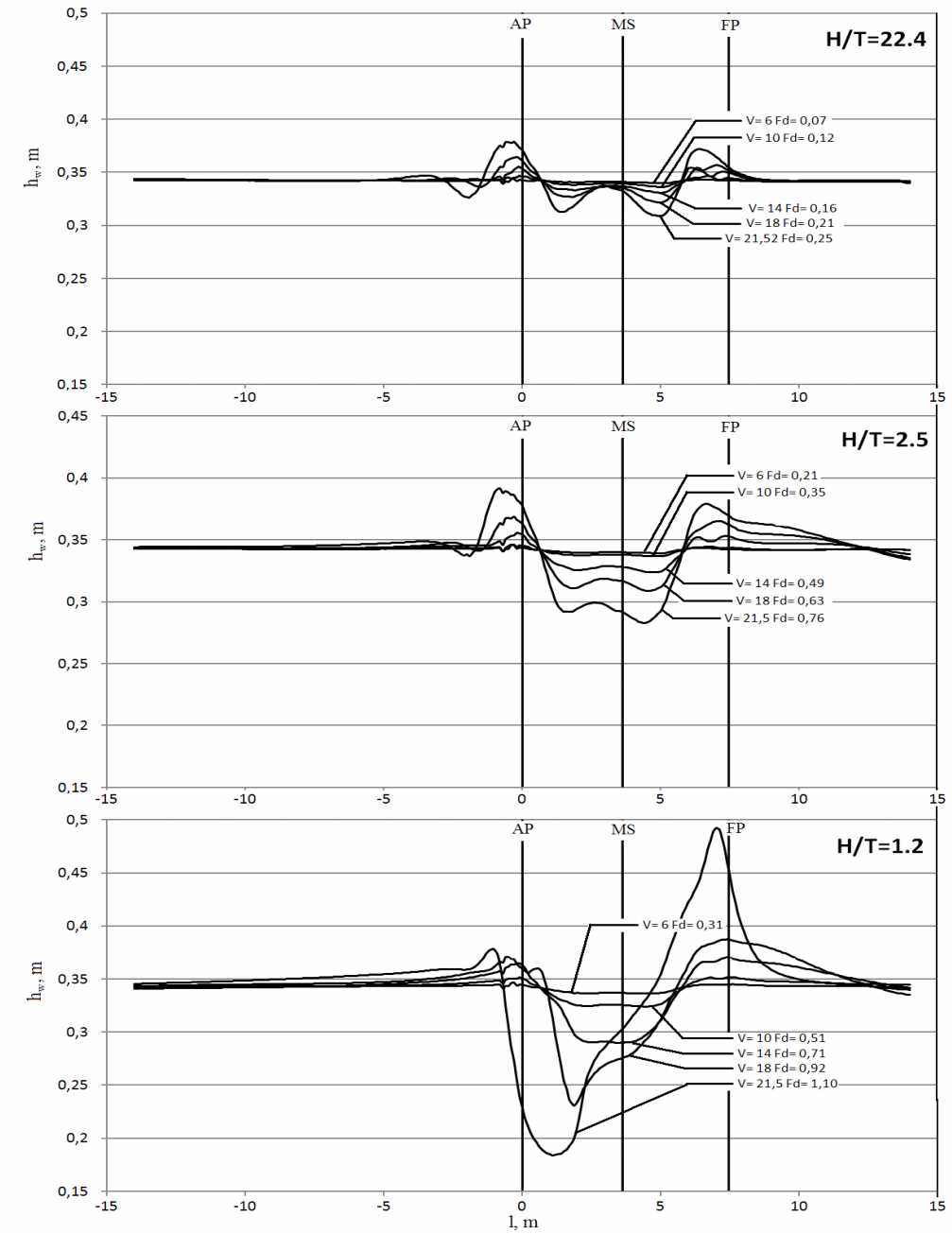

Fig. 8. Wave profiles on model ship board calculated using Fluent for different speed and *H*/*T* values; *AP* – aft perpendicular, *MS* – midship, *FP* – fore perpendicular, *l* – length of domain, h_w – wave height, F_d – depth Froude number

5. Conclusions

The comparison presented above shows the influence of the water depth and ship speed on the squat and wave profile.

In general the calculated wave pattern and wave profile agree qualitatively with observation and with wave theory.

Wave heights are strongly affected by depth to draft ratio.

It seems that the length of domain in calculations of the wave pattern in shallow water should be lengthened in front of the ship.

The computed values of the ship squat were in the range between 0.2 and 0.8m for real ship speed in shallow water.

The comparison of the calculated and measured results shows that:

- the empirical method of Hooft and mean of all empirical methods agree well with the results obtained using Fluent,
- the agreement between present calculations and the empirical methods of Hooft and Eryuzlu was confirmed also by the real experiment data using GPS [2, 3].

The results of the research presented above demonstrate that Fluent can be effectively used for prediction of ship squat in shallow water, but further investigation of restricted waters effect and irregular channel bottom effect is necessary.

References

[1] *FLUENT Tutorial Guide*, Fluent Inc., 2001.

[2] Gucma L., Gucma M., Schoeneich M.: *Weryfikacja modeli określania osiadania statku w ruchu za pomocą badań rzeczywistych na torze wodnym Świnoujście-Szczecin*, Proceedings of the 15-th International Scientific and Technical Conference, Gdynia, Poland, 2006.

[3] Gucma L., Schoeneich M.: *Określanie niepewności metod osiadania na podstawie badań rzeczywistych przeprowadzonych na promie M/F Jan Śniadecki w Porcie Świnoujście*, Praca naukowo-badawcza.

[4] Jałoszyński T.: *Analiza oporu i opływu kontenerowca metodami numerycznej mechaniki płynów.* Politechnika Gdańska, Wydział Oceanotechniki i Okrętownictwa, Katedra Teorii i Projektowania Okrętów, Gdańsk, 2005.

[6] Kraskowski M., Bugalski T.: *CFD and EFD tools for ship flow prediction*, Hydronav 2005, Gdańsk-Ostróda, Poland, 2005.

[7] Kulczyk J., Zawiślak M.: *Determination of suction coefficient and propeller disk velocity field by means of Fluent system*, Hydronav 2003, Gdańsk, Poland, 2003.

Ocena osiadania statku na wodzie płytkiej przy użyciu metod numerycznej mechaniki płynów

W ostatnich latach przeprowadzone zostały liczne badania mające na celu identyfikacje sił hydrodynamicznych działających na manewrujący statek na akwenach portowych przystoso-

wanych dla dużych statków. Problemy związane z bezpieczeństwem nawigacji na tych akwenach odgrywają ważną rolę w projektowaniu akwenów i są przedmiotem badań organizacji morskich. U podstaw jakiejkolwiek nawigacji i analizy projektów leży odpowiednie określenie sił hydrodynamicznych generowanych przez kadłub poruszający się na wodach ograniczonych. Analiza ta powinna zawierać przede wszystkim efekt osiadania, poziome ograniczenia kanałów, dna akwenów, oddziaływania kadłubów mijających się statków itp. Jest więc oczywiste, że do badań w tej dziedzinie stosuje się zaawansowane metody numerycznej mechaniki płynów. Artykuł zawiera wstęp do problemu modelowania efektów wody ograniczonej przy użyciu komercyjnego programu Fluent.

ARCHIVES OF CIVIL AND MECHANICAL ENGINEERING

Vol. VIII 2008 No. 1

Stability of ships: risk assessment due hazards created by forces of the sea

LECH KOBYLIŃSKI
Foundation for Safety of Navigation and Environment Protection, 14-200 Iława-Kamionka

The crucial point in safety assessment is identification of all hazards the ship may be subjected. The most important hazards are those that are created by the forces of the sea. Simple criterion that takes into consideration forces of the sea is weather criterion included in the IMO Intact Stability Code. The author suggests to take account of all hazards posed by forces of the sea when performing risk analysis. For this purpose those hazards should be decomposed into hazardous situations and further in a number of possible capsizing scenarios. As an example fault tree and event tree for parametric resonance in following waves are shown. The trees could be used for evaluation of probabilities of capsizing.

Keywords: *ship's safety, risk analysis, stability of ship, hazard identification, stability in a seaway*

1. Introduction

In the paper presented to Hydronav'07 [16] the author provided a list of hazards to stability identified using various available methods, first of all basis of the analysis of a number of LOSA accidents. Hazards posed by forces of the sea belong to the most serious hazards to safety against capsizing. Although capsizing is an accident that rarely is caused by one single event and in most cases is a sequence of events starting from, sometimes small, initiating event, forces of the sea play important part in this sequence contributing to the end result. Therefore most stability criteria in one way or another take into consideration forces of the sea as most important factor contributing to loss of stability accident. Loss of stability accident, or LOSA, is defined as an accident when the ship capsizes and is foundering but also when it develops heel or list so large, that further operation of the ship becomes impossible and it has to abandoned although it may be not necessarily lost.

2. Present prescriptive requirements that take into account forces of the sea

The present set of stability criteria that are inherent part of the IS Code (obligatory from 2009 by reference in the amended SOLAS convention) [14] includes consideration of the forces of the sea in the form of "weather criterion". Weather criterion was originally adopted as recommendation by Resolution A.562 (14) [11].

The idea behind the weather criterion is to check whether the ship will stand combined effect of side wind and rolling in waves. The following assumptions are adopted:

- the ship is exposed to the beam steady wind with wind force acting horizontally perpendicular to the plane of symmetry and the wind heeling arm is l_{w1},
- the ship is rolling in waves around the heeling angle φ_0 due to steady wind. Amplitude of rolling is equal φ_1 to windward side. Angle of heel due to steady wind should not be larger than 16° or 80% of an angle of deck immersion, whichever is smaller,
- in this situation the ship is subjected to dynamical wind heeling moment l_{w2},
- the area *b* should be equal or greater from area *a* (Figure 1).

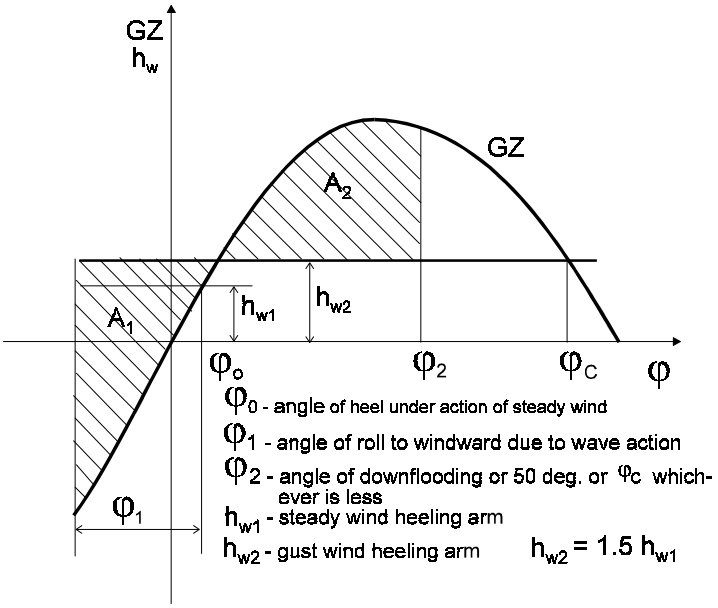

Fig. 1. Weather criterion as in the IS Code

Scenario adopted in development of the weather criterion is based on situation that vessel is exposed broadside to the wind and waves. The structural model adopted is simplified physical model of the behaviour of a ship rolling in beam seas including wind-heeling moment. Adoption of the described prescriptive requirement and structural model was possible only because it was based on statistical evaluation of data for ships capsized and operated safely during the long time of the first formulation of the criteria in 1947 [18]. The crucial element of the criterion, the value of wind pressure was adopted in such a way, that the resulting critical KG value would correspond to average KG values of the population of vessels existing at the time of development of the criterion that were considered safe in operation. Trial calculations shows that the majority of existing at that time ships satisfied adopted weather criterion.

Immediately after weather criterion was adopted it was criticized because of the simplifications and because it was based on the experience with ships of older con-

struction and hull parameters that were in many cases different from those used in more modern design. This caused, that IMO started consideration of possibility to develop improved, or, as it was called at that time, "rational" stability criteria. One possibility of the development of improved criteria is to apply risk analysis.

3. Risk analysis

Recommendation on the application of risk analysis to the rule making process was included in the IMO resolution MSC/Circ 1023 [13]. IMO recommended using Formal Safety Assessment (FSA) methodology, which is risk analysis but formalized.

Risk analysis in rule making process is an alternative to prescriptive requirements. The basic dichotomy between risk based criteria and prescriptive criteria was discussed by the author in other papers [15–16], where also advantages and disadvantages of both approaches were presented

When applying the risk analysis probability of capsizing should be assessed on the basis of structural models applicable to different scenarios of capsizing, on the basis of model tests and on the basis of detailed analysis of loss of stability accidents at sea.

When considering risk of capsizing due to forces of the sea the recommended FSA methodology has to be adjusted according to the specific features of the problem in question. Figure 2 shows block diagram of the risk-based approach for this case.

4. Hazard identification and capsizing scenarios

The main task in the risk analysis in application to hazards caused by forces of the sea is identification of hazards. According to the definition hazard is the situation with the potential of accident to happen. Hazards could be identified using several different methods [16].

General guidance on the methodology of hazard identification is provided by IMO resolution [13]. The IMO SLF Subcommittee discussed hazardous situations for the ship in a seaway that may lead to capsizing in the years 1970–1985 at the time when development of "rational" stability criteria intended to supersede existing statistical criteria and weather criterion was considered [10]. The Subcommittee at that time expressed the opinion that the most serious hazardous situations for the ship in a seaway are:

- in beam sea with wind gusts,
- in following sea, with pure loss of stability and possibility of parametric resonance,
- in quartering sea in conjunction with broaching.

Situation where the ship may experience parametric resonance in head sea was not considered as important. The danger involved in this situation was seriously considered after the accident of container vessel C11 had been analyzed [9], although even earlier parametric resonance in head seas was observed [4]. More recently situation of

meting freak wave was added to hazardous situations requiring consideration [1–2], [7–8]. Also breaking waves that caused capsizing of the fishery research vessel HELLAND HANSEN [5] should be taken into consideration.

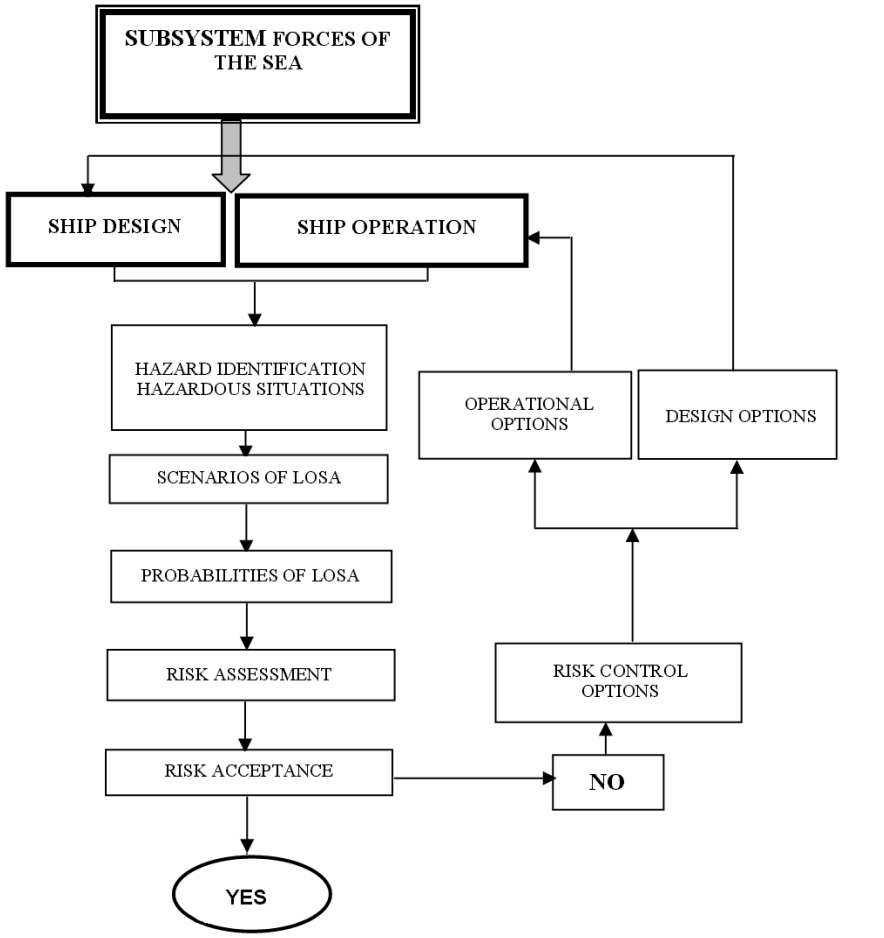

Fig. 2. Block diagram for risk assessment due to hazards created by forces of the sea

In each hazardous situation different capsizing scenarios may develop. Capsizing scenario is the sequence of events leading ultimately to capsizing or, more general, to LOSA accident. Many scenarios of capsizing were identified, mainly based on detailed description of accidents and also on observations of the capsizing of models tested in towing tanks or in open waters in waves. Experts opinions contributed greatly to the creative part of identification of scenarios where operational aspects and human performance played important part. Block diagram in Figure 3 shows hazardous situations and possible capsizing scenarios identified taken from various sources [6], [17].

This should be considered as an example; in reality certainly the number of scenarios may be larger.

5. Probability of capsizing

Risk analysis and development of risk based criteria requires estimation of probability of capsizing in various dangerous situations simulating respective capsizing scenarios. Belenky [1] suggested to apply "vulnerability criteria" consisting of assessment whether particular situation and scenario is relevant for the design considered or not. However the problem is not that simple, because, if under vulnerability criteria hazardous situations and capsizing scenarios are understood, there is necessary to estimate probability of occurring such scenario for the particular ship. This depends not only on the design features of the ship, but also on operational aspects.

Once the probability of occurring dangerous situation is estimated, the probability of capsizing in this situation should be calculated. Constructing event trees or fault trees could do this.

Frequencies of hazards could be assessed on the basis of risk contribution trees (RCT) being a set and combination of all fault trees and event trees as defined below.

A fault tree is a logic diagram showing the casual relationship between events, which singly or in combination occur to cause the occurrence of higher-level event. It is used to determine the probability of the top event. Fault tree is top-down procedure systematically considering the causes and events at levels below the top event. An event tree is logic diagram used to analyse the effect of an accident, a failure or an unintended event. The diagram shows the probability or frequency of the accident linked to those safeguard actions required to be taken after occurrence of the event to mitigate or prevent escalation. An event tree is down-top procedure starting from the undesired event and leading to possible consequences.

One or more events from the lower level must be present in order to cause the event in upper level happens. Those events are then connecter with the functor (gate) "AND". If only one of two or more events in the lower level is necessary to cause upper event to happen, then those events are connected with gate "OR". An example of fault tree where the primary event is parametric resonance is shown in Figure 4. Those functors or gates mean addition or multiplication of probabilities when calculating the probability of upper level event.

As it seen from Figure 4 three events must happen in order to cause parametric resonance: ship parameters, heading and direction of waves. Only one of them depends on design. Therefore even if the events in the lover levels of the fault tree are neglected, assessment of the probability of parametric resonance could only be estimated on the basis of organized experts opinion (e.g. using Delphic method).

Event tree is constructed assuming that parametric happens and then possible consequences are investigated. Figure 5 shows simplified event tree for the scenario of parametric resonance in following seas. The important event in this tree is operational factor, i.e. the decision of the master.

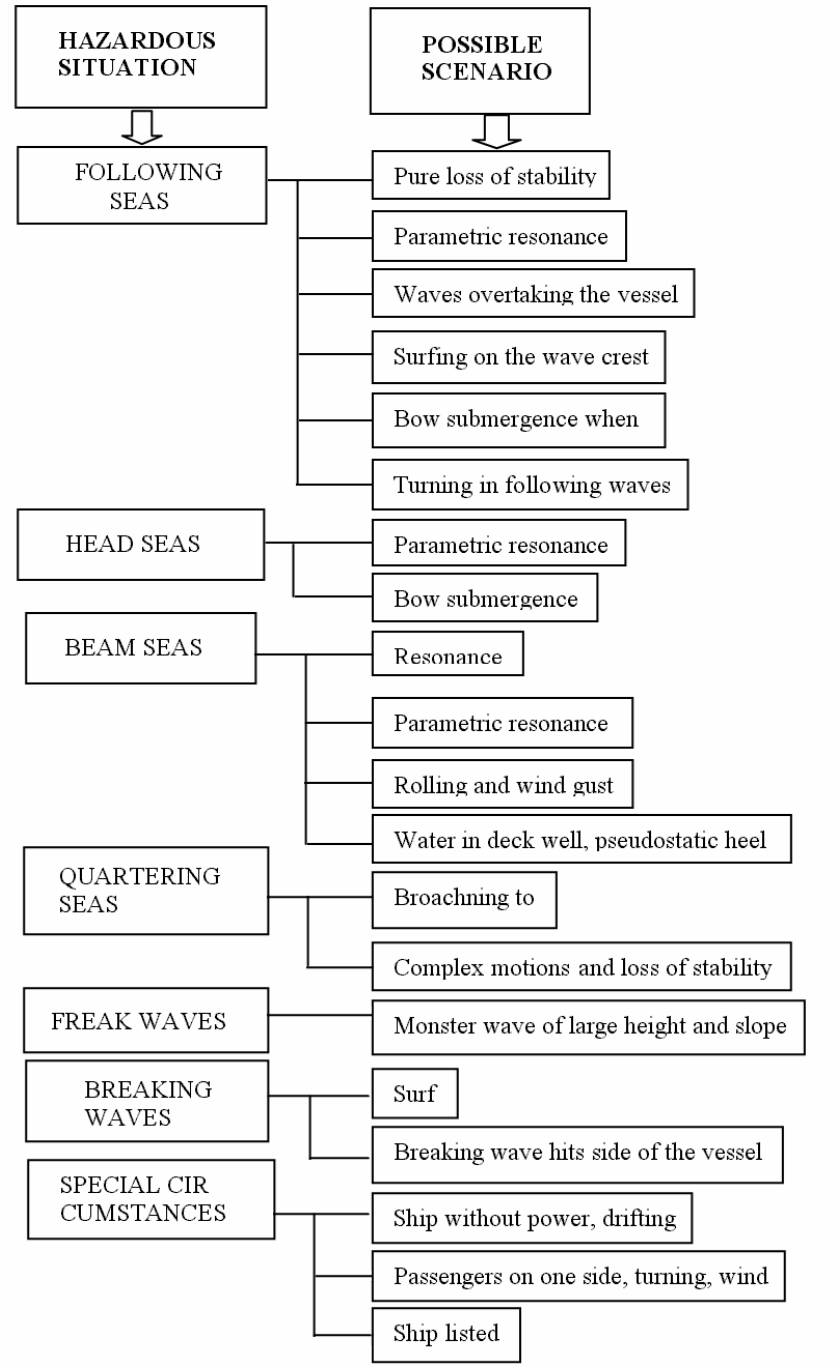

Fig. 3. Schematic presentation of hazardous situations and possible scenarios of capsizing

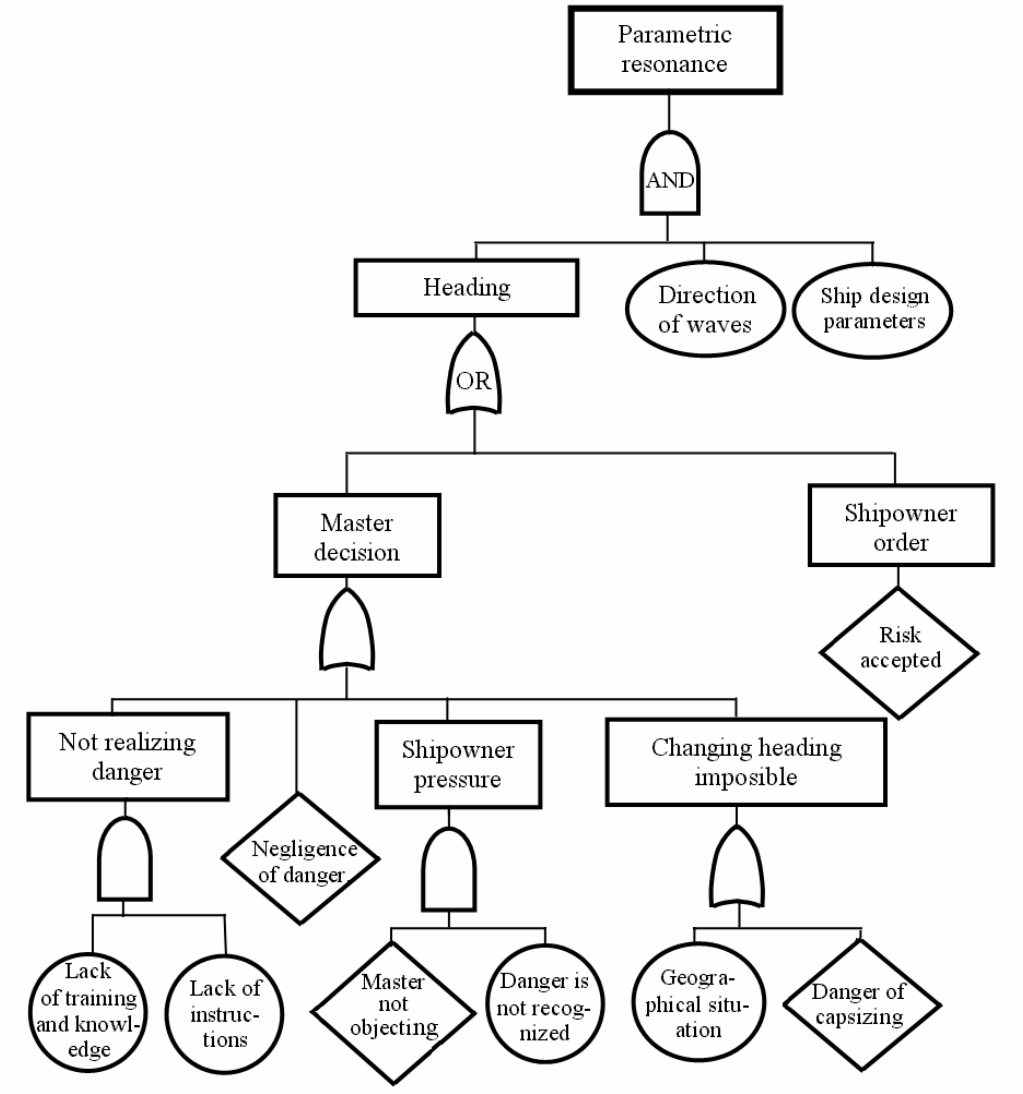

Fig. 4. Fault tree for parametric resonance

The basic probability of capsizing not taking into account operational aspect could be calculated in many cases using structural formulae or numerical simulation provided computer codes are available. However this is not the probability that has to be taken in further risk assessment. The probabilities related to operational factors could be only estimated by evaluation by experts on the basis of experience, statistics etc. In the case of parametric resonance it is rather improbable, that observing increasing amplitudes of rolling in following seas the master will take no action at all. Operational

guidance, as e.g. [12] provide necessary guidance in this respect. There is also possibility of installing barriers that will force the master to take action. All this is possible within methodology of risk analysis.

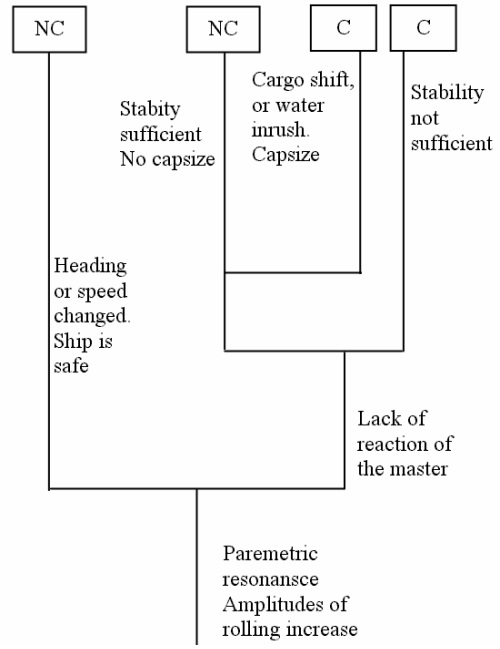

Fig. 5. Event tree for parametric resonance

6. Conclusions

As the majority of existing ships satisfying stability criteria included in the revised IMO Intact Stability Code are reasonably safe this code could be used as the main instrument to assure safety of ships against capsizing. In those cases where maritime administrations, ship owners or designers consider those criteria inadequate, risk analysis should be performed. Within risk analysis all hazards relevant to the particular ship must be taken into consideration. The most important hazards are hazards created by forces of the sea. The way, how the risk analysis could be performed is shown on an example of parametric resonance in following seas.

References

[1] Belenky V., de Kat J.O., Umeda N.: *Towards performance-based criteria for intact stability*, To be published in Marine Technology, 2007.
[2] Buckley W.H.: *Extreme and climatic wave spectra for use in structural design of ships*, Naval Engineers Journal, 1988.

[3] Buckley W.H.: *Critical capsizing conditions in survivability seaways*, International Conference Design and Operation for Abnormal Conditions, RINA, Glasgow, 1997.
[4] Burcher R.K.: *Experiments into the capsize of ships in head seas*, 4th STAB Conference, Naples, 1990.
[5] Dahle E.A., Kjaerland O.: *The capsizing of M/S HELLAND HANSEN*, Transactions RINA, 1979.
[6] de Kat O., Brouwer R., McTaggart K., Thomas, W.L.: *Intact ship survivability in extreme waves: new criteria from research and navies perspective*, STAB'94, Conference, Melbourne, Florida, 1994.
[7] Faulkner D., Buckley W.H.: *Critical survival conditions for ship design. Design and Operation for Abnormal Conditions*, International Conference, Glasgow, 1997.
[8] Faulkner, D., Williams, R.A.: *Design for abnormal wave climates*, RINA Spring Meeting, 1996.
[9] France W.N., Levadou M., Treakle T.W., Paulling J.R., Michel R.K., Moore C.: *An investigation of head sea parametric rolling and its influence on container lashing systems*, SNAME Annual meeting, 2001.
[10] IMO: *Intact Stability*, Report of the ad hoc working group. Doc. SLF29/WP.7, 1984.
[11] IMO: *Recommendation on Resolution A.562*, No. 14, 1987.
[12] IMO: *Guidance to the master for avoiding dangerous situations in following and quartering seas*, Doc. MSC/Circ.707, 1995.
[13] IMO: *Guidelines for Formal Safety Assessment (FSA) for use in the IMO rule-making process*, Doc. MSC/Circ.1023; MEPC/Circ.392, 2002.
[14] IMO: *Subcommittee on Stability, subdivision and Safety of Fishing Vessels*, Report of 50th session. Doc.SLF 50/WP.6, 2007.
[15] Kobyliński L.: *Appraisal of risk assessment approach to stability of ships*, International Workshop on Ship Stability, Istambul, 2005.
[16] Kobyliński L.: *Stability of ships: Risk assessment due to hazards created by forces of the sea*, Hydronav Intern. Conference, 2007.
[17] Kobyliński L.: *Capsizing scenarios and hazard identification*, 8th International STAB Conference, Madrid, 2003.
[18] Register of Shipping of the USSR: *Interim standards of stability for merchant sea-going vessels and coasters*, Morskoj Transport, Moscow, 1948.

Stateczność statku: ocena ryzyka w stosunku do zagrożeń spowodowanych siłami morza

Podstawowym elementem w analizie bezpieczeństwa jest identyfikacja zagrożeń. Najbardziej istotnymi zagrożeniami dla bezpieczeństwa statecznościowego statku są zagrożenia wywołane siłami morza. Proste kryterium uwzględniające to zagrożenie, znane pod nazwa kryterium pogody, znajduje się w Kodeksie Stateczności IMO. Autor proponuje uwzględnienie wszystkich zagrożeń wywołanych siłami morza przy wykonywaniu analizy ryzyka.. W tym celu należy dokonać dekompozycji tego zagrożenia na szereg sytuacji zagrażających a następnie te sytuacje dekomponować na możliwe scenariusze przewrócenia się statku. Jako przykład podano drzewa błędów i zdarzeń dla przypadku scenariusza polegającego na wystąpieniu rezonansu parametrycznego na fali nadążającej. Drzewa te mogą być wykorzystane dla określenia prawdopodobieństwa przewrócenia się statku.

ARCHIVES OF CIVIL AND MECHANICAL ENGINEERING

Vol. VIII 2008 No. 1

A computer system for the complete design of ship propellers

TADEUSZ KORONOWICZ, PATRYK CHAJA
The Szewalski Institute of Fluid-Flow Machinery PASci, ul. Fiszera 14, 80-952 Gdańsk

JAN SZANTYR
Gdansk University of Technology, ul. Narutowicza 11/12, 80-952 Gdańsk

The integrated computer system presented in this paper is capable of conducting the complete design calculations of ship propellers, including their analysis in the conditions of a real inflow velocity field behind the ship hull.
The system enables solution of the following tasks:

- calculation of the scale effect on the velocity field in the area of propeller operation,
- correction of this velocity field due to the presence of the rudder,
- maximization of the propeller efficiency,
- optimization of the propeller blade geometry on the basis of the cavitation and strength requirements,
- optimization of the propeller number of blades and of the blade geometry on the basis of the level of induced pressure pulses and unsteady bearing forces.

The computer system contains numerous options for visualization of the input data and the results of calculations.

Keywords: *ship propellers, design methods, computational fluid dynamics*

1. Introduction

The process of ship propeller design leads to the determination of the propeller geometry on the basis of an optimum compromise fulfillment of several, often conflicting, requirements:

- suitable strength of the blades,
- possibly high propeller efficiency,
- lack of cavitation or cavitation limited to a harmless level, not leading to vibration, noise etc.,
- acceptable level of pressure pulses induced on the hull surface,
- acceptable level of the unsteady bearing forces.

In order to fulfill the above requirements, the designer should be equipped not only with the high quality basic propeller design program and with information about the radial distribution of the circumferentially averaged inflow velocity field, but he should know the details of the three-dimensional non-uniform design velocity field and he should be equipped with a suitable program for the analysis of all aspects of unsteady propeller operation in this velocity field. Consequently, the complete design system should incorporate 3 mutually interacting computer programs:

- program for the determination of the design velocity field,
- program for the basic propeller design,
- program for the analysis of propeller operation in the design velocity field.

In the design practice of the past all three above listed computer programs were used independently and the transfer of data between them required manual corrections of the data files. The system described in this paper is fully integrated and it can perform complete design calculations under supervision of the designer without any necessity for manual modification of the data files. The system is equipped with many graphical procedures, which enable control of the input data and calculation results. The correction of propeller geometry at the intermediate stages of the design development may be made directly from the computer screen.

2. The design velocity field

The standard model experiments usually supply the so called nominal velocity field behind the ship hull, excluding the scale effect, propeller operation effect and presence of the rudder. Accurate determination of the true design velocity field at propeller location requires complicated calculations, taking into account all the above listed effects. The suitable calculation procedure based on the Computerized Model Basin (CMB) "PANSHIP" is presented below.

2.1. The discretization of the ship hull

The system is equipped with the specially developed procedure for easy discretization of the ship hull, i.e. representation of its geometry be a set of flat quadrilateral panels. The scaling of the velocity field behind the hull does not require very dense discretization. Experience shows that the application of 60 panels along the hull and 20 panels around the half-frame is fully sufficient. The standard definition of hull geometry, shown in Figure 1 is quite adequate for this purpose.

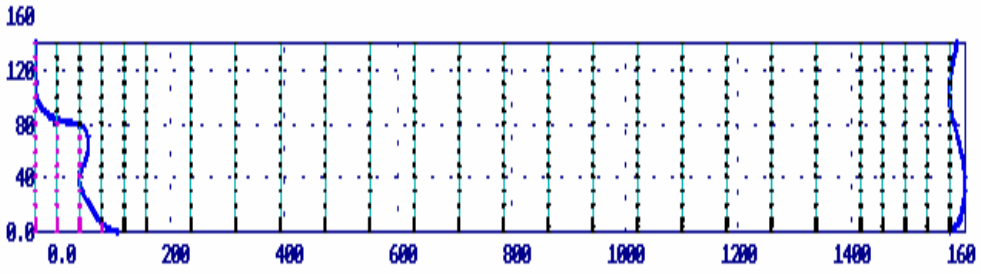

Fig. 1. The standard frame division of the ship hull

The discretization of the ship hull surface is performed automatically and it may be controlled and if necessary further corrected from the computer screen. An example of

the discretized hull of a general cargo ship is shown in Figure 2. Such discretized hull, including similarly discretized rudder, is the basic input data for the CMB "PAN-SHIP".

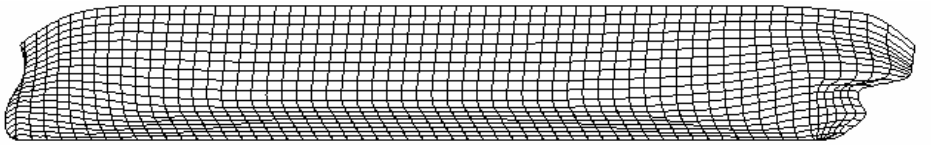

Fig. 2. The discretized ship hull

2.2. The Computerized Model Basin "PANSHIP"

The development of the CMB "PANSHIP" [1] was started in the 1990s as the computational fluid dynamics program for determination of the ship hull flow, including free surface and water viscosity effects. At the present stage of development "PANSHIP" is unable to perform an independent prediction of the propeller design velocity field with acceptable accuracy, but it can be used effectively for the determination of the scale effect, the effect of the propeller operation and the effect of rudder or other appendages on this velocity field. Consequently, a procedure for prediction of the full scale propeller design velocity field based on CMB was developed [3]. An input to this procedure consists of the following:

- the nominal velocity field measured in typical model scale experiments,
- the discretized hull geometry,
- the discretized rudder geometry,
- the propeller geometry and its operating parameters.

The main result of calculations is the full scale propeller design velocity field.

2.3. The scale effect

The calculation of the velocity field in "PANSHIP" may be performed at an arbitrary scale. The scale coefficient is one of the input parameters. Figures 3–5 show the differences in the computed velocity field for the ship model having length of 6.52 m

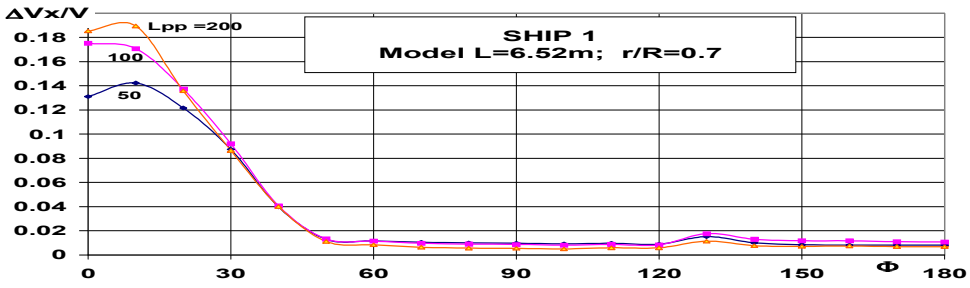

Fig. 3. Axial component of the nominal velocity field calculated for the model and for the geometrically similar full scale ships of different lengths

and for geometrically similar full scale hulls of different lengths. Analysis of these diagrams shows that the scale effect corrections can not be represented accurately by simple formulae and they should be determined using special calculation procedures.

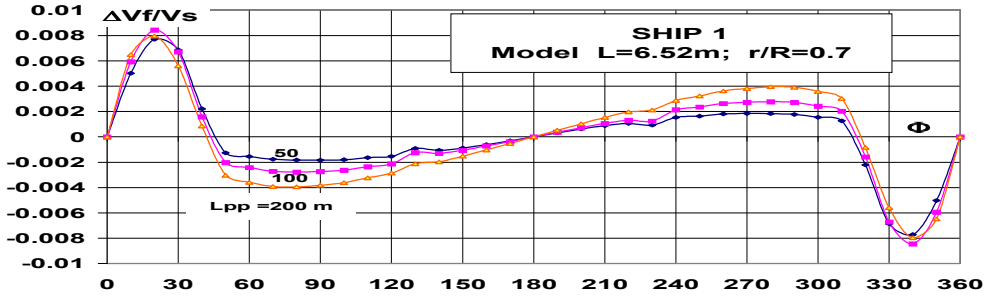

Fig. 4. Tangential component of the nominal velocity field calculated for the model and for the geometrically similar full scale ships of different lengths

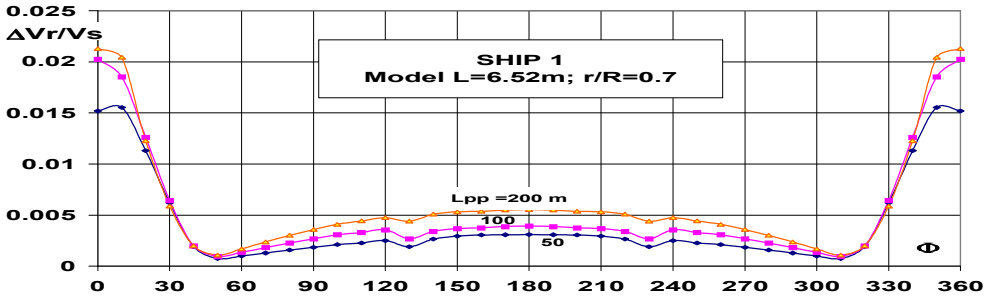

Fig. 5. Radial component of the nominal velocity field calculated for the model and for the geometrically similar full scale ships of different lengths

2.4. The influence of the rudder

The calculations performed using “PANSHIP” demonstrate a visible effect of the rudder on the propeller design velocity field. This effect is present not only in the three-dimensional non-uniform velocity field but also in the radial distribution of the

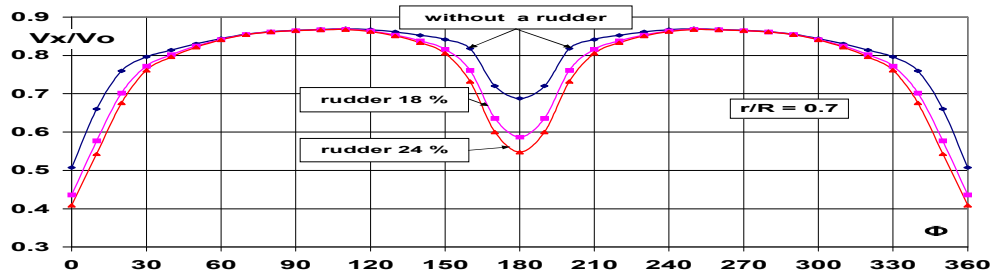

Fig. 6. Axial component of the nominal velocity field calculated without a rudder and with rudders of different thickness

circumferentially average axial component of this field, which is an essential element of the input data in the basic propeller design (cf. Figures 6–9). This means that either the model measurements of the nominal velocity field should be performed with rudder or the appropriate correction, taking into account the influence of the rudder, should be introduced through appropriate calculations based on "PANSHIP".

Fig. 7. Tangential component of the nominal velocity field calculated without a rudder and with rudders of different thickness

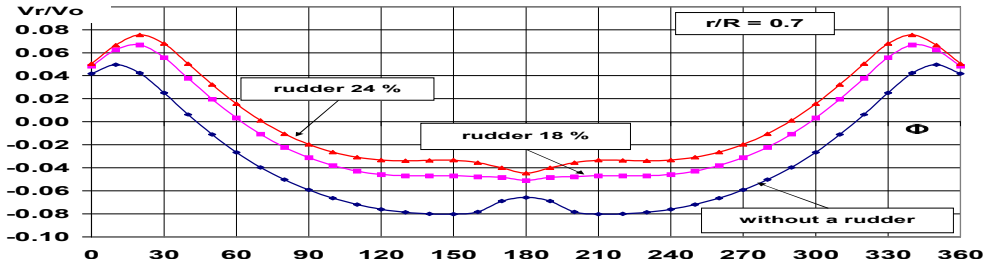

Fig. 8. Radial component of the nominal velocity field calculated without a rudder and with rudders of different thickness

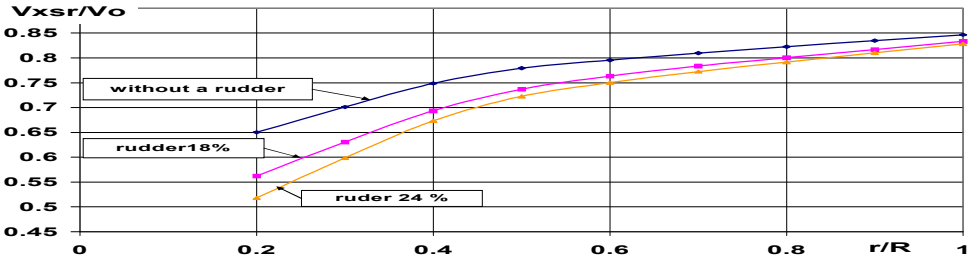

Fig. 9. Radial distributions of the circumferentially averaged axial velocity calculated without a rudder and with rudders of different thickness

2.5 The influence of the propeller operation

The influence of the propeller operation on the design velocity field may be determined through appropriate calculations, provided they are based on suitable interpre-

tation of the Biot Savart formula [4]. In order to verify the accuracy of such a prediction, calculations were performed for full scale ships for which the results of appropriate measurements were available. The results presented in Figures 10 and 11 show qualitative agreement between computations and measurements. The degree of quan-

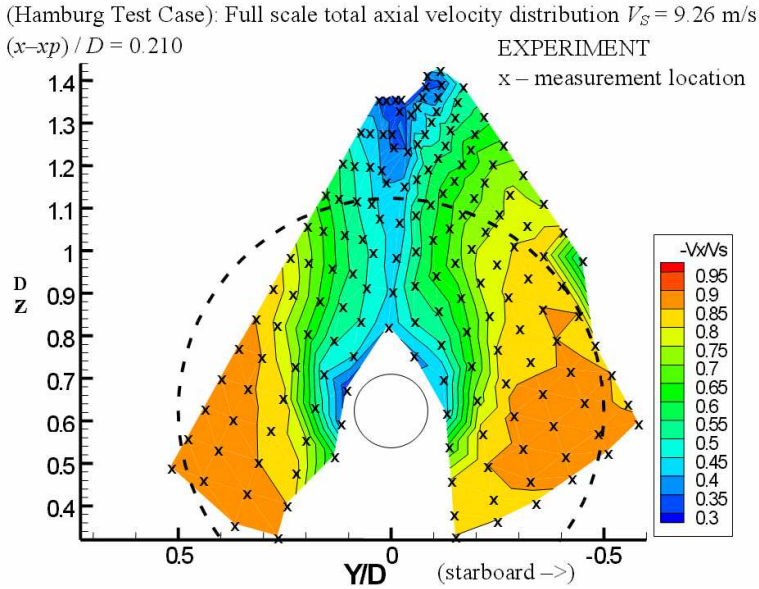

Fig. 10. Axial component of the velocity field measured on full scale ship with operating propeller

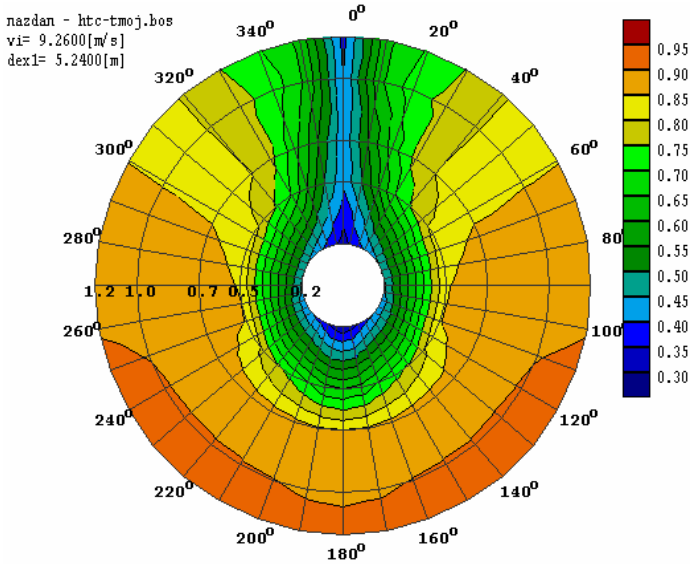

Fig. 11. Axial component of the velocity field calculated for a full scale ship with operating propeller

titative agreement may be assessed more closely from the velocity distribution at a specific radius of the propeller, as shown in Figure 12. These results confirm the ability of "PANSHIP" to predict accurately the effect of propeller operation on the design velocity field.

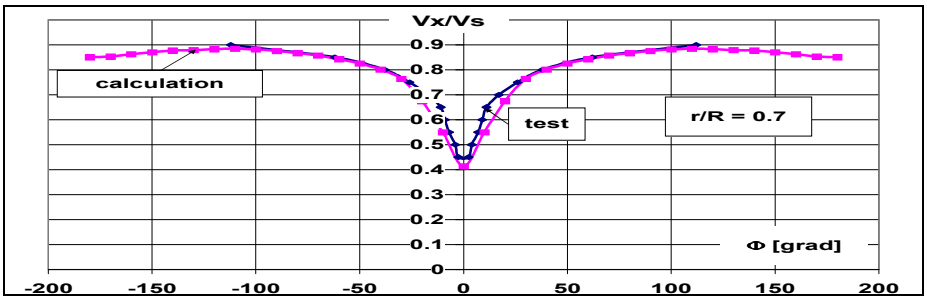

Fig. 12. Comparison of the measured and calculated axial velocity component on the radius r/R=0.7 for a full scale ship with operating propeller

3. The basic propeller design program

In the system described in this paper an extensively verified computer program based on the vortex lifting surface theory is used for the basic propeller design. The initial phase of the design calculation is performed using lifting line model according to Lerbs. The final geometry of the propeller blade is determined using the lifting surface model, composed of vortex elements representing blade loading and source elements representing the blade thickness, as shown in Figure 13.

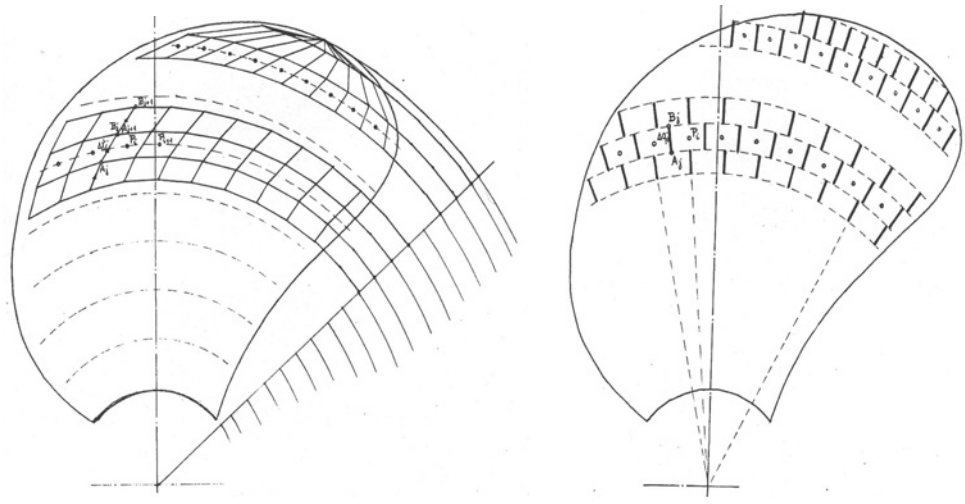

Fig. 13. Scheme of the vortex grid and the source grid of the lifting surface model

The results of lifting surface calculations have the form of corrections determining the final distributions of propeller blade pitch and mean line camber. These corrections, developed by T. Koronowicz [2], are the functions of radius, number of blades, hydrodynamic pitch angle, blade area coefficient and hydrodynamic loading distribution along the chord. The results of the basic design calculation include:

- blade outline described by the blade section chord lengths,
- blade pitch described by the pitch coefficients,
- blade mean line camber,
- blade thickness.

4. The program for analysis of propeller operation in the non-uniform inflow velocity field

The program for analysis of propeller operation is based on the unsteady deformable lifting surface theory [5]. This theory integrates the vortex lifting surface with the unsteady sheet cavity. The presence of the sheet cavity is treated as the time-dependent deformation of the blade geometry. The idea of this original approach is explained in Figure 14, where the dynamic boundary condition on the cavity surface leads to determination of the local velocity of cavity expansion or collapse. This process of dynamic cavity expansion (or collapse) is modeled by the additional distribution of sources (or sinks) on the lifting surface. The deformation of the original geometry of the lifting surface due to sheet cavity is included in the kinematic boundary condition on this surface.

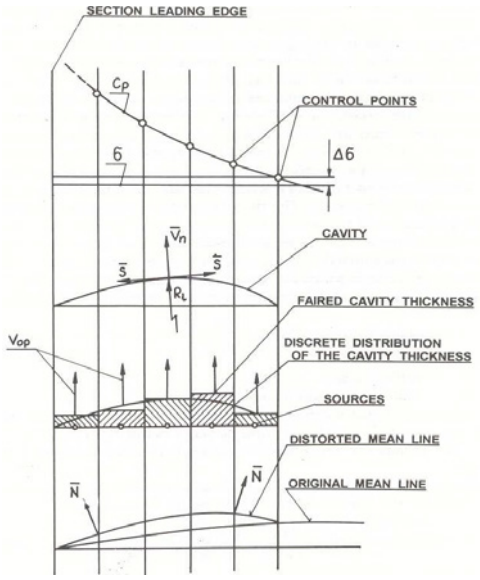

Fig. 14. The model of unsteady sheet cavitation on the propeller blade section

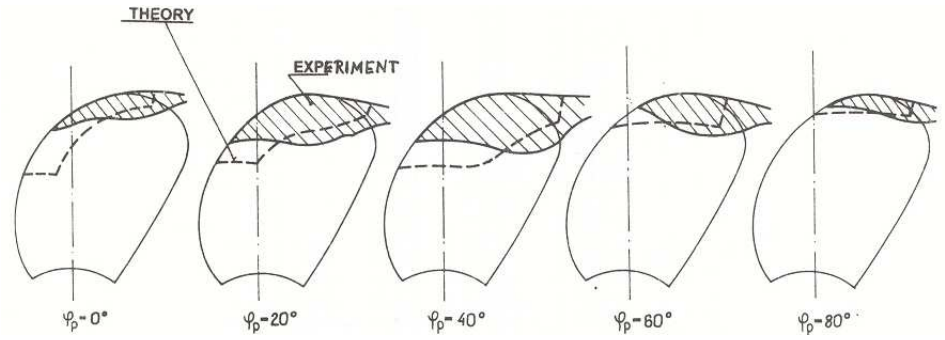

Fig. 15 Comparison of the calculated and observed time-dependent sheet cavity extent

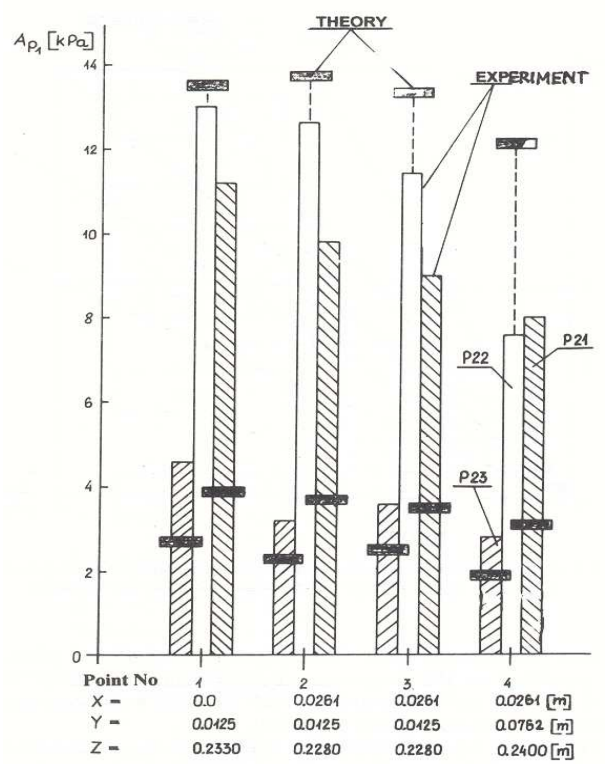

Fig. 16. Comparison of the calculated and measured propeller-induced pressure pulses

The program is able to detect the inception and describe the development of sheet, vortex and bubble cavitation on the propeller blade. It also calculates the pressure pulses induced by the cavitating propeller in the surrounding space (including ship hull) and the unsteady hydrodynamic bearing forces on the propeller shaft. Examples of calculations compared with appropriate experimental measurement results are shown

in Figures 15 and 16. The propeller-induced pressure pulses are presented in the form of harmonic amplitudes starting with the blade frequency. In Figure 16 the first harmonic amplitude is shown for four points on the hull and for three different propellers P21, P22 and P23 designed for the same hull. Despite visible differences between calculations and measurements the program can distinguish correctly between "good', "bad" and "average" propeller design.

5. Conclusion

The integrated computer system for complete design of ship propellers has been presented. This system consists of three main programs enabling: prediction of the design velocity field behind ship hull, calculation of the basic propeller design and effective multi-criterial optimization of the propeller on the basis of a thorough analysis of propeller operation in the non-uniform velocity field. All three programs have been extensively validated experimentally and the accuracy of produced results ensures high quality of the propeller designs developed using this system. New and original feature of the system is its ability to determine scale effect, rudder effect and propeller operation effect on the design velocity field. Future development of the system may include introduction of the fully automatic optimization procedure, based for example on the genetic algorithm approach.

References

[1] Bugalski T., Koronowicz T., Szantyr J., Waberska G.: *Computer System for Calculation of Flow, Resistance and Propulsion of Ship at the Design Stage*, CADMO'94 Southampton, 1994.
[2] Jarzyna H., Koronowicz T., Szantyr J.: *Design of Marine Propellers*, Maszyny Przepływowe, t. 20, Ossolineum, 1996.
[3] Koronowicz T., Tuszkowska T., Wacławczyk T.: *A computer method for prediction of the velocity field behind a full-scale ship hull*, Polish Maritime Research, Vol. 10, No 1, 2003.
[4] Koronowicz T., Krzemianowski Z.: *Investigations of influence of screw propeller operation on water flow around stern part of ship hull*, Polish Maritime Research, Vol. 14, No. 1, 2007.
[5] Szantyr J.A.: *A Method for Analysis of Cavitating Marine Propellers in Non-uniform Flow*, Intern. Shipbuilding Progress, Vol. 41, No. 427, 1994.

System komputerowy do kompleksowego projektowania śrub okrętowych

Zintegrowany system komputerowy przedstawiony w referacie pozwala na przeprowadzenie kompleksowych obliczeń projektowych śrub okrętowych połączonych z analizą ich pracy w rzeczywistym polu prędkości za kadłubem statku. System umożliwia rozwiązanie następujących zadań:

- określenie wpływu efektu skali na pole prędkości w miejscu pracy śruby,
- skorygowanie tego pola ze względu na wpływ steru,
- maksymalizację sprawności śruby,
- optymalizację geometrii skrzydła śruby na podstawie wymagań kawitacyjnych i wytrzymałościowych,
- optymalizację liczby skrzydeł śruby i ich geometrii na podstawie poziomu indukowanych pulsacji ciśnienia i zmiennych sił łożyskowych.

Opisany system komputerowy posiada wiele możliwości wizualizacji danych wejściowych i wyników obliczeń.

ARCHIVES OF CIVIL AND MECHANICAL ENGINEERING

Vol. VIII 2008 No. 1

Recent developments in the field of ship hydrodynamics at the Ship Laboratory of Helsinki University of Technology

J. MATUSIAK, T. MIKKOLA
Helsinki University of Technology, Ship Laboratory, Tietotie 1, 02150 Espoo, Finland

Some recent developments in the fields of ship hydrodynamics, stability and hydroelasticity at the ship laboratory of Helsinki University of Technology are briefly described.

Keywords: *PIV, CFD, hydroelasticity*

1. Introduction

Helsinki University of Technology (TKK) is the main and largest university of technology in Finland. It was founded in 1849 and received university status in 1908. The university employs about 250 professors with a total staff of around 3600. The combined number of students, including post-graduate students, is roughly 15000. The Ship Laboratory belongs to the Faculty of Mechanical Engineering. It provides degrees and carries out research in naval architecture including ship design and ship structures, marine engineering, hydrodynamics, arctic marine technology and maritime safety. At present, the Ship Laboratory employs four professors and a permanent staff of roughly 20 persons consisting of research scientists and technical staff. Additionally the laboratory employs about 5 graduate students and 10 post graduate students.

About 50% of the laboratory's budget is obtained from national funding. The rest of the budget is covered by external funding in the form of project work. The external funding is obtained from the EU, the industry, the Academy of Finland, the Technology Development Centre and various other sources of minor significance. Regarding EU-projects, several ones have been successfully planned for the industry and carried out in the Ship Laboratory.

Development of different type of mathematical models and the appropriate numerical tools yielding solutions to them is the main field of activity in Ship Hydrodynamics at the Ship Laboratory. Mainly this means activities within Computational Fluid Dynamics (CFD). However, other fields such as intact and damaged ship stability, hydroelasticity, hydrodynamic aspects of ice-breaking and special propulsors have also been recent subjects of investigations. The relatively broad scope of research stems from the fact that the Finnish shipbuilding industry is very active and it is involved in different type of activities. In addition to the shipyards there is a vivid activity of design and consultancy offices, software developers and equipment suppliers.

The theoretical research at the laboratory is complemented by experimental research. Model test techniques as well as equipment are also being actively developed. The most important developments in this regard have been the purchase and commissioning of a Particle Image Velocimeter (stereo-PIV) and of an optical system (Krypton) capable of measuring model motions in 6 degrees-of-freedom. Taylor-made design and construction of wave-maker for laboratory's towing tank is also important and challenging development serving the laboratory's experimental research.

2. CFD in the naval context

The process of using Computational Fluid Dynamics in the naval applications was initiated in 1995 within the national research program funded by the Technology Development Centre. Within this five-year program the FINFLO-SHIP RaNS solver was developed. It is capable of computing viscous flows with free surfaces at model and full scale. Numerous ships have already been computed at model scale giving an estimation of the total resistance with an accuracy of about three to five percent. Recently, also at full scale, encouraging results with respect to the evaluation of the wave profile and the resistance have been obtained. At present, the FINFLO-SHIP code is transformed into a practical design tool. Furthermore, the implementation of an iterative propeller module based on the body-force concept was completed. Therefore, the FINFLO-SHIP code is applicable to the simulation of turbulent ship flows with complex geometries, appendages, propellers and free surfaces at model and full scale, resulting in an improved understanding of the physics of the flow around ships.

In the recent years, the research has been focused on the evaluation of free surfaces using structured and unstructured grids, full scale computations of ships, computations of realistic modern hull forms and the evaluation of the stability of damaged ships.

3. Examples of recent research

In the following some examples of the recent research at the laboratory in the fields of numerical and experimental hydrodynamics as well as hydroelasticity are briefly presented. References to additional information are provided for the interested reader.

3.1. Simulation of model- and full-scale ship flows

It is only within the recent years, when the increased computing capacities have enabled computations of viscous ship flows in full scale. One significant contribution to study the possibilities of the numerical ship-flow simulations has been the European Union project European Full-Scale Flow Research and Technology, EFFORT (Verkuyl and Raven, 2003).

The project has focused on the applicability of different RANS methods to full-scale viscous flow computations of ships, and the results of several computational cases obtained with different RANS methods have been compared. In addition to

Helsinki University of Technology (TKK), the other CFD partners of the project have been Ship Design and Research Centre (CTO) from Poland, Chalmers University of Technology from Sweden, Ecole Centrale de Nantes and Centre National de la Recherche Scientifique (ECN/CNRS) from France, HSVA from Germany, MARIN from the Netherlands and National Technical University of Athens (NTUA) from Greece.

The simulations at the TKK Ship Laboratory have been performed using FINFLO-SHIP flow solver. This is a RANS solver based on cell-centred finite volume method on multiblock strutured grids. The free surface is evaluated by a moving-grid technique with regridding. An actuator disk approach based on elliptic thrust distribution is used for the modeling of the influence of the propeller. A more detailed description of the full method is given in e.g. Hänninen and Schweighofer (2006), Li et al. (2001), Mikkola (2000) and Siikonen et al. (1990).

In total, seven different vessels have been considered in the project. The cases have been simulated in both model- and full-scale with and without an operating propeller. Some results for two of the cases – namely the Polish research vessel Navigator XXI and a container ship known as the Hamburg Test Case – are presented in Figures 1 and 2. More results can be found in Hänninen and Schweighofer (2006) and Schweighofer et al. (2005).

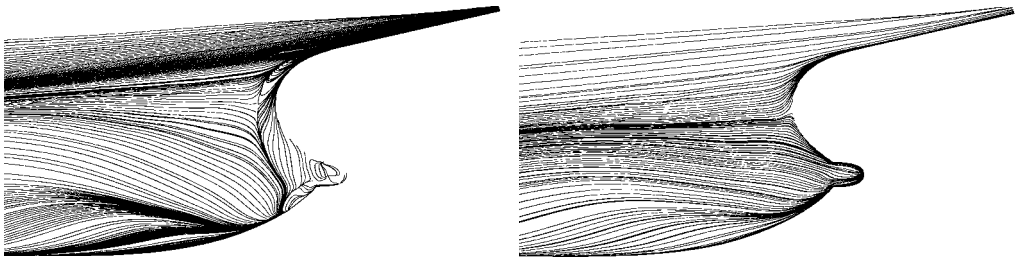

Fig. 1. The effect of the Reynolds number for the streamlines on the hull; Hamburg test case. Left: model scale ($Re = 1.0\times10^7$), right: full scale ($Re = 1.2\times10^9$)

3.2. Development of an unstructured flow solver

Due to the growing geometric complexity of the cases to be considered within the field of ship hydrodynamics TKK Ship Laboratory has also initiated research on unstructured solution methods. One part of this work is the development of a finite volume flow solver for time accurate free surface flows.

The solver (Yet Another Fine Flow Analyser – YAFFA) is based on SIMPLE/SIMPLEC type pressure correction method on unstructured 2D grids. Unsteady problems are treated with a dual time step approach and a three level fully implicit scheme. For free surface flows a surface tracking approach is used. Main features of the approach include deformations in the direction of the boundary normals, semi-implicit treatment

of the kinematic boundary condition and a partial coupling of the free surface and the pressure correction equations. Updating of the grid is handled with linear/torsional spring analogy and/or with Laplacian smoothing. Further details on the method can be found in e.g. Mikkola (2006).

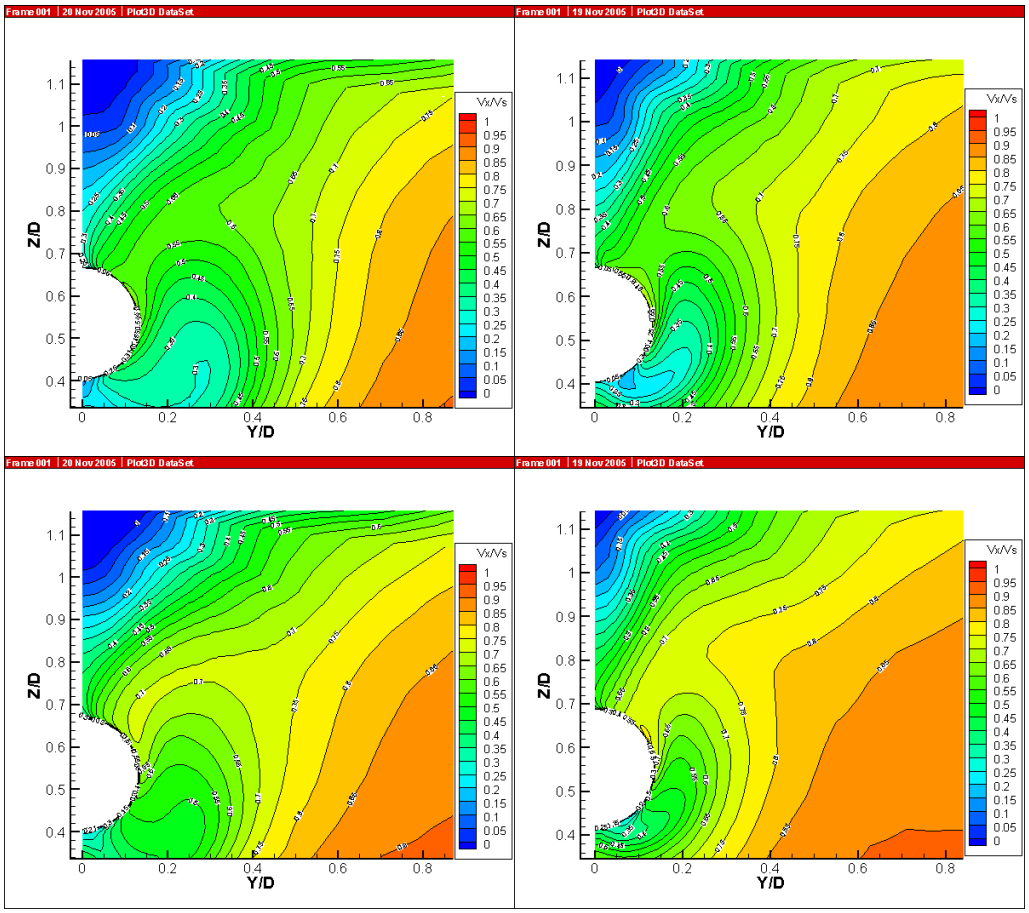

Fig. 2. Simulated wake at the propeller plane for Nawigator XXI at 10 kn. Top: nominal wake in model scale ($Re = 7.328\times10^6$) and full scale ($Re = 2.234\times10^9$), bottom: total wake in model and full scale

One example of the application of the method is fully nonlinear time accurate flow simulation of heaving bodies for the design and sizing of a plunger type wave maker. This is a part of the ongoing wave maker renewal project for the towing-tank at TKK Ship Laboratory. The task of the project has been to assess the quality of the wave generated by triangular wedges of different angles and to estimate the size and power requirements of the traversing gear for the new wave maker. In addition to this a lot of work in the project has been put in the validation of the new flow solver. For valida-

tion of the wave field prediction additional measurements have been made with the wave maker at the multi-purpose basin of the Ship Laboratory. Some of these results are presented in Figure 3. The interested reader is referred to Mikkola (2006) for the full results.

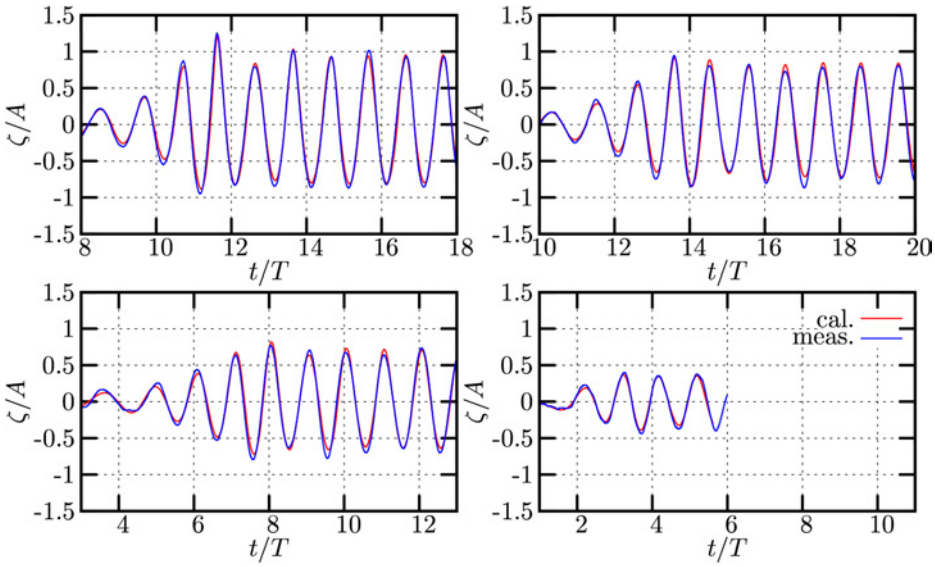

Fig. 3. Calculated and measured wave as a function of time for the wave maker at the Ship Laboratory with motion amplitude A = 150 mm. Motion period T: on the top 1.6 s and 1.8 s, on the bottom 2.0 s and 3.0 s

3.3. Simulation of Progressive Flooding

A novel simulation method for progressive flooding has been developed at TKK Ship Laboratory in close co-operation with Napa Ltd. This method is based on the pressure-correction technique and the compartments of the ship are considered as a staggered and unstructured computational grid. Hydrostatic pressures (water heights) and air pressures are solved in the centres of the rooms and flow velocities in the openings. Bernoulli's equation with semi-empirical discharge coefficients is used to represent the conservation of momentum. The method is implicit and iterative. A more detailed description of the simulation method is presented in Ruponen (2006a).

Model tests with a box-shaped barge were performed in the towing tank of TKK Ship Laboratory (Ruponen, 2006b). The studied cases included slow progressive flooding in a complex system of rooms and openings as well as compression of air in an air pocket. The results of the model tests have been made available for an ITTC Benchmark Study. Some examples of the validation results are shown in Figure 4. More results are presented in Ruponen et al. (2006).

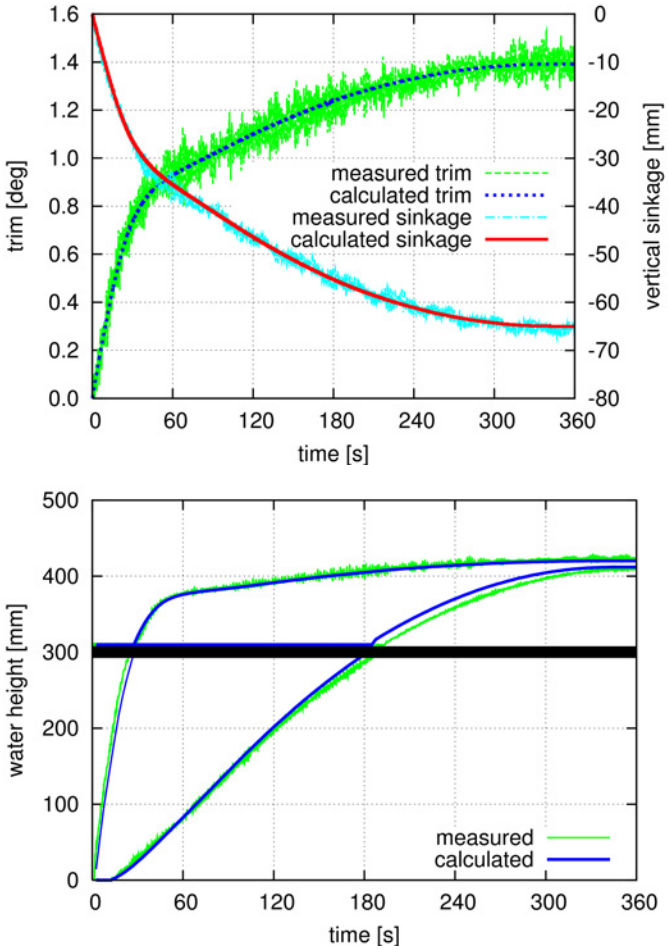

Fig. 4. Simulated and measured results for a box-shaped barge (Ruponen, 2006b). Top: the time histories of the simulated and measured trim and sinkage. Bottom: the time histories of the water height. The horizontal, black line is a deck between two compartments

One of the advances of this new simulation method is the efficient solution of air pressures and airflows that can have a significant effect on the flooding process, especially in voids. Thus the method can also be used for the calculation of cross-flooding times instead of the traditional IMO Resolution A.266 in order to achieve more realistic results with the counter air pressure taken into account. Furthermore, the implicitness ensures time-accurate solutions for progressive flooding in complex systems of rooms and openings, typical for passenger ships with dense internal non-watertight subdivision. Also the collapsing of non-watertight structures, such as fire doors, can be taken into account.

3.4. Effect of ship main dimensions on springing-type vibration

Increasing ship size has made springing an important matter in ship design. Literally, ship springing is considered to be the two-node vertical vibration of the hull girder, but the same kind of two-node transversal and torsional vibration can be remarkable as well. Typically, the amplitude of the resulting vibration is small in comparison to severe whipping cases, but it is dangerous for ship structures in the long-term and annoying for the passengers onboard also momentarily. The elimination of springing is not possible by stiffening the hull girder, as the vibration of the two-node mode shapes excites the whole ship hull from bow to stern. Regarding the occurrence of springing-type vibration, the critical factor is the relation between the two-node natural frequencies of the hull girder and the frequency content of the wave loads that the vessel encounters.

An approach to predict the effect of ship main dimensions on the vibratory level has been developed at the laboratory. The basic idea is to estimate how the changes in ship main dimensions affect the parameters that define the degree of springing-type vibration. The problem of predicting exact springing level is overcome by using a reference ship with known vibratory level. The approach is based on the maximum vibratory response given by the Euler-Bernoulli beam theory. It considers the responses of the two-node vertical and transversal mode shapes, and the harmonic and slamming loads are treated separately. The harmonic excitation is modelled by using the basic ideas of the potential flow theory and the slamming excitation by assuming a series of successive weak slams. The theory has been applied to two cases by comparing the displacement and acceleration responses onboard three vessels with one of the cases being a reference with assumed known values. As the coupling of two-node transversal and torsional mode shapes in these cases can be significant, the effect of the torsional mode shape on the total transversal responses is approximated.

On the basis of the developed approach, it is possible to point out general effects of the ship main dimensions on the vibratory responses. Some results are presented in Table and Figure 5. Further information on the approach and the results can be found in Hänninen et al. (2007).

3.5. Study on propeller-rudder interaction with stereo-PIV

Further improvement of the performance of ships in terms of propulsive efficiency, noise and cavitation requires more detailed information of the flow and particularly of interaction of the propulsor and different appendages of the ship. These matters have been studied recently at TKK Ship Laboratory using flow measurements of the propeller slipstream and propeller-rudder interaction for a fast twin-screw vessel.

Table. The data of the ships used for the study of the effect of the main dimensions on springing-type vibration

	Length L	Breadth B	Draught T
Ship B / Ship A	1.10	1.00	0.99
Ship C / Ship A	1.20	1.22	1.08

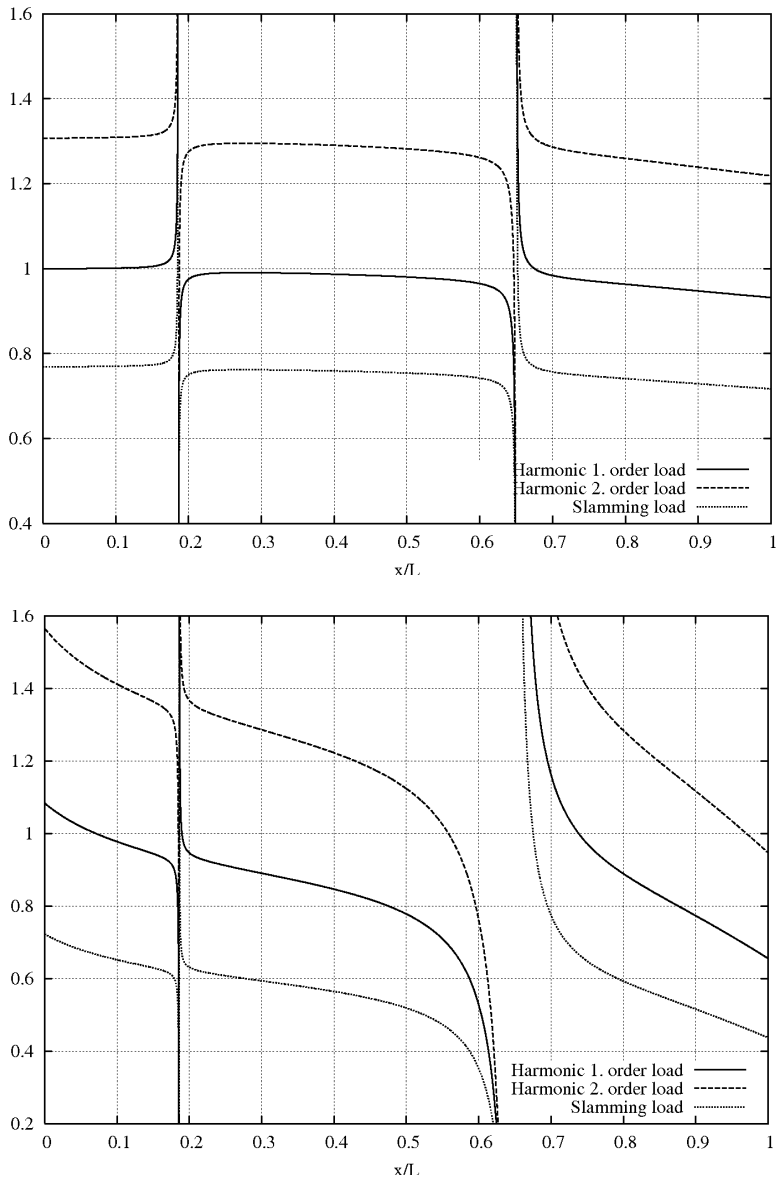

Fig. 5. The vertical accelerations for Ship B (left) and Ship C (right) relative to Ship A

The measurements were performed with a towed stereo-PIV system shown in Figure 6. Phase-averaging was applied by synchronising individual image acquisitions with the blade angle. Six-different angular positions with 15 degrees separation were used assuming periodicity for a four-bladed propeller. The instantaneous results for each blade position were averaged in order to get a phase-averaged flow field.

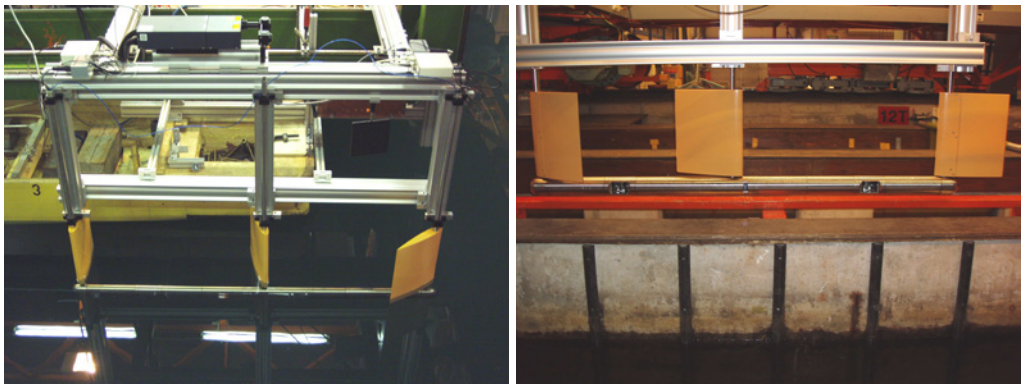

Fig. 6. The measurement setup for towed stereo-PIV measurements. On right: The underwater part of the measurement system. The cameras and the lenses are located in the outermost sections. The sections with windows are filled with water and house mirrors. The sheet optics are located in the middle section

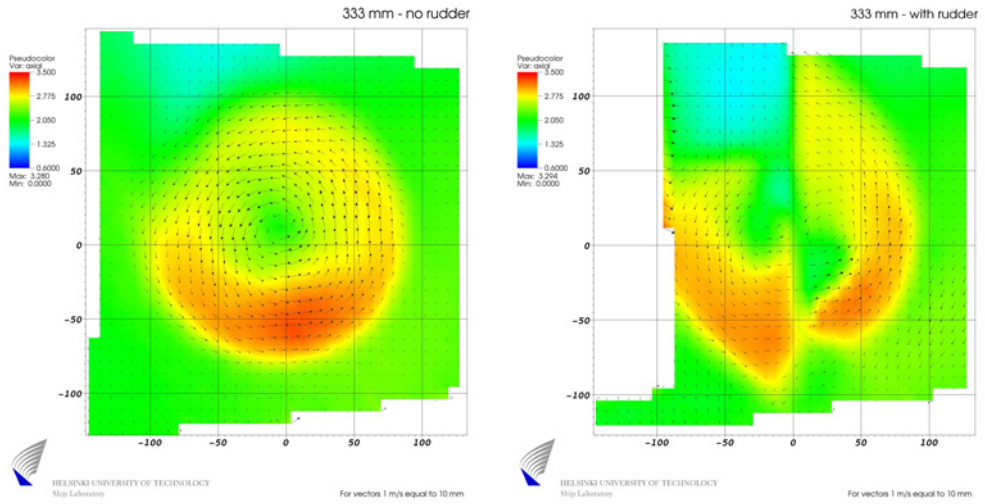

Fig. 7. Influence of the rudder on the propeller slipstream for a fast twin-screw vessel. The measurement plane is roughly a quarter of the chord length behind the rudder trailing edge

Four different planes perpendicular to the main flow direction were considered. The measurements were performed without any rudder and for three rudder configurations. The results reveal the complicated interaction of the propeller slipstream and the rudder as shown in Figure 7.

Acknowledgements

The authors wish to thank Mr. Pekka Ruponen and Ms. Satu Hänninen for their help in preparing the paper.

References

[1] Hänninen S. K.-M., Matusiak J., Niemelä A.: *Effect of ship main dimensions on springing-type vibration*, Marine Structures, in preparation, 2007.
[2] Hänninen S. K.-M., Schweighofer J.: *Numerical Investigation of the Scale Effect on the Flow around a Ship Hull*, Ship Technology Research, Vol. 53, 2006, pp. 17–25.
[3] Li T., Matusiak J., Lehtimäki R.: *Numerical simulation of viscous flows with free surface around realistic hull forms with transom*, International Journal for Numerical Methods in Fluids, Vol. 37, 2001, pp. 601–624.
[4] Mikkola T.: *Implementation of an implicit scheme into a free surface RANS solver in order to improve the convergence*, Ship Laboratory Report M-257, 2000, pp. 76.
[5] Mikkola T.: *Time accurate simulation of a plunger type wave maker using unstructured finite volume solver with surface tracking*, 26th Symposium on Naval Hydrodynamics, Rome, Italy, 2006.
[6] Ruponen P.: *Pressure-Correction Method for Simulation of Progressive Flooding and Internal Air Flows*, Schiffstechnik – Ship Technology Research, Vol. 53, 2006a, No. 2, pp. 63–73.
[7] Ruponen P.: *Model Tests for the Progressive Flooding of a Box-Shaped Barge*, Helsinki University of Technology, Ship Laboratory Report M-292, 2006b, pp. 88.
[8] Ruponen P., Sundell T., Larmela M.: *Validation of a Simulation Method for Progressive Flooding*, Proceedings of the 9th International Conference on Stability of Ships and Ocean Vehicles, Rio de Janeiro, Brazil, 25–29.9.2006, Vol. 2, 2006, pp. 607–616.
[9] Schweighofer J., Regnström B., Starke A. R., Tzabiras G.: *Viscous-flow computations of two existing vessels at model- and full-scale ship Reynolds numbers – A study carried out within the European Union project, Effort*, International Conference on Conputational Methods in Marine Engineering, MARINE 2005, Oslo, Norway.
[10] Siikonen T., Hoffren J., Laine S.: *A multigrid LU factorization scheme for the thin layer Navier-Stokes equations*, In Proceedings of the 17th ICAS Congress, Stockholm, Sweden, 1990.
[11] Verkuyl J.-B., Raven H.: *Joint EFFORT for Validation of Full-Scale Viscous-Flow Predictions*, The Naval Architect, January, 2003.

Najnowsze prace badawcze z dziedziny hydrodynamiki okrętu w Laboratorium Okrętowym w Helsinki University of Technology

W referacie pokrótce opisano najnowsze prace badawcze z dziedziny hydrodynamiki okrętu, stateczności i hydrosprężystości prowadzone w laboratorium okrętowym w Helsinki University of Technology.

ARCHIVES OF CIVIL AND MECHANICAL ENGINEERING

Vol. VIII 2008 No. 1

The crucial contemporary problems of the computational methods for ship propulsor hydrodynamics

J. A. SZANTYR
Gdańsk University of Technology, ul. Narutowicza 11/12, 80-958 Gdańsk

The paper presents the state-of-the-art review of the contemporary computational methods in ship propulsor hydrodynamics, pointing out the crucial problems on which the international researchers community attention is, or should be, focused. The review is based on papers presented at important international conferences within the last four years. At the beginning four basic categories of the computational fluid mechanics methods are briefly presented: traditional lifting line and lifting surface, Boundary Element Methods, Reynolds Averaged Navier Stokes Equations and Large Eddy Simulation or Direct Numerical Simulation methods. Then the problems with application of these methods to specific propulsor hydrodynamic problems are discussed in greater detail. This presentation starts with the narrowly defined design procedures, i.e. determination of propeller geometry fulfilling the required dynamic parameters: ship speed, propeller thrust and rpm with maximum efficiency. Then the computations of the complicated flow around a propeller of given geometry are presented, including the complicated cases of manoeuvring propellers or hydro-elastic effects. Subsequently the important problems of determination of propeller-generated vortex wakes and prediction of the different forms of cavitation and their hydrodynamic consequences are discussed. A separate section is devoted to unconventional propulsors, concentrating on the most important: pod propulsors and waterjets. The paper ends with a summary pointing out the directions for future research and applications of computational methods in propulsor hydrodynamics.

Keywords: *ship propulsors, hydrodynamics, computational methods*

1. Introduction

The advanced computational methods, driven by the relentless progress in computer technology, dominate nearly all fields of contemporary science and engineering. Fluid mechanics and within it, ship hydrodynamics, are no exception. The decisive role of computational methods may be illustrated by the following example: the basic equation of fluid mechanics, namely the Navier Stokes equation, has been known in its present form for over 150 years. However, during the first 120 years of its existence it played no practical role in applied technology. It was the advent of numerical methods about 30 years ago which enabled effective solution of the Navier Stokes equation for real engineering problems. Nowadays the realistic numerical solutions of this equation govern the progress in aerospace industry, marine industry, automotive industry, civil engineering, chemical engineering, oceanography, meteorology, biology, medicine and many other fields. Naval architecture and especially ship hydrodynamics, is also the field of growing application of the advanced computational fluid mechanics.

The subject of this paper is limited to the seemingly narrow field of ship propulsor hydrodynamics. However, a closer look at this field distinguishes a number of specific difficult problems such as high Reynolds numbers, complicated geometry of the flow boundaries, effect of realistic surface roughness and manufacturing tolerances, free surface effects, flows dominated by the interaction of moving and stationary elements, flows with different forms of cavitation, generation and propagation of pulsating pressure fields, hydroelasticity and many others. The complicated nature of these problems creates several ambitious tasks for computational fluid mechanics.

The central problem of the ship propulsor hydrodynamics is in fact a design problem, i.e. determination of the propulsor geometry and its operating parameters fulfilling in an optimum way a variety of often conflicting criteria. These criteria include: fulfilling required design conditions, high propulsive efficiency, low level of variable hydrodynamic forces and pressure pulsations, limited and harmless cavitation, low acoustic emission, low weight and cost etc. Consequently, this design problem is a multi-parameter optimization task, which is seldom solved using formalized optimization methods. In the current practice solution of the above design problem is achieved using a mixture of model experiments and computational methods, which are controlled either by a computerized optimization procedure or, more often, by the intuition of an experienced project leader.

This paper presents the computational methods used in the process of ship propulsor design and analysis. These methods may be based on four different approaches, namely:

- lifting line or lifting surface methods (also known as “vortex methods”),
- boundary element methods,
- Reynolds Averaged Navier Stokes Equation methods,
- Large Eddy Simulation or Direct Numerical Simulation methods.

These methods may be especially developed and used for a variety of tasks, such as:

- initial design of a propulsor geometry as the starting point for further optimization, which is typically based on the results of the following computations
- determination of flow around a propulsor of given geometry, including the effect of ship hull, appendages and rudders,
- prediction of propeller-generated vortex wakes,
- prediction of different forms of cavitation and their hydrodynamic consequences,
- analysis of unconventional propulsors.

The more detailed presentation and discussion of the above methods applied to specific problems is included in the following sections of the paper. This presentation is concentrated on the application to the most popular propulsor, namely the screw propeller. A separate section is devoted to unconventional propulsors, such as pod propulsors and waterjets.

2. Review of contemporary computational methods in propulsor hydrodynamics

Contemporary computational methods used in propulsor hydrodynamics may be divided into two major groups:

- potential flow methods, including lifting line, lifting surface and boundary element methods,
- viscous flow methods, including Reynolds Averaged Navier Stokes Equations (RANSE), Large Eddy Simulation (LES) and Direct Numerical Simulation (DNS).

Potential flow methods are gradually losing their importance, but they are still widely used. They are cheap and simple to use and the extensive accumulated experience and validation makes them still acceptably effective for most calculations. Lifting line methods date back from pre-computer era. Their essence lies in substituting propeller blade with a single vortex line of variable strength (cf. Figure 1), which is visibly inadequate for the modeling of flow around contemporary low aspect propeller blades. Lifting surface methods in which vortices or dipoles are distributed on infinitely thin surfaces (cf. Figure 2) represent correctly the true propeller blade outline, but they are unable to predict flow in the crucial leading edge region. This shortcoming is removed by the boundary element methods (cf. Figure 3), in which vortices or dipoles are located on the true surface of propeller blades and hub. Still, every potential method must be supplemented with empirical corrections for viscosity effects.

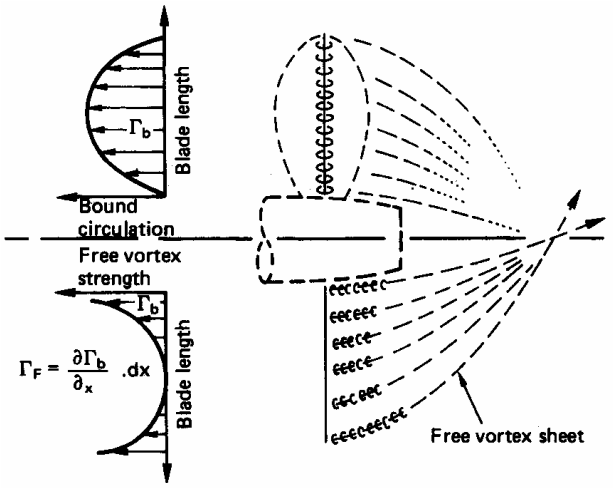

Fig. 1. Scheme of the lifting line model of a propeller [1]

Viscous flow methods are rapidly gaining ground in propulsor flow analysis. The most popular are RANSE (cf. Figure 4) methods which employ a variety of empirically calibrated turbulence models for closing the Reynolds equations for turbulent

flow. The solutions of these methods include in principle the effects of viscosity, but their results depend strongly on the adequacy of the particular turbulence model to the specific flow and on the structure of discretization of the flow domain. Another step forward towards modeling physical reality of viscous flows are LES methods, in which the turbulence cascade of vortices is divided into anisotropic high energy large eddies simulated numerically and smaller isotropic low energy eddies modeled using semi-empirical relations similar to those used in RANSE. At the end of this development lie DNS methods, in which all turbulence scales (i.e. all sizes of eddies) are simulated numerically. DNS requires very dense discretization of the flow domain, which with available computer technology limits the practical application to simple flows at relatively low Reynolds numbers only. Figure 5 shows schematically the basic difference between LES and DNS in the scales of simulated eddies and the resulting velocity variation in a point.

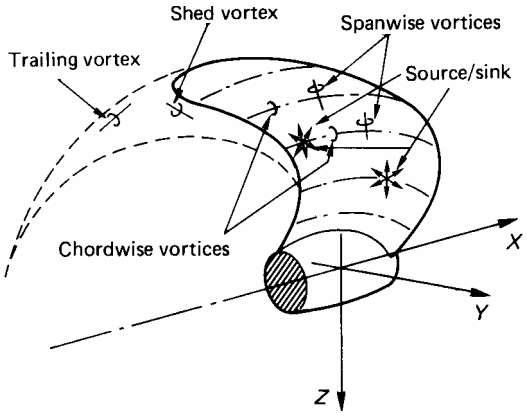

Fig. 2. Scheme of the lifting surface model of a propeller [1]

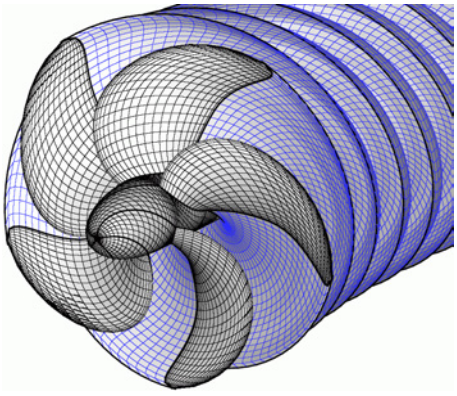

Fig. 3. Scheme of the boundary element method model of a propeller [21]

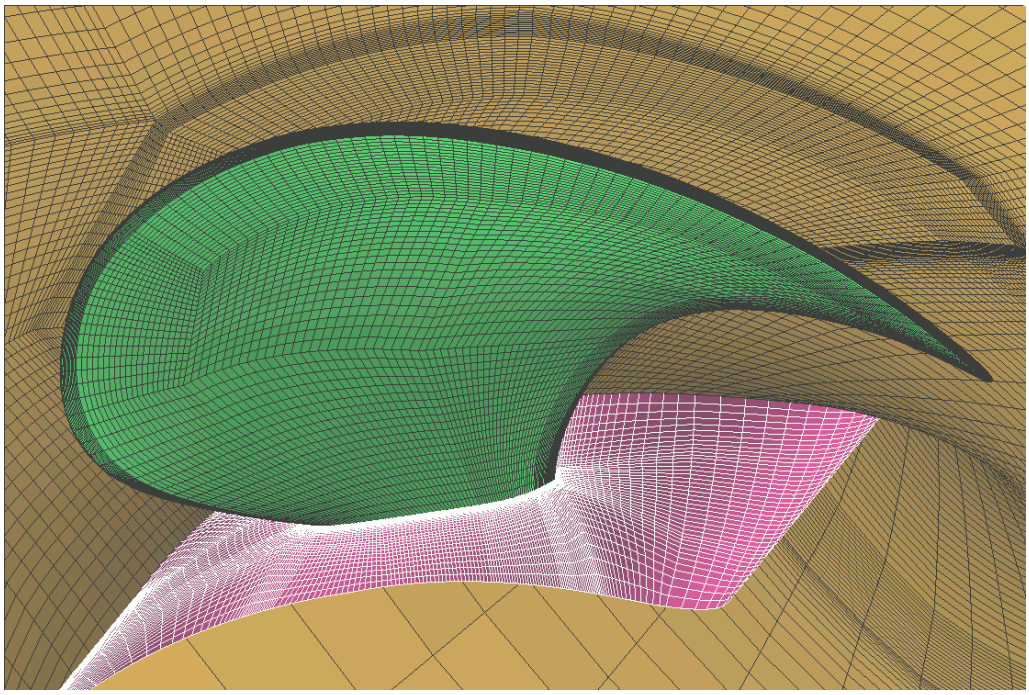

Fig. 4. Scheme of discretization for the RANSE calculation of propeller flow [2]

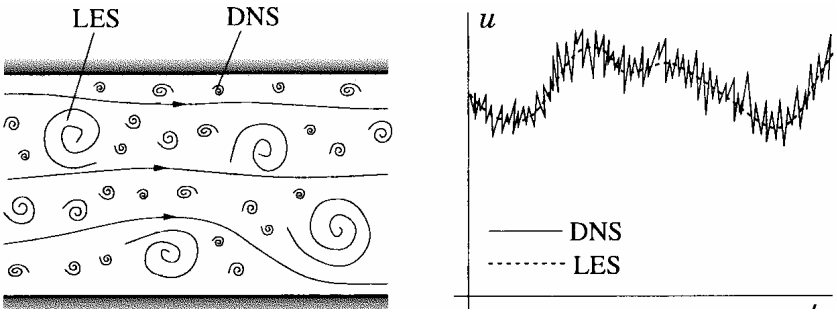

Fig. 5. Principle idea of the Large Eddy Simulation and Direct Numerical Simulation methods [3]

3. Design of ship propellers

Design of ship propellers means determination of their geometry in the course of multi-criteria optimization process. This optimization is in most cases performed manually, only occasionally automatic optimization procedures are used. In this process a variety of computational procedures are used, often interacting with model experiments and other empirical data. An example of the computational method which may be used for this purpose is the higher order boundary element method presented

in [4]. This method approximates the propeller blade by B-splines (cf. Figure 6), which enables local increase of accuracy of the propeller geometry representation, thus leading to increased accuracy of the results. The practically achievable accuracy may be assessed from the comparison the calculated and measured pressure distribution on the blade section (Figure 7) and from the comparison of calculated and measure propeller open water characteristics shown in Figure 8.

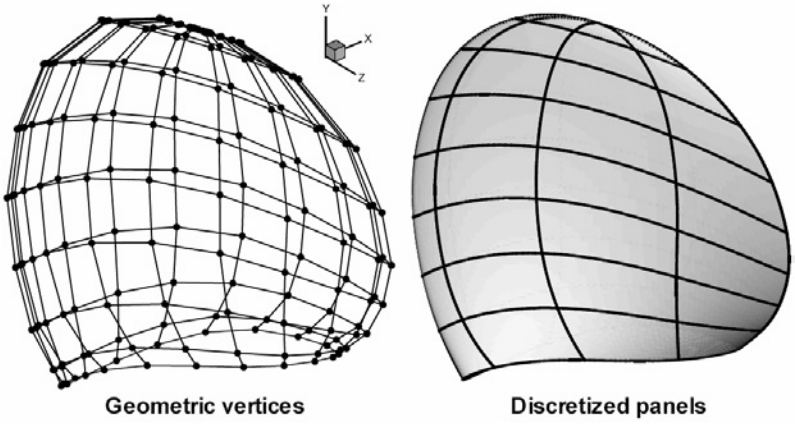

Fig. 6. Higher order discretization of a propeller blade [4]

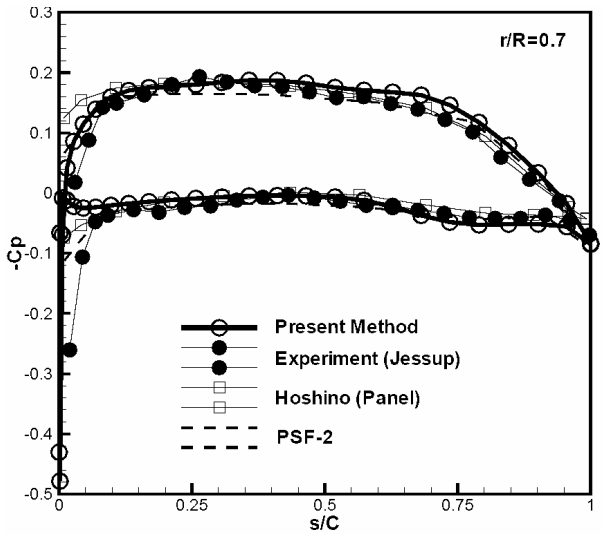

Fig. 7. Calculated and measured pressure distribution at $r/R = 0.7$ [4]

The tendency to develop propeller design procedures incorporating automatic optimization is quite visible in the recent years. Often genetic algorithms are used for

this purpose. Another possible way is a variational approach to the lifting surface algorithm, as presented in [5]. This procedure minimizes propeller torque at given propeller thrust and given advance coefficient. The varied parameters are propeller pitch distribution and mean line camber distribution of the blade sections. The results of automatic optimization of these parameters may be seen in Figures 9 and 10. It is visible that the method reduces blade pitch and increases mean line camber at blade root and tip. According to the author application of the optimization procedure increases propulsive efficiency by 1–2 per cent.

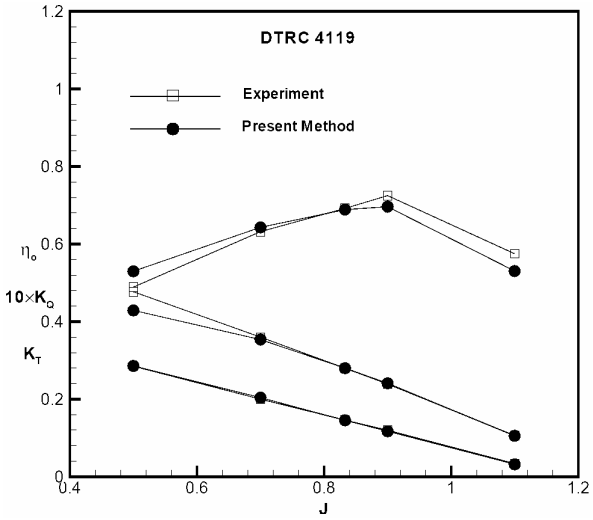

Fig. 8. Calculated and measured hydrodynamic characteristics of a propeller [4]

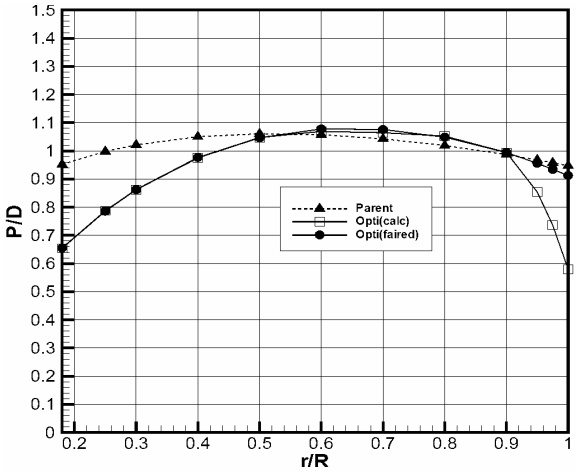

Fig. 9. Optimised pitch distribution of a propeller [5]

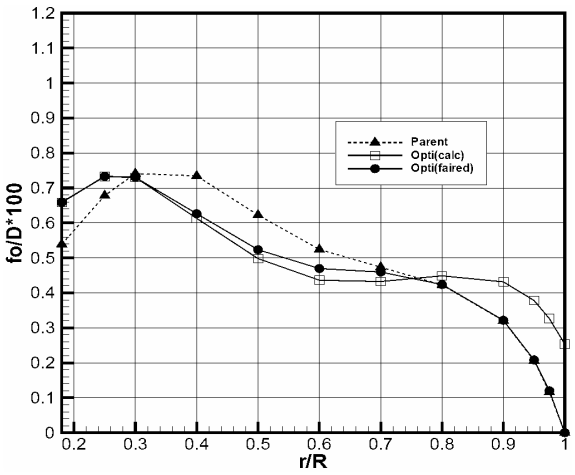

Fig. 10. Optimised mean line camber of a propeller [5]

Another approach to automatic optimization is presented in [6], where an Adaptive Range Genetic Algorithm is used in conjunction with RANSE method for optimization of propellers in behind condition. Four different grid densities were tested from the sparsest G4 to the densest G1 and the summary of optimization is given in Table 1, showing the gain in efficiency and resulting changes in propeller pitch and camber. The corrections listed result from the constraint of steady-state self propulsion condition. It is reassuring that all grid densities produce similar results.

Table 1. Summary of propeller optimization results [6]

Quantity changed (%)	G1	G2	G3	G4
Delivered power	-2.1	-2.2	-2.4	-1.9
Correction on delivered power	0.8	0.7	0.7	0.0
Final delivered power	-1.3	-1.5	-1.7	-1.9
Check in Grids	-1.3	-1.5	-1.7	-1.9
Camber	-1.5			
Revolution speed	0.7			
Pitch	-1.7	-1.7	-1.7	-1.7
Correction on pitch	0.4	0.3	0.3	0.0
Final pitch	-1.3	-1.4	-1.4	-1.7

However, a true propeller optimization process should take into account many more criteria than just the propulsive efficiency. The following criteria are as important as maximization of efficiency:

- extent of cavitation phenomena,
- level of propeller induced pressure pulses,
- level of propeller generated fluctuating shaft forces,
- risk of cavitation erosion,
- propeller weight and moment of inertia in water,

- cost of manufacturing.

Even propulsive efficiency as the optimization criterion should be evaluated for the realistic propeller-hull interaction, not for the axi-symmetrical inflow velocity field as in [5]. Development of an effective procedure for such multi-criterial automatic optimization is one of the urgent tasks of contemporary propeller hydrodynamics.

4. Computation of propeller flow

Effective computation of propeller flow is a pre-requisite in any propeller design and analysis task. Nowadays majority of these computations employ CFD methods, in most cases RANSE. The accuracy of RANSE predictions depends strongly on the grid structure and on the turbulence models. Propellers generate specific flows markedly different from e.g. hull flows, and they require special grid structures and turbulence models. Considerable research effort is devoted to investigating these problems, for example in [7] three turbulence models were tested, namely k–ω, k–ε and RNG. The influence of these models on the calculated propeller forces is shown in Table 2. This table shows three numerical predictions of thrust, torque and efficiency coefficients for model and full scale, compared with model experiment data and full scale prediction using ITTC78 method. The differences between turbulence models are quite visible.

Table 2. Effect of turbulence models on the accuracy of RANSE calculation of propeller forces [7]

	Conventional propeller			Error: [Model/Exp-1]		
Model Scale	K_{Tm}	$10K_{Qm}$	η_{0m}	ΔK_T [%]	ΔK_Q [%]	$\Delta\eta_o$ [%]
Exp	0.1650	0.1950	0.5387	-	-	-
SST	0.1679	0.2129	0.5021	1.8	9.2	-6.8
RKE	0.1677	0.2183	0.4891	1.6	11.9	-9.2
RNG	0.1677	0.2184	0.4888	1.6	12.0	-9.3
				Scaling: [Full/Model-1]		
Full Scale	K_{Ts}	$10K_{Qs}$	η_{0s}	ΔK_T [%]	ΔK_Q [%]	$\Delta\eta_o$ [%]
ITTC' 78 method	0.1655	0.1896	0.5556	0.3	-2.8	3.1
SST	0.1743	0.2009	0.5523	3.8	-5.6	10.0
RKE	0.1779	0.2098	0.5398	6.1	-3.9	10.4
RNG	0.1776	0.2087	0.5418	5.9	-4.4	10.8

Computations of typical propeller flows are nowadays regarded as standard analysis tasks. The frontline of advanced applications lies today in special geometries, dynamic unsteady flow phenomena and special effects like for example hydro-elasticity. For example in [8] the RANSE computations of flow around the propeller with endplates are presented. The computational grid for such a case is shown in Figure 11, while Figure 12 shows the calculated pressure for model scale (model diameter 0.239 m) and full scale (propeller diameter 4.30 m). The calculated scale effect on pressure distribution looks very interesting, however, it lacks experimental confirmation.

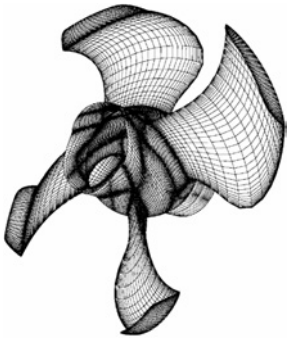

Fig. 11. Computational grid for propeller with endplates [8]

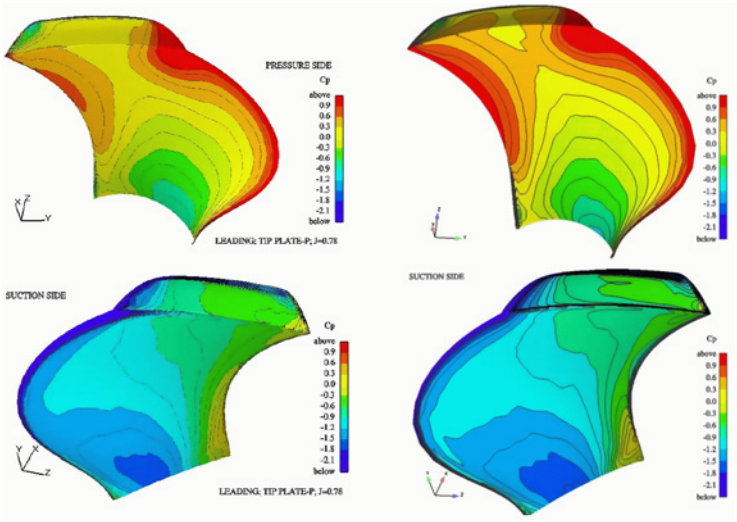

Fig. 12. Calculated pressure distribution on an endplate propeller in model and full-scale [8]

A crash stop of a propeller leads to highly dynamic and very complicated re-circulating flow around the propeller, which for a long time has escaped attempts to calculate it. Contemporary computational methods enable effective determination of such flows (cf. Figure 13) using for example RANSE approach. The primary purpose of such calculations is to determine fluctuations of propeller blade pressure distribution, with further objective of blade stress analysis. Experiments show that during the crash stop maneuver the amplitudes of blade forces reach the order of mean thrust, leading to acute blade strength problems. RANSE calculation exhibits large errors in prediction of blade forces and in general it underestimates the amplitudes of fluctuations. Application of LES method [10] markedly improves the accuracy of predictions. Figure 14 shows the comparison of calculated and PIV measured velocity fluctuations around a propeller during crash stop maneuver.

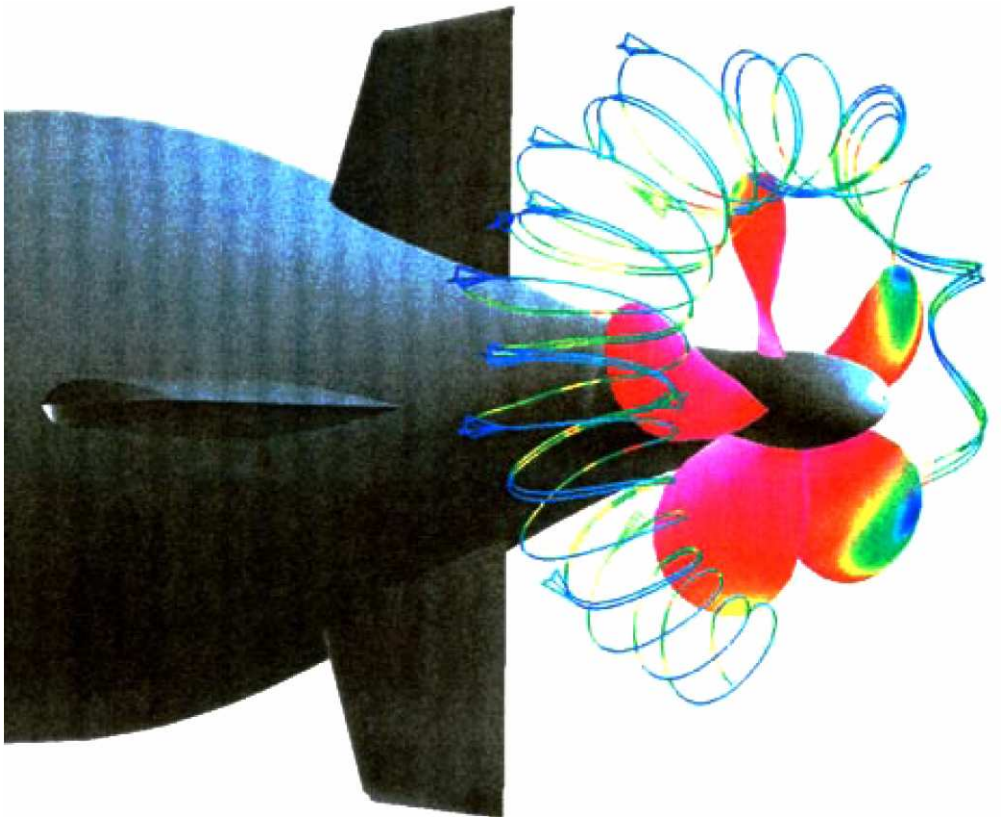

Fig. 13. Flow during propeller crash stop computed using RANSE method [9]

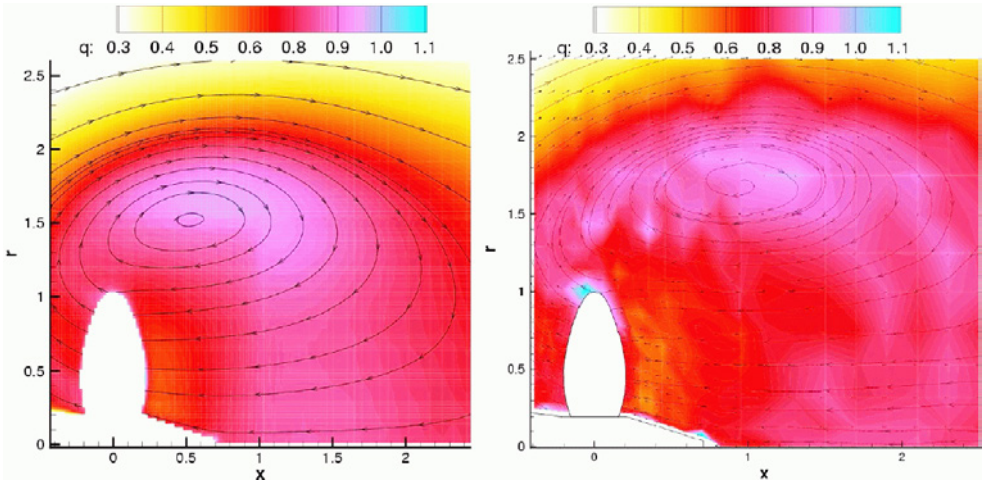

Fig. 14. Calculated using LES method and measured velocity fluctuations during propeller crash stop [10]

Contemporary marine propellers usually have skewed blades and they are susceptible to hydro-elastic effects under loading. These lead to the deformation of geometry and to changes in the hydrodynamic characteristics under loading. These effects should be taken into account during propeller design. In order to evaluate them the combination of flow and strength analysis procedures must be used. In [11] a combined BEM/FEM method was used. Table 3 shows experimentally determined coefficients of thrust, torque and efficiency for a rigid and flexible propeller model at two loading conditions. Analysis of these results reveals the practical importance of the hydro-elastic effect. Figure 15 presents the calculated and experimentally determined propeller hydrodynamic characteristics demonstrating the hydro-elastic effect.

Table 3. Changes in propeller thrust and torque due to hydro-elastic effects [11]

454 rpm	K_T	$10K_Q$	η
open water, rigid	0.243	0.384	0.665
open water, flexible	0.232	0.361	0.675
wake inflow, rigid	0.245	0.382	0.674
wake inflow, flexible	0.235	0.361	0.685
909 rpm	K_T	$10K_Q$	η
open water, rigid	0.243	0.384	0.665
open water, flexible	0.206	0.311	0.698
wake inflow, rigid	0.245	0.382	0.674
wake inflow, flexible	0.212	0.313	0.710

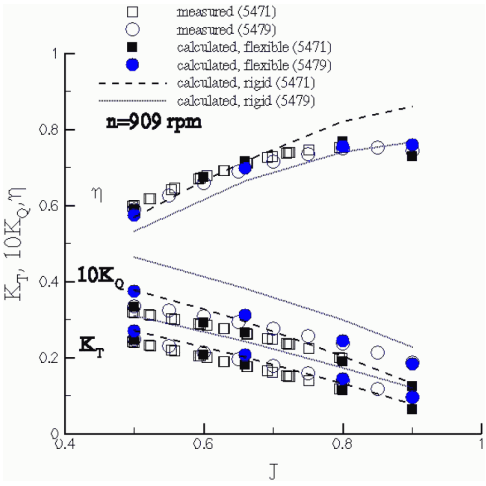

Fig. 15. Comparison of calculated vs. measured propeller characteristics showing hydroelastic effects [11]

5. Prediction of propeller-generated vortex wakes

Prediction of propeller-generated vortex wakes is a task of special importance because of at least three reasons:

- vortex wakes interact with rudders and elements of ships, creating strongly unsteady flow phenomena,
- vortex wakes generate specific forms of unsteady cavitation, leading to high level of acoustic pressure and to cavitation erosion,
- vortex wakes lead to destruction of bottoms and walls of channels in confined waters.

A variety of calculation methods are applied for the prediction of propeller wakes. In [12] a relatively simple potential flow theory is used, incorporating the flow alignment of the near field vortex wake. The accuracy of the results obtained from such an approach may be assessed in a comparison between calculations and PIV measurement shown in Figure 16. It is visible that the potential flow predictions is rather inaccurate in the close vicinity to the propeller. The authors attribute the discrepancy to the different definition of vortex centre location in calculations and in measurements.

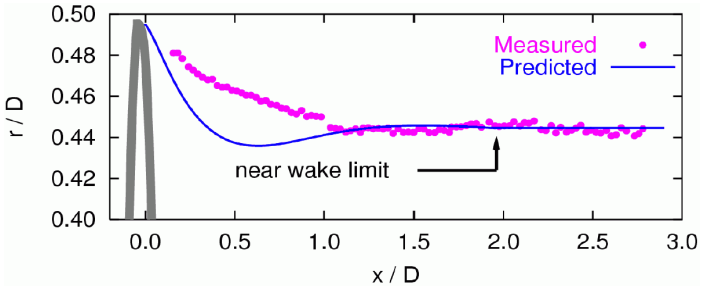

Fig. 16. Comparison of the trajectory of the propeller tip vortex measured and calculated using potential flow theory [12]

A more practical problem is treated in [13], where the vortex wake behind three different propeller hubs: convergent, divergent and convergent-divergent is calculated using RANSE and measured using LDV and PIV. The objective is to find the hub geometry which most effectively disperses the hub vortex wake and reduces the resulting noise, vibration and risk of cavitation erosion on the rudder. Figure 17 shows a very good agreement between the results of computation and two kinds of measurements. The results of the analysis point to the convergent-divergent hub as the most effective one.

The most important problem in propeller wake prediction is the accurate computation of the location and intensity of the tip vortices. If this problem is solved using RANSE, the results are strongly influenced by the grid structure and by the turbulence models. Analysis of this influence is presented in [14], where four turbulence models were tested: one equation Spalart-Almaras model (SA), the realizable k–ε (RKE) model, the shear stress transport model k–ω (SST) and the Reynolds stress transport model (RSTM). Figure 18 shows the comparison of calculated and experimentally measured minimum pressure at the centre of the tip vortex. It is obvious that only

RSTM gives sufficient accuracy of prediction, while other models seriously underestimate the pressure reduction in the vortex centre. This effect may invalidate any cavitation inception prediction based on such computations.

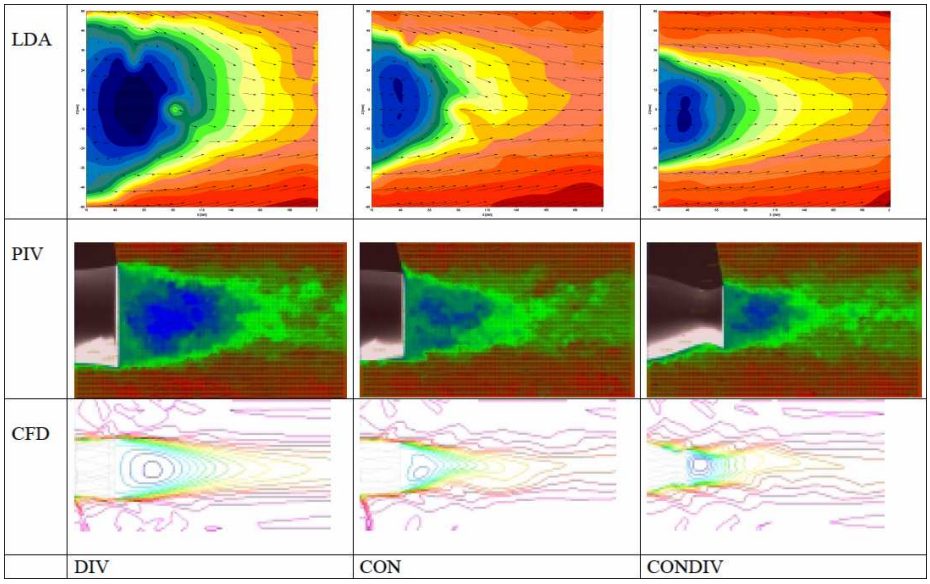

Fig. 17. Comparison of the axial velocity field behind propeller hub measured and calculated using RANSE [13]

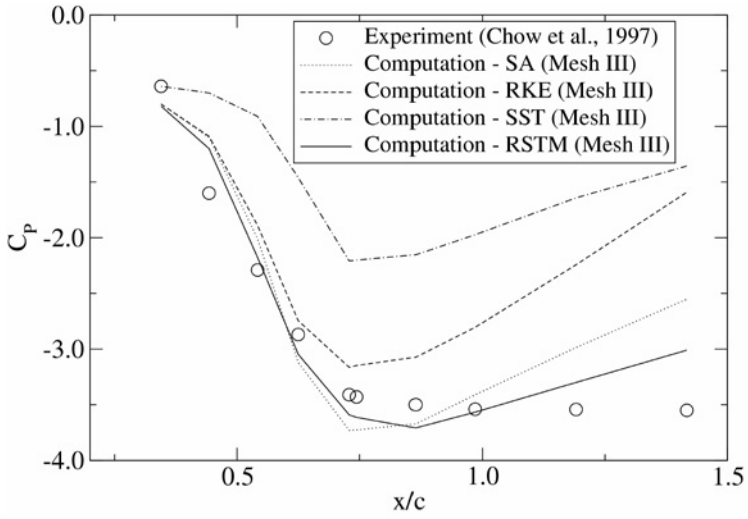

Fig. 18. Minimum pressure in the propeller tip vortex using RANSE with different turbulence models [14]

The continuous progress in computer technology enables nowadays much more complicated numerical simulations that those possible only a few years ago. An example of such a case is presented in [15], where the flow field generated by a propeller tip vortex is predicted using LES. The calculations were performed in model scale with propeller diameter of 0.228 m and blade tip Reynolds number of 10^6. The unstructured tetrahedral grid had a cell size of 0.3 mm. Figure 19 shows the calculated induced velocity in the propeller wake with visible locations of the tip vortex.

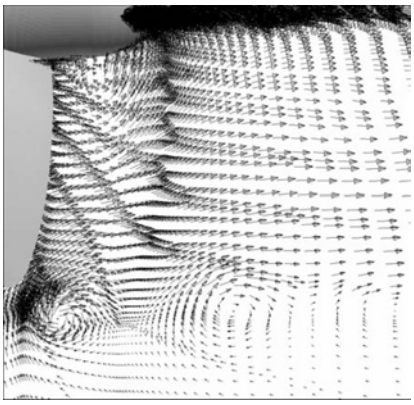

Fig. 19. Induced velocity field in the propeller wake calculated using LES [15]

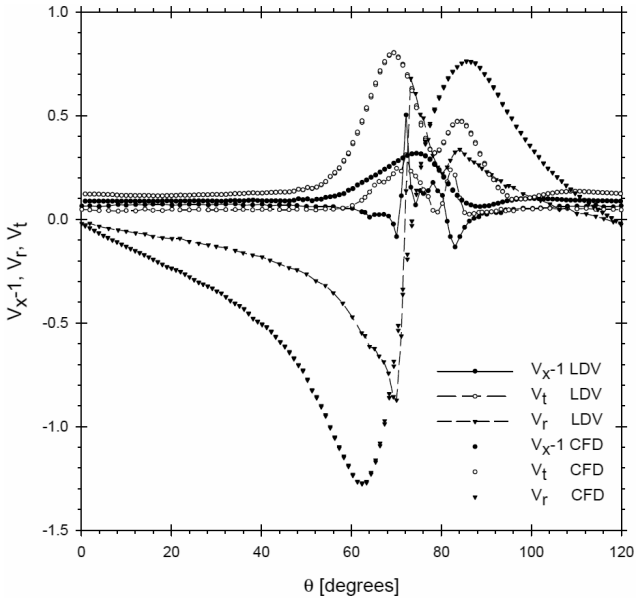

Fig. 20. Comparison of the velocity field in the cross-section of the propeller tip vortex measured and computed using RANSE [16]

One of the serious problems of the tip vortex flow computations is that the location of the vortex is not known *a priori*. On the other hand a very dense grid structure is necessary to capture high cross-flow velocity near the vortex centre. It would be impractical to use such a dense structure in the entire flow domain. One of the possible solutions to this problem is described in [16], where an automatic grid adaptation is applied. Initial computation based on a coarse grid locates the vortex and then the grid density is locally automatically increased until a sufficiently accurate solution is obtained. The results of such an approach using RANSE with k–ω turbulence model is shown in Figure 20, where results of computations are compared with LDV measurements.

6. Prediction of propeller cavitation and its consequences

A comprehensive review of the contemporary propeller cavitation research problems is given in [17]. Computational prediction of propeller cavitation is a difficult task, because cavitation takes different forms: sheet, vortex, bubble and cloud. Moreover, the process of cavitation inception, development and decay is strongly dynamic and physically very complicated. Much of the researchers' attention is concentrated on tip vortex cavitation, because this form of cavitation is responsible for high noise emission and for cavitation erosion. Inception of tip vortex cavitation depends on the behaviour of the cavitation nuclei in the velocity and pressure field generated by the tip vortex. Advanced computational methods of today enable much more realistic and accurate simulation of these processes than those available only a few years ago.

The successful numerical simulation of the complicated behaviour of the cavitation nuclei in the centre of the propeller tip vortex is described in [18]. The computations were performed using the Unsteady RANSE for vortex flow calculation and the boundary element method for non-spherical bubble dynamics calculation. The results are presented in Figure 21, where the consecutive stages of the bubble development and decay are shown. It is visible that the shape of individual bubbles is far from spherical, what precludes application of the Rayleigh Plesset equation used traditionally for studying their dynamics.

The accurate prediction of tip vortex velocity and pressure fields is an obvious prerequisite for the analysis of tip vortex cavitation. However, in real propeller flows the tip vortex is often a complicated structure, resulting for example from the mutual interaction of the tip vortex and leading edge leakage vortex. Such a flow may be nowadays effectively simulated using the most advanced approach, namely through direct numerical simulation of the Navier-Stokes equation DNS [19]. Figure 22 shows the computational domain behind the blade tip with the very dense grid required for DNS. In this figure the calculated pressure field is also shown. Figure 23 presents the velocity field generated by the interacting tip vortex and the leading edge leakage vortex, computed using DNS. Figure 24 shows the astonishingly strong effect of 10 per cent fluctuation in the inflow velocity on the formation of the cavitating tip vortex.

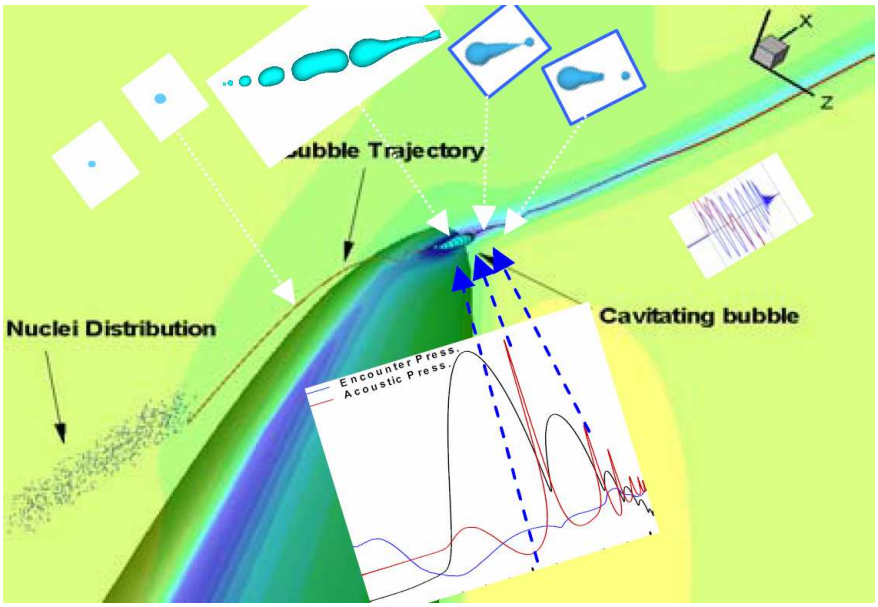

Fig. 21. Cavitation bubble behaviour in vortex flow calculated using URANSE [18]

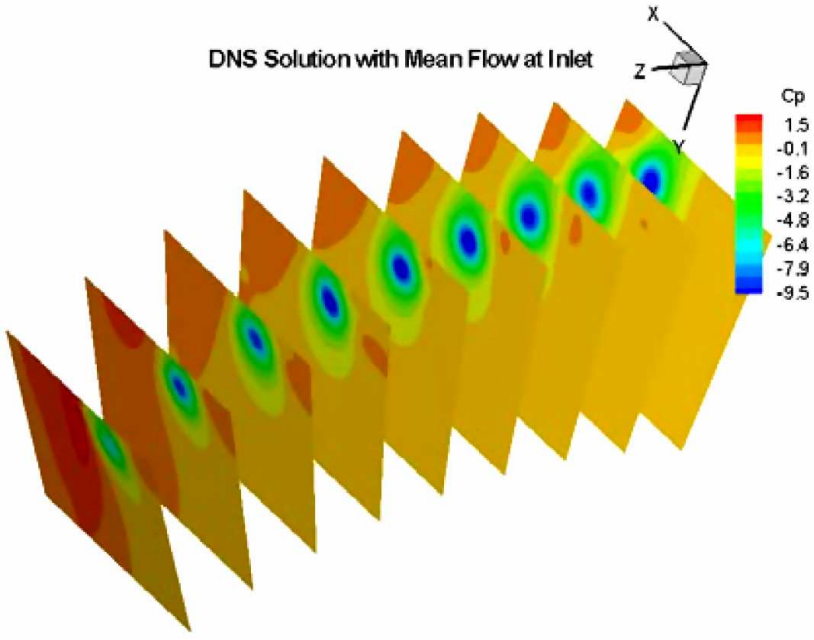

Fig. 22. Pressure field around a propeller tip vortex calculated using DNS [19]

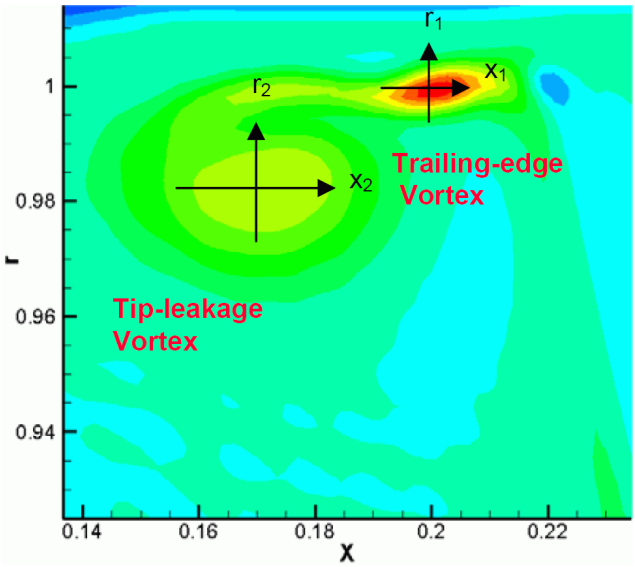

Fig. 23. Tip leakage and trailing vortices velocity distribution calculated using DNS [19]

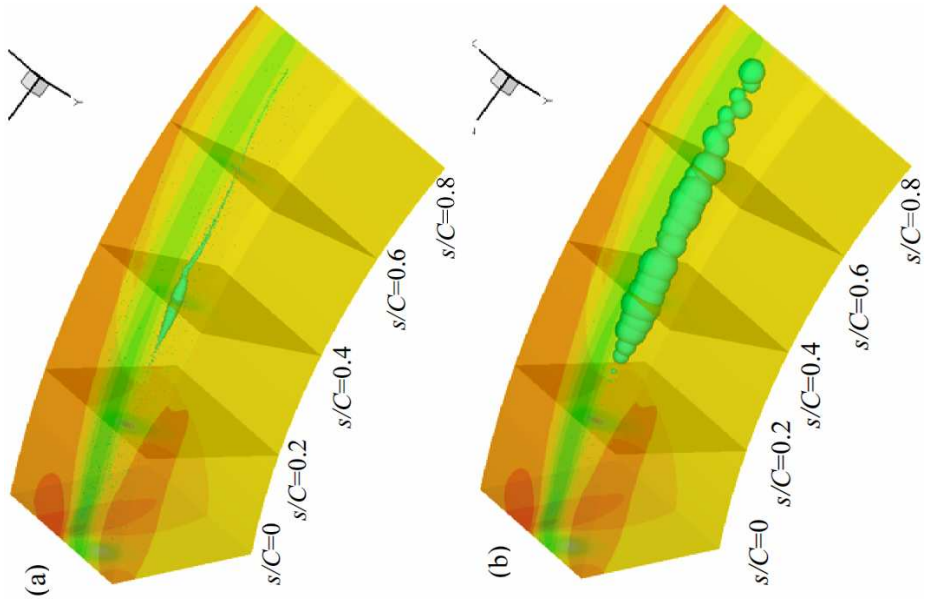

Fig. 24. Influence of inflow velocity fluctuation on the formation of the cavitating tip vortex calculated using DNS [19]

Sheet cavitation on propeller blades seems much easier to calculate and for several years it has been successfully calculated using lifting surface methods. Here also the

most advanced methods demonstrate their advantage. In [20] the LES method combined with the Volume of Fluid Method (VOF) are used for modeling the unsteady sheet and vortex cavity on a hydrofoil of finite span. Numerical simulation of large anisotropic eddies, carrying high kinetic energy, gives this approach a marked advantage over RANSE, where all vorticity scales are modeled using simplified equations and the influence of certain specific flow characteristics on the cavity inception and development may be overlooked. Figure 25 shows the calculated sheet cavity formation on a mid-span profile of the hydrofoil at four consecutive moments in time, while Figure 26 presents the calculated complicated geometry of the tip vortex cavitating kernel at a given moment in time. These two pictures demonstrate the ability of the contemporary advanced CFD method to describe accurately complicated dynamic two-phase flow phenomena.

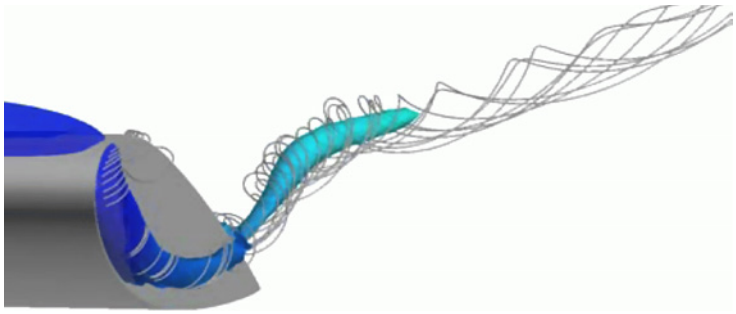

Fig. 25. Cavitating tip vortex formation calculated using LES [20]

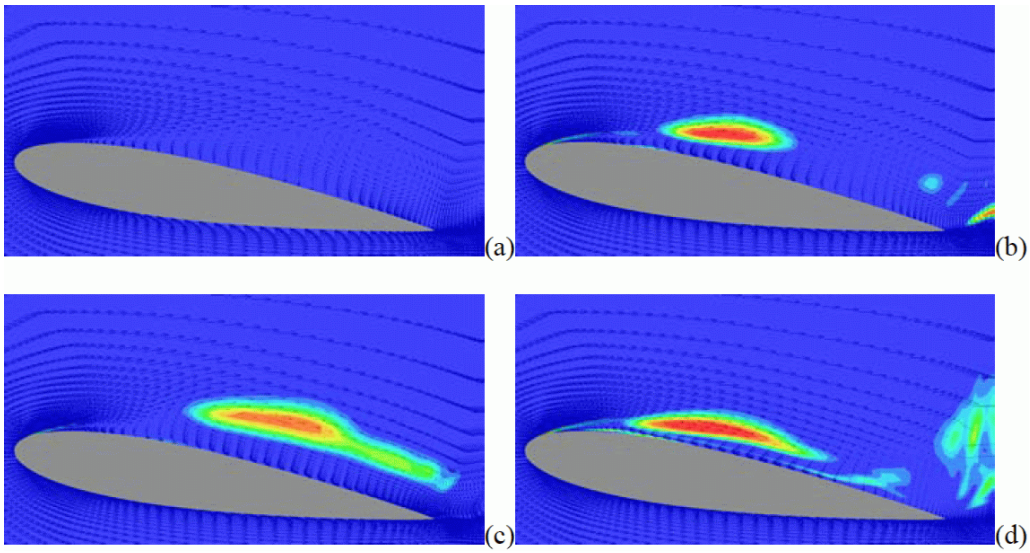

Fig. 26. Development of sheet cavity on a blade section computed using LES [20]

Propeller sheet cavitation may be also quite effectively predicted using simpler, more traditional approach. In [21] the almost classical formulation of the BEM is used for the analysis of unsteady sheet cavitation on the propeller operating in a wake. Figure 27 shows the comparison of calculated and experimentally observed sheet cavity at different angular blade positions in the non-uniform inflow velocity field.

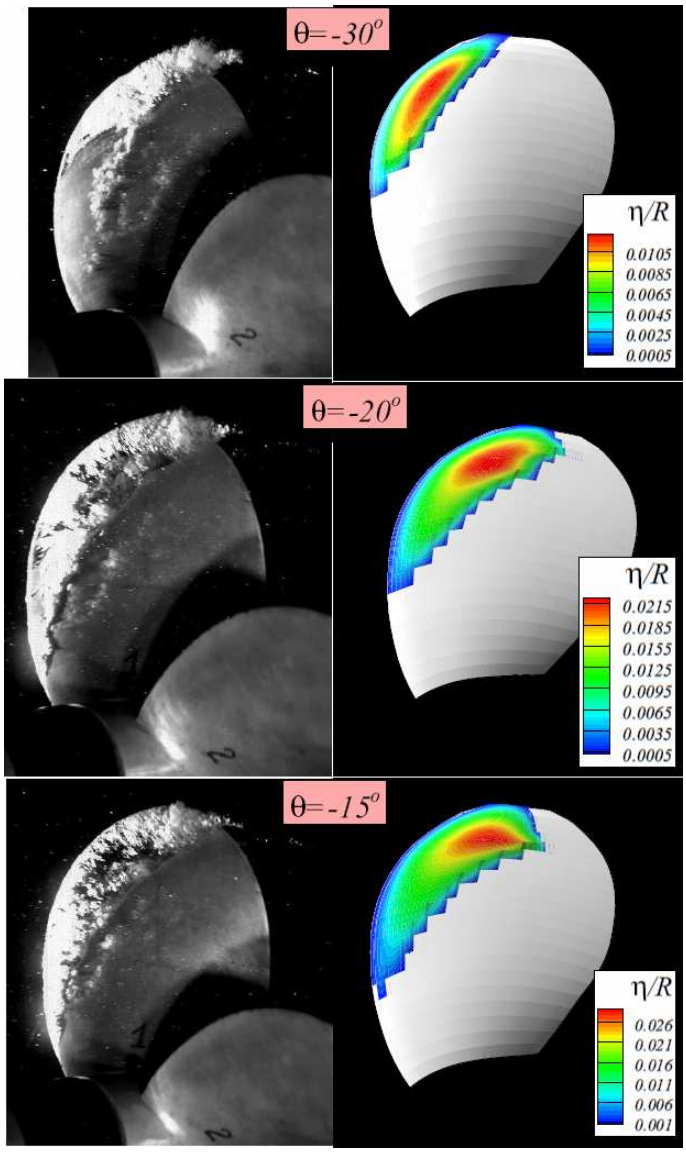

Fig. 27. Comparison of time-dependent sheet cavity extent on a propeller observed and computed using BEM [21]

Cloud cavitation is very difficult to predict theoretically. It is governed by the complicated interactions of a large number of small bubbles located in a small volume of fluid and behaving in a very dynamic way. An example of the effective application of LES algorithm for the analysis of the cloud cavity formation behind a cavitating hydrofoil is described in [22]. Figure 28 presents a comparison of the calculated and PIV measured velocity field and void fraction in the region of the cloud cavity. Despite the extremely complicated physical phenomena the accuracy of the numerical prediction seems remarkable.

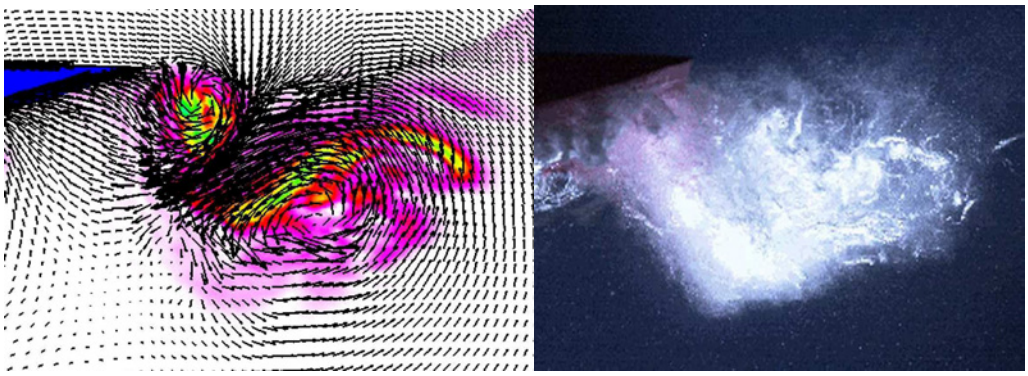

Fig. 28. Comparison of wake behind a cavitating profile observed and computed using LES [22]

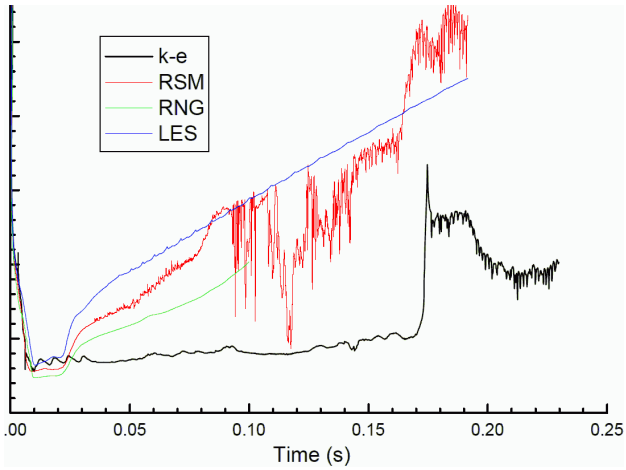

Fig. 29. Drag coefficient of a supercavitating missile computed using LES and RANSE with different turbulence models [23]

Computational methods are often used for very specialized tasks, like for example for prediction of flow around supercavitating objects like missiles etc. In [23] three different turbulence models were used in RANSE methods and compared with LES in

calculation of flow around a supercavitating missile. Figure 29 shows a comparison of the hydrodynamic drag coefficient during initial stages of the supercavity formation, calculated with different approaches. This figure may serve as an illustration of uncertainty still associated with CFD calculations when applied to a new and unrecognized problem.

7. Problems of unconventional propulsors

In this paper the term "unconventional propulsors" means any propulsor other than the classical fixed pitch propeller. In the recent years many variants of unconventional propulsors were invented and applied, but only problems concerning the two most popular of them are presented below, namely pod propulsors and waterjets.

Pod propulsors are an interesting combination of a propulsive and steering device, composed of rotating and stationary elements in complicated mutual hydrodynamic interactions. Despite many full scale implementations, various aspects of the hydrodynamic performance of these propulsors are still not fully recognized. Therefore numerical methods for prediction of flow around pod propulsors are in great demand. In [24] such a method based on RANSE is described. Figure 30 shows the applied discretization of a pod propulsor, while Figure 31 presents the calculated pressure field on a pod propulsor. This enables further calculation of the hydrodynamic forces and the resulting propulsive and manoeuvring characteristics of a pod propulsor.

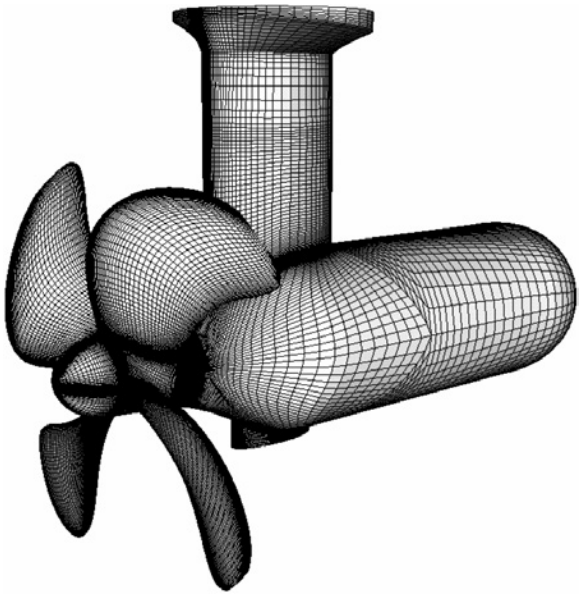

Fig. 30. Discretisation of a pod thruster [24]

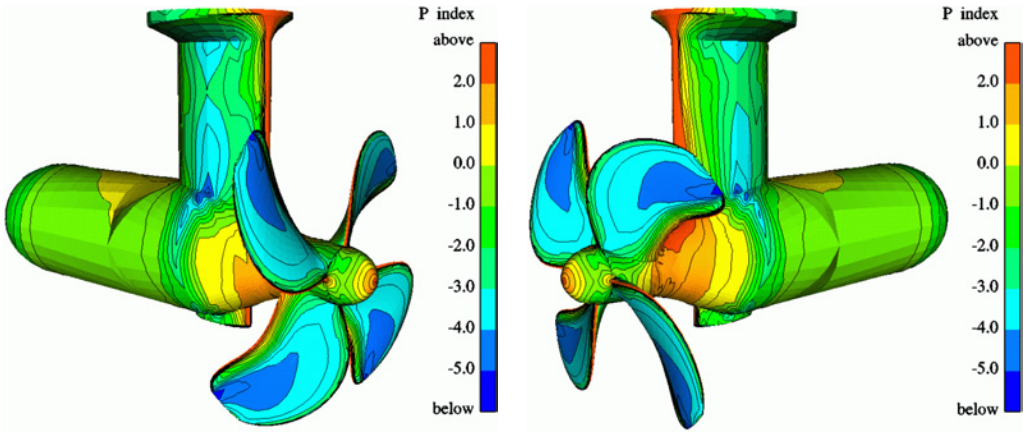

Fig. 31. Pressure distribution on a pod thruster calculated using RANSE [24]

Waterjets are nowadays widely applied for propulsion of many kinds of vessels with speeds above 25 knots. Design of waterjets leads to a number of specific hydrodynamic problems. One of them is the interaction between the rotor and stator in the pump of a high speed waterjet. Scheme of the axial flow pump is shown in Figure 32, with the rotor having 5 blades and stator having 8 blades. Analysis of the rotor/stator interaction presented in [32] is carried out using RANSE (k–ε turbulence model) with so called mixing plane approach, where average interaction velocities between rotor and stator are computed. The comparison of calculated and measured rotor torque is shown in Figure 33. This comparison shows the tendency to underestimate torque in calculations, which points to some deficiency of the applied computational method.

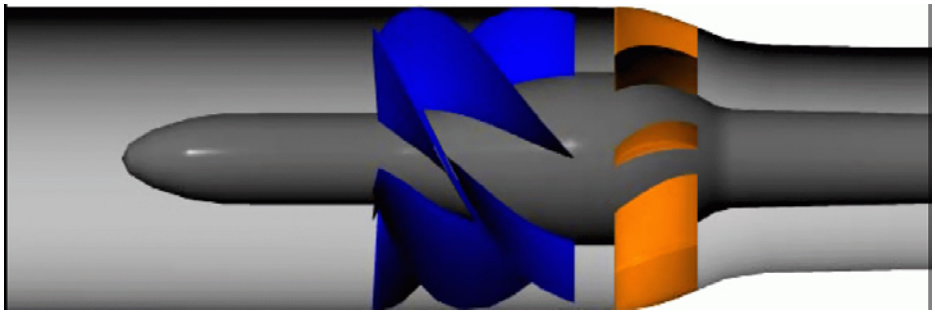

Fig. 32. Scheme of the axial waterjet pump [25]

In today's practice waterjet propulsors are designed by specialized manufacturers. However, it is the responsibility of the ship designer to provide an optimum inflow to these propulsors by the appropriate design of the hull geometry. Solution of such a task for a twin propulsor ship is described in [26]. Figure 34 presents the RANSE

calculated velocity profile in the hull boundary layer and at the pump inlet (excluding the shaft effect). In Figure 35 the comparison of RANSE computed and experimentally measured axial velocity distribution at the waterjet pump inlet is shown (including the shaft). The agreement between calculation and experiment seems to be quite satisfactory.

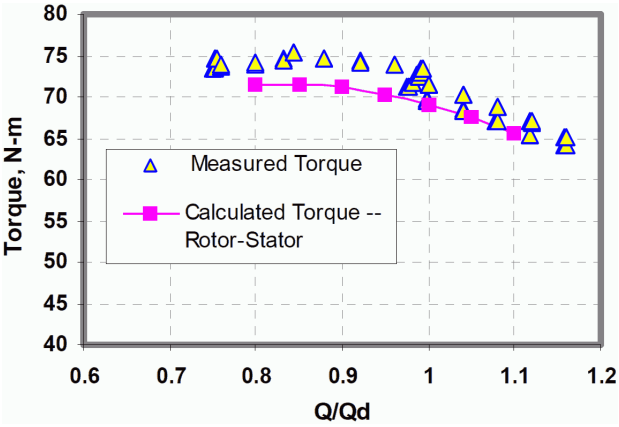

Fig. 33. Measured and calculated rotor torque [25]

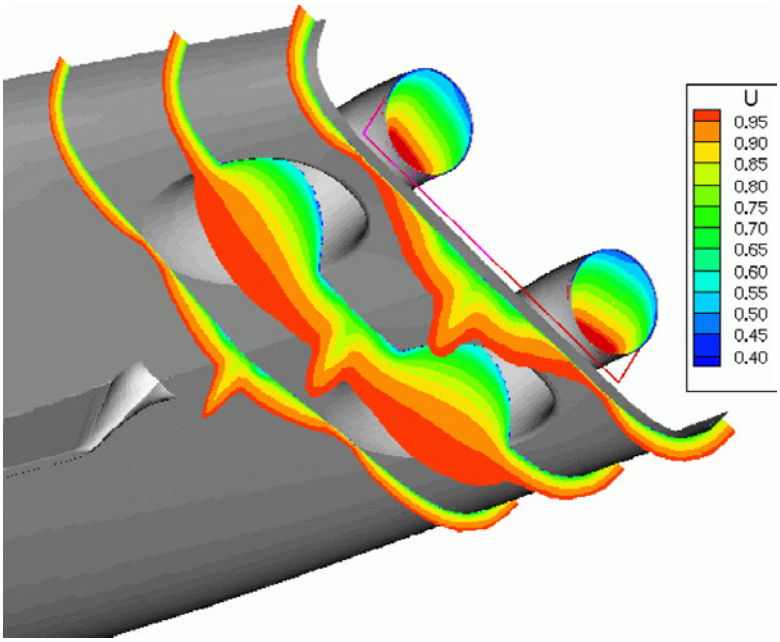

Fig. 34 Calculated velocity at twin waterjet inlet [26]

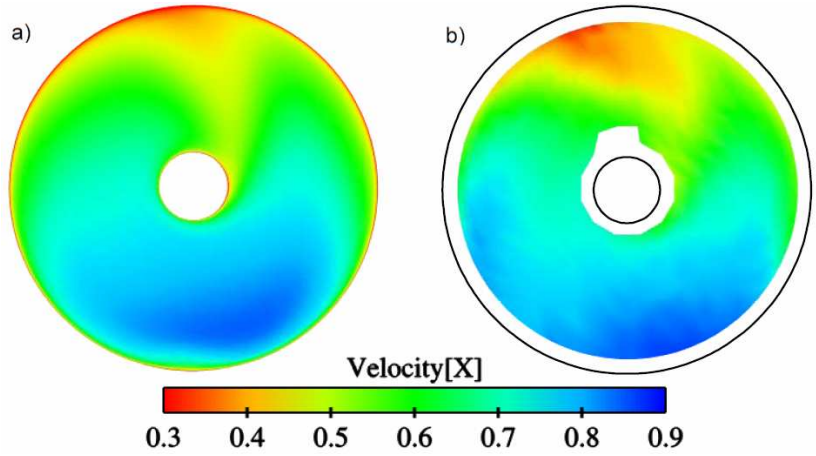

Fig. 35. Comparison of the calculated and measured velocity at waterjet pump inlet [26]

8. Summary

The detailed analysis of the above presented problems of computational fluid dynamics methods applied to ship propellers leads to the following conclusions:

- thanks to the rapid progress in computer technology the most advanced CFD methods like LES and DNS are becoming a practical tool for analysis of the complicated propulsor flow problems,
- these methods give unprecedented new possibilities of deeper insight into complex phenomena like tip vortex formation, strongly dynamic flows associated with unsteady propeller operation and development of different forms of propeller cavitation,
- RANSE methods are today a routine approach to propulsor flow analysis, however they require further refinement of the discrete grid structures and turbulence models optimized for this specific category of flows,
- "old methods" like lifting surface or BEM are still an effective tool for more traditional propulsor flow computations, thanks mainly to the extensive accumulated experience and validation results,
- all Computational Fluid Dynamics methods can be effective only in close mutual inter-relation with advanced experimental techniques used in model and full scale experiments. This inter-relation generates synergetic effects, which stimulate progress both in CFD and in the field of experimental fluid mechanics.

References

[1] Carlton J.: *Marine Propellers and Propulsion*, Butterwoths&Heinemann, London, 1995.
[2] Dymarski P. *Calculation of the viscous flow around a foil and a propeller using finite volume method*, Ph D. Thesis (in Polish), Gdańsk University of Technology, 2007.

[3] Ferziger J.H., Peric M.: *Computational methods for fluid dynamics*, Springer, 1999.
[4] Lee C.S., Kim G.D., Kerwin J.E.: *A B-Spline based higher order panel method for analysis of steady flow around marine propeller*, 25th ONR Symp. on Naval Hydrodynamics, Newfoundland, Canada, 8–13 August, 2004.
[5] Lee C.S. et al: *Propeller steady performance optimisation based on discrete vortex method*, 26th ONR Symp. on Naval Hydrodynamics, Rome, Italy, 17–22 September, 2006.
[6] Han K.J., Larsson L., Rengstroem B.: *Numerical optimisation of the propeller behind a ship hull at full scale*, 26th ONR Symp. on Naval Hydrodynamics, Rome, Italy, 17–22 September, 2006.
[7] Li D.Q., Berchiche N., Janson C.E.: *Influence of turbulence model on the prediction of full scale propeller open water characteristics with RANS methods*, 26th ONR Symp. on Naval Hydrodynamics, Rome, Italy, 17–22 September, 2006.
[8] Sanchez Caja A., Sipla T.P, Pylkkanen J.V.: *Simulation of the incompressible viscous flow around an endplate propeller using a RANSE solver*, 26th ONR Symp. on Naval Hydrodynamics, Rome, Italy, 17–22 September, 2006.
[9] Jessup S., Fry D., Donelly M.: *Unsteady propeller performance in crashback condition with and without a duct*, 26th ONR Symp. on Naval Hydrodynamics, Rome, Italy, 17–22 September, 2006.
[10] Vysohlid M., Mahesh K.: *Large eddy simulation of crashback in marine propellers*, 26th ONR Symp. on Naval Hydrodynamics, Rome, Italy, 17–22 September, 2006.
[11] Young Y.L. et al: *Numerical and experimental investigation of composite marine propellers*, 26th ONR Symp. on Naval Hydrodynamics, Rome, Italy, 17–22 September, 2006.
[12] Greco L., Salvatore F., Di Felice F.: *Validation of a quasi-potential flow model for the analysis of marine propeller wake*, 25th ONR Symp. on Naval Hydrodynamics, Newfoundland, Canada, 8–13 August, 2004.
[13] Abdel-Maksoud M., Helkig K., Blaurock J.: *Numerical and experimental investigation of the hub vortex flow of a marine propeller*, 25th ONR Symp. on Naval Hydrodynamics, Newfoundland, Canada, 8–13 August, 2004.
[14] Kim S.E., Rhee S.H.: *Towards high fidelity prediction of tip vortex around lifting surfaces*, 25th ONR Symp. on Naval Hydrodynamics, Newfoundland, Canada, 8–13 August, 2004.
[15] Bensow R.E., Lieferdahl M., Wikstroem N.: *Propeller near wake analysis using LES with a rotating mesh*, 26th ONR Symp. on Naval Hydrodynamics, Rome, Italy, 17–22 September, 2006.
[16] Turnock S.R., Pashias C., Rogers E.: *Flow feature identification for capture of propeller tip vortex evolution*, 26th ONR Symp. on Naval Hydrodynamics, Rome, Italy, 17–22 September, 2006.
[17] van Terwisga T.: *Cavitation research on ship propellers – A review of outstanding problems and research strategies*, CAV'06 Intern. Conf. on Cavitation, Wageningen, The Netherlands, September, 2006.
[18] Chahine G.L.: *Nuclei effects on cavitation inception and noise*, 25th ONR Symp. on Naval Hydrodynamics, Newfoundland, Canada, 8–13 August, 2004.
[19] Hsiao C.T., Join A., Chahine G.L.: *Effect of gas diffusion on bubble entrainment and dynamics around a propeller*, 26th ONR Symp. on Naval Hydrodynamics, Rome, Italy, 17–22 September, 2006.

[20] Persson T. et al: *Large eddy simulation of the cavitating flow around a wing section*, CAV'06 Intern. Conf. on Cavitation, Wageningen, The Netherlands, September, 2006.
[21] Vaz G., Bosschen J.: *Modelling 3D sheet cavitation on marine propellers using BEM*, CAV'06 Intern. Conf. on Cavitation, Wageningen, The Netherlands, September, 2006.
[22] Wosnik M., Arndt R.E.A.: *Identification of large eddy structures in the wake of cavitating hydrofoils using LES and time resolved PIV*, CAV'06 Intern. Conf. on Cavitation, Wageningen, The Netherlands, September, 2006.
[23] Xiong Y.L., Gao Y., An W.G.: *Comparison of turbulence models in predicting unsteady supercavitating flows*, CAV'06 Intern. Conf. on Cavitation, Wageningen, The Netherlands, September, 2006.
[24] Sanchez-Caja A. et al.: *Simulation of incompressible viscous flow around a tractor thruster in model and full scale*, 8th Intern. Conf. On Num. Ship Hydrodynamics, Busan, Korea, 22–25 September, 2003.
[25] Brewton S., Gowing S., Gorski J.: *Performance prediction of a waterjet rotor and R/S combination using RANS calculation*, 26th ONR Symp. on Naval Hydrodynamics, Rome, Italy, 17–22 September, 2006.
[26] Ebert M.P., Gorski J.J., Coleman R.M.: *Viscous flow calculation of waterjet propelled ships*, 8th Intern. Conf. On Num. Ship Hydrodynamics, Busan, Korea, 22–25 September, 2003.

Kluczowe współczesne problemy metod obliczeniowych hydrodynamiki pędników okrętowych

Referat przedstawia przegląd aktualnego stanu współczesnych metod obliczeniowych używanych w hydromechanice pędników okrętowych, wskazując na kluczowe problemy, na których uwaga międzynarodowej społeczności badaczy jest, lub powinna być, skoncentrowana. Przegląd jest oparty na referatach wygłoszonych na ważnych konferencjach międzynarodowych w ciągu ostatnich czterech lat. Na wstępie pokrótce przedstawiono cztery podstawowe kategorie metod obliczeniowych mechaniki płynów: tradycyjne metody linii i powierzchni nośnej, metody elementów brzegowych (BEM), metody uśrednionych przez Reynoldsa równań Naviera-Stokesa (RANSE) oraz metody numerycznego symulowania koherentnych struktur wirowych (LES) i bezpośredniego numerycznego rozwiązania równań Naviera-Stokesa (DNS). Następnie problematyka zastosowania tych metod do specyficznych problemów hydromechaniki pędników okrętowych jest przedstawiona bardziej szczegółowo. Ta prezentacja rozpoczyna się od wąsko zdefiniowanego zadania projektowego, czyli określenia geometrii śruby napędowej spełniającej zadane parametry dynamiczne: prędkość statku oraz napór i obroty śruby. Potem przedstawiono problemy wyznaczania skomplikowanego opływu śruby okrętowej o zadanej geometrii, również w trakcie manewrowania lub z udziałem zjawiska hydroelastyczności. Następnie przedyskutowano problem określania generowanych przez pędniki śladów wirowych oraz przewidywania różnych form zjawisk kawitacyjnych i ich hydrodynamicznych konsekwencji. Oddzielna część referatu jest poświęcona pędnikom niekonwencjonalnym, koncentrując się na dwóch najważniejszych: pędnikach gondolowych i pędnikach strugowodnych. Referat kończy podsumowanie wskazujące kierunki przyszłych badań i zastosowań metod obliczeniowych w hydromechanice pędników okrętowych.

ARCHIVES OF CIVIL AND MECHANICAL ENGINEERING

Vol. VIII 2008 No. 1

Computation of flow around inland waterway vessel in shallow water

TOMASZ TABACZEK
Wrocław University of Technology, Wybrzeże Wyspiańskiego 27, 50-370 Wrocław

Flow around an inland waterway vessel in shallow water was computed in model scale using CFD software Fluent. Theoretical data were compared to the results of measurements in towing tank. The comparison comprises ship resistance, wave profile on hull surface, and distribution of velocity in flow around bow and stern.

Keywords: *inland waterway vessel, ship flow, shallow water*

Nomenclature
C_F – frictional resistance coefficient,
$C_{F(\text{wofs})}$ – frictional resistance coefficient computed using $R_{F(\text{wofs})}$,
C_{F0} – frictional resistance coefficient of a corresponding plate, calculated acc. to the ITTC'57 model-ship correlation line,
C_T – total resistance coefficient,
$C_{T(\text{wofs})}$ – total resistance coefficient computed using $R_{T(\text{wofs})}$,
Fn – Froude number,
Fn_h – depth Froude number,
h – water depth,
k – form factor,
R_F – frictional resistance,
$R_{F(\text{wofs})}$ – frictional resistance computed without the free surface effect,
R_{PV} – pressure resistance due to viscosity effect,
R_T – total resistance,
$R_{T(\text{wofs})}$ – total resistance computed without the free surface effect,
R_V – viscous resistance,
R_W – wave resistance,
Rn – Reynolds number,
T – ship draught,
V – ship speed.
Subscript $_M$ refers to model scale.

1. Examined vessel

The vessel considered in these computations consisted of two dumb barges coupled stern to stern, an arrangement usual in inland waterborne transportation. A pushboat that provides propulsion for barge train was excluded for simplicity. Hull form of a single barge and main particulars are presented in Figure 1.

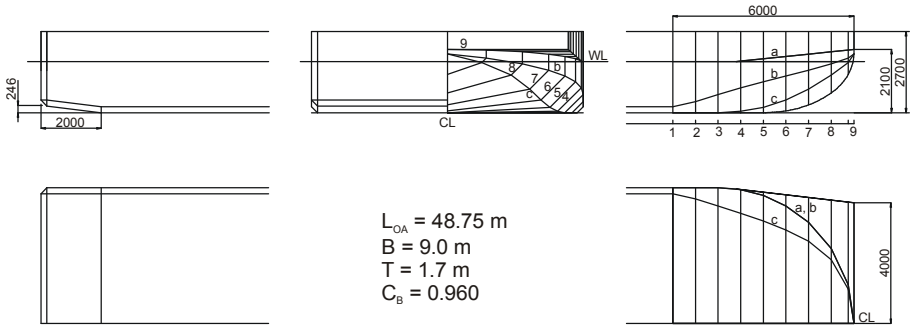

Fig. 1. Hull form of considered vessel

Because the present author intended to compare the results directly (without scaling) to the available experimental data (outcomes from model tests [1]), all computations were carried out in model scale 1:14. All values presented hereafter in this paper refer to model scale.

2. Results

Ship flow was computed for the following 3 cases:

Table 1

Case No.	Model draught T_M [m]	Full scale draught T [m]	Water depth in model scale h_M [m]	Water depth in full scale h [m]	Depth to draught ratio h/T
1	0.0714	1.0	0.0840	1.176	1.176
2	0.1214	1.7	0.1429	2.0	1.176
3	0.1214	1.7	0.2429	3.4	2.0

The first two cases correspond to extremely shallow water.

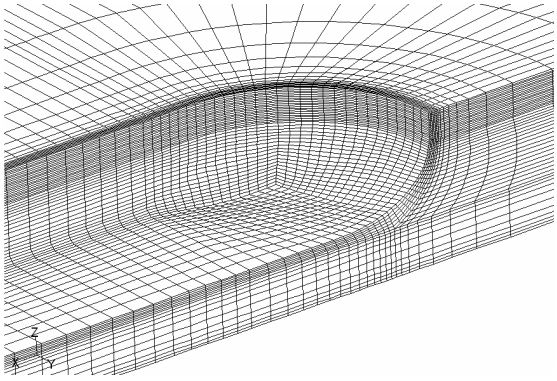

Fig. 2. Computational grid

CFD computations were carried out using the Fluent software. Neither trim nor sinkage were taken into account. Computational domain was extended 2.95 m in front of bow and behind stern and 3.25 m away from ship side. The grid consisted of 92.000 to 188.000 cells (cf. Figure 2), depending on case, and was constructed to capture flow phenomena close to hull surface. Cell dimensions increase rapidly towards the borders of computational domain and it was impossible to reproduce the wave pattern in present computations. In order to account for the effect of free water surface around vessel the volume of fluid (VOF) model was used in computations.

2.1. Resistance

Computed model ship resistance was compared to measured data in Figure 3.

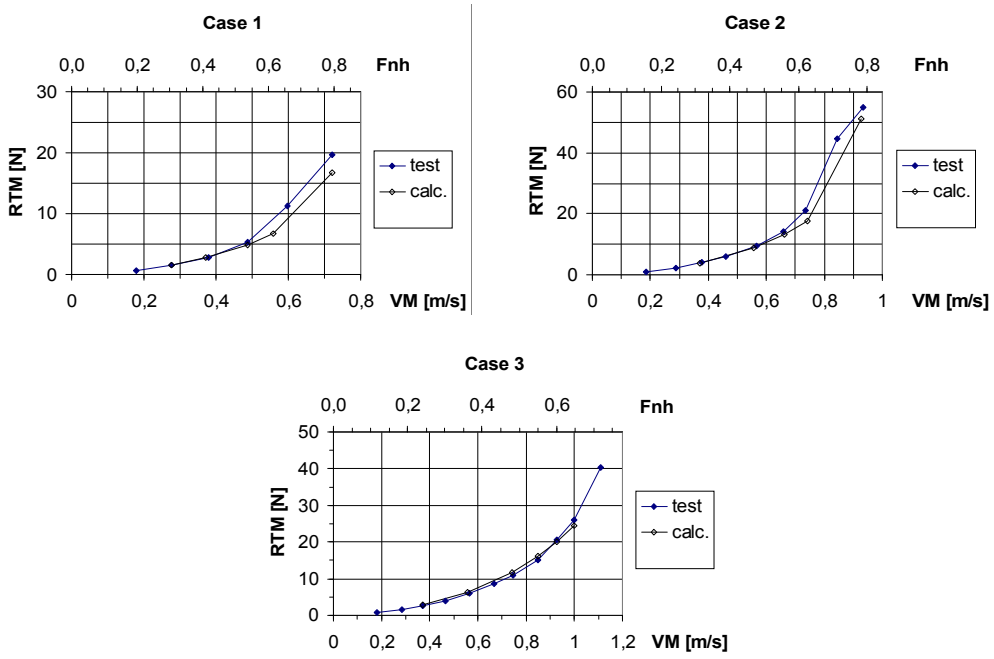

Fig. 3. Model ship resistance

Computations predicted the resistance quite well at ship speed up to Fn_h of about 0.55. Above that speed the results of test and computations start to diverge. The measurements in towing tank were carried out with model free to trim and sinkage. Closer investigation of test results, especially of trim data, revealed that at $Fn_h \approx 0.55$ trim rapidly starts to increase (Figure 4). One may consider the CFD computations without account for trim as reliable up to that specific speed. At higher speeds ship trim and presumably sinkage have to be taken into account for better results of computations. On the other hand it is well known that operation of inland waterborne vessels at

Fn_h > 0.6 is not economically justified. In the following the discussion of data will be confined to ship speed below Fn_h of 0.55.

Despite its shortcomings, CFD enables easier insight into flow than measurement. That advantage was used to examine the share of frictional, viscous and wave resistance.

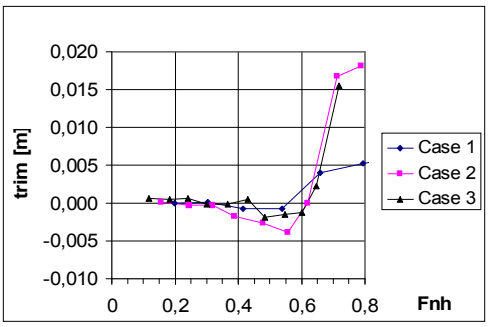

Fig. 4. Trim of vessel measured in model test

Total resistance is usually decomposed into viscous and wave resistance:

$$R_T = R_V + R_W.$$

Viscous component consists of frictional resistance and pressure resistance due to viscosity effect:

$$R_V = R_F + R_{PV}.$$

The frictional resistance R_F is understood as resistance component due to tangential stress on hull surface and is directly computed by Fluent (the term "viscous force" used in Fluent manuals is misleading, in fact that force is computed by integration of tangential stress). In the following viscous resistance is approximated by total resistance computed without the free surface effect:

$$R_{VM} = R_{TM(\text{wofs})}.$$

The wave resistance can than be evaluated indirectly by subtracting the total resistance computed without free surface effect from the total resistance computed with free surface effect:

$$R_{WM} = R_{TM} - R_{TM(\text{wofs})}.$$

The proportions between the resistance components are illustrated in Figure 5. In considered range of ship speed (Fn < 0.102) the wave resistance in model scale R_{WM} makes 20 to 37% of total resistance R_{TM}.

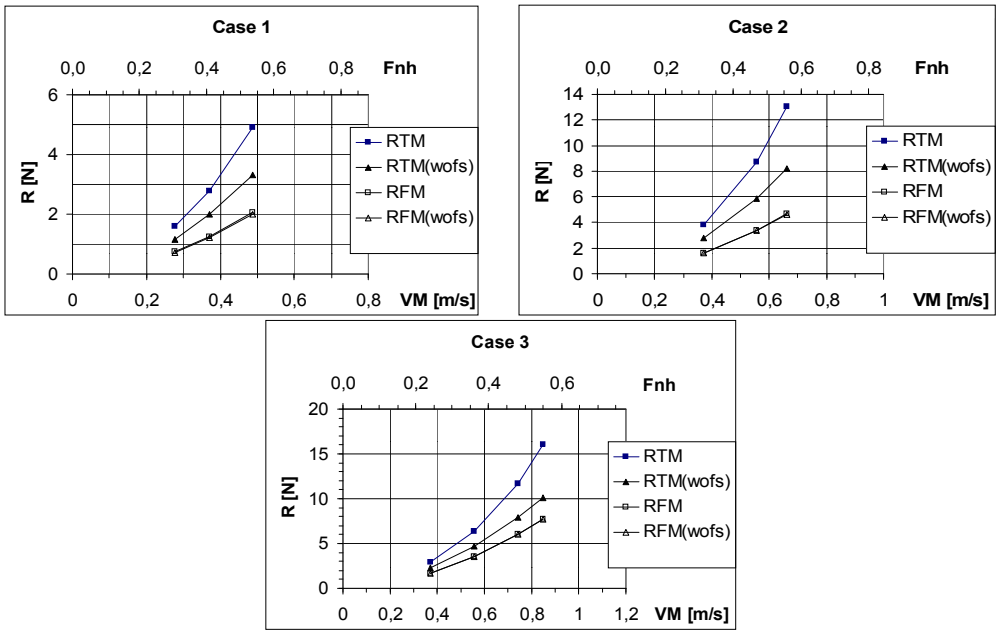

Fig. 5. The share of resistance components in model scale

The computed values of resistance were applied to estimate the form factor k that is used in scaling the model ship resistance to full scale according to the method of 3D-extrapolation, the procedure that is still in common use. Values of $1 + k$ presented Table 2 were calculated using the resistance computed without free surface effect and the resistance coefficient of flat plate C_{F0M} based on the ITTC'57 model-ship correlation line:

$$1 + k = C_{TM(\text{wofs})}/C_{F0M}$$

Table 2.

V_M [m/s]	Fn_h	Fn	$Rn_M \times 10^{-6}$	$C_{TM(\text{wofs})} \times 10^3$	$C_{FM(\text{wofs})} \times 10^3$	$C_{F0M} \times 10^3$	$1 + k$	$1 + k$ acc.to [2]
Case 1								
0.277	0.305	0.034	1.70	5.88	3.62	4.19	1.40	
0.371	0.409	0.045	2.28	5.61	3.40	3.95	1.42	1.59
0.488	0.538	0.059	3.00	5.35	3.26	3.74	1.43	
Case 2								
0.371	0.313	0.045	2.30	6.77	3.88	3.94	1.72	
0.557	0.471	0.067	3.45	6.41	3.66	3.64	1.76	1.56
0.663	0.560	0.080	4.10	6.32	3.57	3.52	1.79	
Case 3								
0.371	0.240	0.045	2.30	5.76	4.31	3.94	1.46	
0.557	0.361	0.067	3.45	5.28	4.00	3.64	1.45	1,27
0.742	0.481	0.090	4.60	5.01	3.81	3.45	1.45	
0.847	0.549	0.102	5.25	4.90	3.73	3.37	1.46	

2.2. Wave profile on hull surface

In Figure 6 the computed free surface profiles on hull surface are compared to the profile recorded on photographs during model test. Experimental data were adjusted to general frame of reference using the measured trim. It was impossible to read the height of wave profile at hull center plane from photographic documentation. The remaining data reveal that wave lengths are reproduced well but heights of wave crests and depths of troughs are underestimated. This is due to the computational grid that was not fine enough to capture the wave propagation.

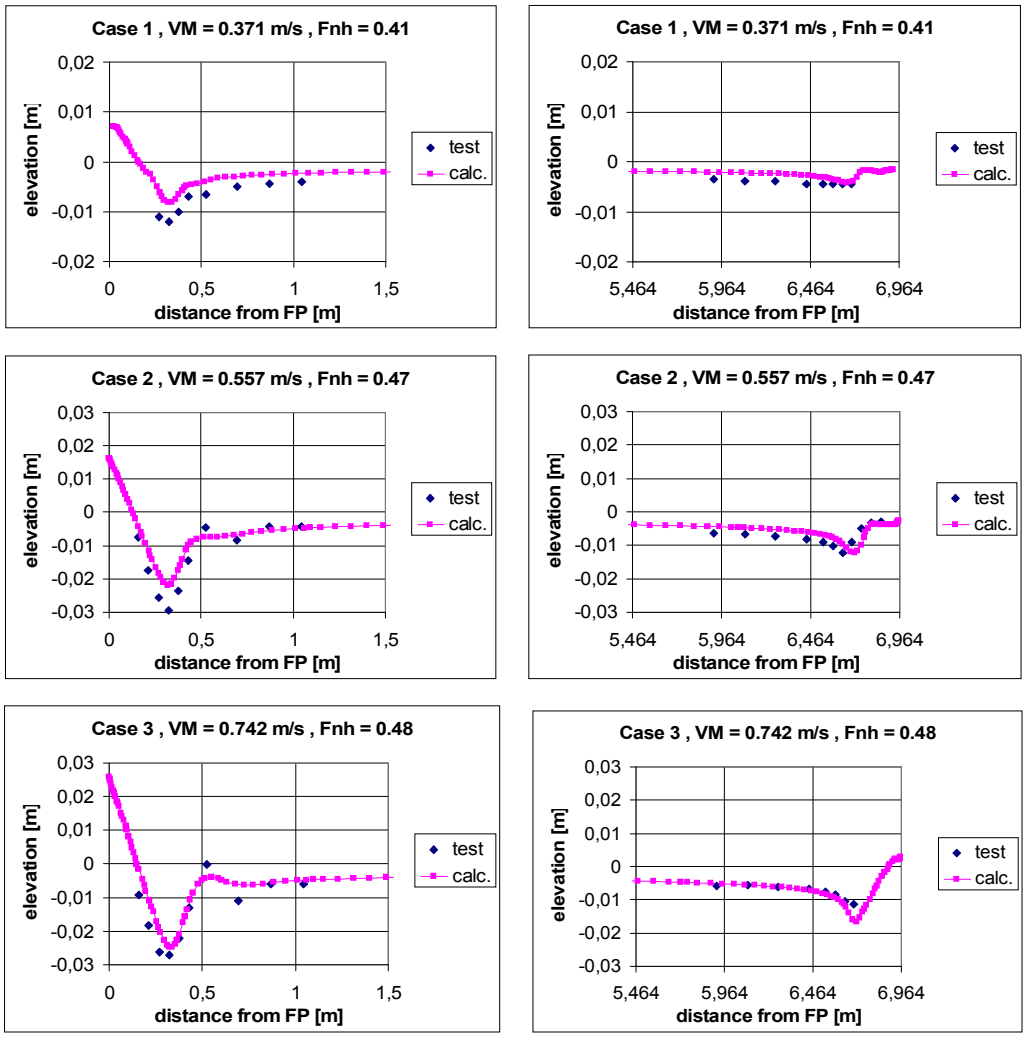

Fig. 6. Wave profile on hull surface

2.3. Distribution of velocity in flow around vessel

Three components of velocity in flow were computed and measured in transverse planes located 0.214 m from fore and aft transoms towards midship. Both computation and test were carried out for Case 2 and model speed of 0.663 m/s. The velocity was measured using the 5-hole pressure probe. Sample results of computations are shown in Figure 8 and 9, on the background of rough results of measurement.

X and Z velocity components were predicted by computations well in comparison with test data. Computed Y-components are overestimated, but the profiles are similar. The reason of that regular discrepancy remains unknown.

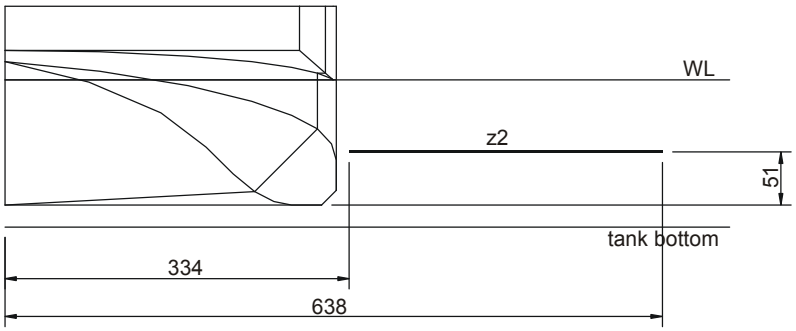

Fig. 7. Position of velocity profiles shown in Figures 8 and 9

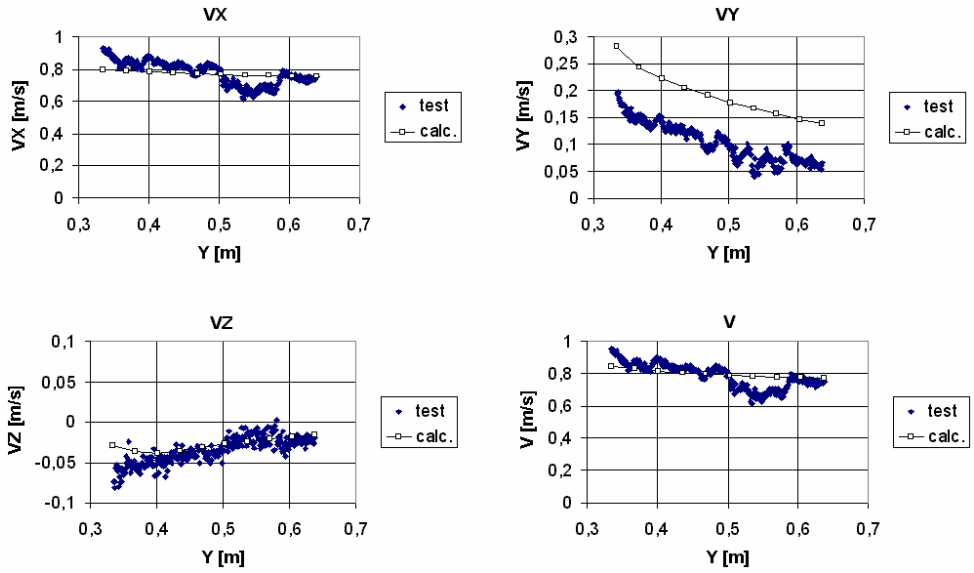

Fig. 8. Components of velocity in flow around bow, the profiles along line z2 located 0.051 m above base plane

3. Conclusions

CFD software Fluent is capable to compute the free surface flow around inland waterway vessel in shallow water to the extent enough to predict ship resistance with satisfactory precision. More thorough tests and uncertainty analysis would quantify that precision. At ship speed below Fn_h of 0.55 the resistance was computed quite precisely without account for trim and sinkage.

Based on results of computations with and without free surface effect one is able to separate the frictional, viscous and wave resistance.

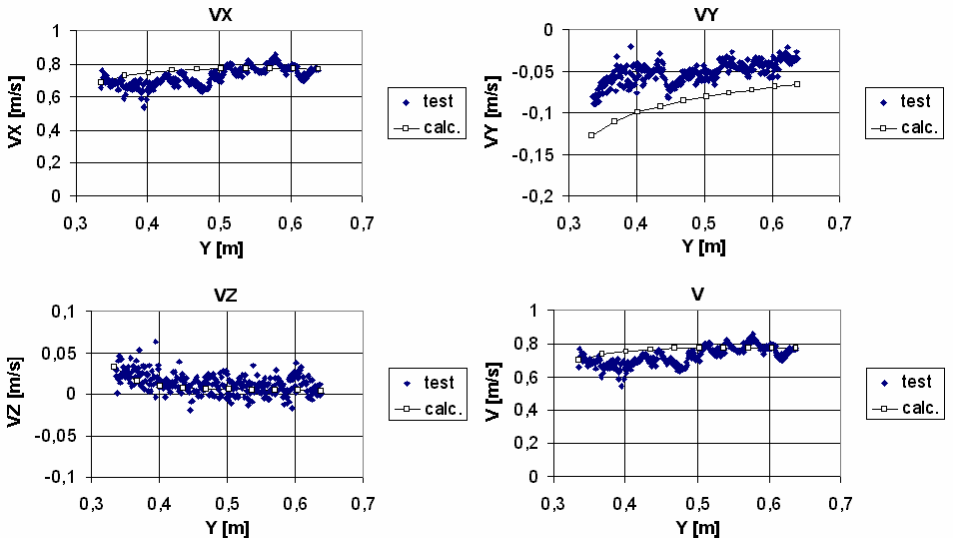

Fig. 9. Components of velocity in flow around stern, the profiles along line z2 located 0.051 m above base plane

The resistance computed without free surface effect is a reasonable alternative in determination of the form factor to be used in extrapolation of ship resistance from model to full scale in shallow water.

The density of computational grid was not enough to reproduce precisely the wave pattern on free surface, even the wave profile on hull surface. Correct results of total resistance suggest, however, that the height of profile at hull center plane, that is crucial for wave resistance, was predicted accurately.

References

[1] Grzybowski, P.: *Zestaw barek śródlądowych, model M659, wyniki prób modelowych na wodzie płytkiej - opór, pomiar fali, pole prędkości*, Report RH-2006/T-040, Ship Design and Research Centre S.A., Gdańsk, June, 2006.

[2] Millward, A.: *The Effect of Water Depth on Hull Form Factor*, International Shipbuilding Progress, Vol. 36, No. 407, 1989.

Obliczanie przepływu wokół statku śródlądowego na wodzie płytkiej

Przy użyciu programu komputerowego Fluent obliczany był przepływ wokół kadłuba statku śródlądowego w skali modelu. Wyniki obliczeń zostały porównane z wynikami pomiarów w basenie holowniczym. Porównanie obejmuje opór kadłuba, profil fali na powierzchni kadłuba i rozkład prędkości przepływu w pobliżu dziobu i rufy.

ARCHIVES OF CIVIL AND MECHANICAL ENGINEERING

Vol. VIII 2008 No. 1

The affect of human feelings on creation of housing

B. GRONOSTAJSKA
Wrocław University of Technology, Wybrzeże Wyspiańskiego 25, 50-370 Wrocław

In the paper the relation between architects and human being and the role of places in creation of human architecture are analyzed. It was shown that even the most of results are obvious on the base of observation the expensive empirical researches are needed to find the proper solution in relation between architects, human being and environment. How relevant should research be to solving the problems is very important for architect and planners. The answer is a particularly difficult question because architecture involves different connections, which are considered on various levels. Architects and planners have designed neighbourhoods, cities, and transportation systems, which attempt to achieve the maximum accessibility to places and facilities for all people who live there. Some people have little choice in moving around within the environment and so have limited opportunity to use a variety of places. When a place is design and constructed, certain assumptions should be also made about its share use. Some places are designated for exclusive use of a specific person or group, but in order for certain activities to occur, many environments must be shared for large number of people, but cannot function for just one individual. In order to judge a place, people need standards and/or criteria to identification it. Problems can only be solved if people have some basis for comparison.

Keywords: *housing, human feelings, creation, design, places, factors*

1. Relation between architects and humans being

Many architects spend time and energy at experimental researches that have been heavily criticized from the point of view that most of the results are obvious on the base of usual considerations without expensive empirical researches. The question is while in such situation a lot of effort, energy and money have been spent on such researches, while they could be used on the most effective targets. It can be seen that such criticism true on the first view, after more precise investigations could be wrong [1].

Since every kind of human reaction is conceivable, it is of great important to know which reaction actually is most probable in defined circumstances. Only then a more advanced understanding of the man - environment relationship can be received, which should undoubtedly have substantial effects upon behaviour of architects.

How relevant should research be to solving the problems is very important for architect. The answer is a particularly difficult question because architecture involves different connections which can be considered on various levels. Is the design at conceptualization stage more relevant than design when the information how the people use designed buildings are available by architect? Such diversity of information could

be valuable, but it depends on people particular needs and characters. It is the first difficulty in definition of relevance of actual solution.

The second difficulty in definition of relevance is numerous number of variables involved in each solution. The answer to the problem solved in Poland do not must be the same as solution of similar problem in Egypt, because a different political, economical and social situation in both countries exist. Before architect could apply the same solution in both countries, he ought to be sure that the results in one country is valid in the other one. Besides many environmental conditions are difficult to quantify and the use of subjective judgments is questionable, and interdependence of large number of different variables against environmental conditions makes analysis even harder. People respond not only to one incident at a time but to the total event, the response depends on age, sex, experience and emotion state.

The third degree of confidence of experimental results will influence their relevance. Even if the results are statistically significant and proper determined sometimes they cannot be accepted because of suspecting that independent, substantial variables have not been taken into account. The following example confirms this sentence, that not child-birth causes tooth decay as it common thought, but calcium deficiency. Sometimes it can be possible to find relevant answer to a problem without understanding why that is, without understanding the complex phenomena involved.

Some of the problems related to research and applicability are named as "data paradox", that means the better is examined the problem the more remote to everyday life it is, though it is scientifically respectable; on the other hand the grater the number of variables involved the more relevant will be to everyday life, though it solution maybe scientific dubious.

Taking into account the above difficulties about proper determination of reality, architect may be convinced that the best and easiest way is to forget the whole things and design completely by his own intuition. It results from the fact that architect is not trained and educated to distinguish which is reality and which is fiction, and the easiest way out is to built his own preconceived ideas, theories and design philosophy.

The architect should be educated in such a way to appeal to three philosophical methods: authority, tenacity and intuition. The authority method states that something is true. The tenacity method is to believe something is true because one has always believed it. According to intuition method a statement is felt to be true because it is self-evident.

Architect who practices on the basis of his own personal design philosophy or by applying his own creative talent should not be condemned. But he should test his ideas against knowledge of people both from psychology and from those architects who have succeeded in designing pleasing and humane environments.

The redefinition of architect's role in relation to his understanding of people is needed because the people should not be convinced that they are content with what architect providing for them, but he should ask people what they want. Architecture is designing beautiful buildings, full of fantastic qualities. Architecture is something

which will enable architect to express himself, blow his mind without any constrains. From the other hand the beautiful and fantastic buildings create the different reaction of people. Architectural psychology seeks to find out why people react to building differently [2].

In recent years serious attempts in education to influence the quality of teaching take place, the example there are habitat conferences organized by Bać [3]. There are great difference between reading about human behaviour and understanding it in a fashion which will be useful for design. Architecture integrates information from other sciences (psychology, physics, engineering, zoology, anthropology, sociology and others) in attempt to understand people.

The crucial task for architectural investigation is to tell architects the truth how much people do know and what they are likely to find out in the near future in the pursuance of empirical science. People need to establish which experiments have direct or indirect design implications, what type of work is helpful in identyfing problems and which studies are interesting or simulating.

Nor should people pursue further the question of relevance. People must accept that some findings will and some will not be relevant to them. It would be presumptuous to define the limits of diversity or to state categorically what specific relevance the work should have.

Getting people involved at all levels of decision making, from social planning to the later stage of architectural and urban design, so that they feel they are an active and contributing part of the environment they live in, has led since then to become the subject of a serious and ongoing debate. The word democracy means that the decisions about people are made by the demos, i.e. by the people themselves. Within each democracy the way in which participation and involvement is effected by people in their day-to-day affairs depends primarily on political, economic and social conditions. Some argue that architects and planners have very little to do with the way in which people's lives and that the quality of live is overwhelmingly the product of political and economic considerations.

Planning for people is the title of book by Broady [4] in which he advocates that people, through voluntary associations and other bodies should be much more involved in social planning. Planning has to be thought of not only as a matter of physical design and economic policy, but also as an educational social process which seeks to encourage the contributions which people themselves can make to the improvement of their own social environment.

If dwellers can be able to control the major decisions and are free to make their own contribution to the design, construction or management of their housing both the process and the environment product simulate individual and social needs. When people have no control over nor responsibility for key decisions in the housing process, dwelling environments may instead become a barrier to personal fulfillment and a burden on the economy.

Citizen participation, consultation, fashionable phrases lead to conclusion so many people feel that too much is being said about the process and that very little has been done about it. The importance of real participation in practice can hardly be over –estimated, provided that the right participatory approach is used in the right circumstances and is acted after the problem has been identified. Participation must not become a mere cosmetic attempt to appease people or to hide other considerations.

One of the most important results of this paper is the directive towards the redefinition of the role of the architect. Without ignoring aesthetics the architect should fill a basically support role, helping people to be more resourceful and to identify and participate with their environments in every possible way, and liberating their latent creativity, so often suppressed in by industrialized society.

By referring to human needs the architect might aspire to understand people better. But danger is that he will become more confused than ever, or even that he will take up the false position of eloquently justifying his design decisions by reference to some obscure conscious or unconscious human need. The complexity and richness of personality patterns. the multiplicity of biological and socio-cultural determinants make his task of formulating an adequate understanding of personality extremely difficult until he tempers his knowledge with real-life experience. The most likely outcome is that architect will tend towards one particular standpoint, instead of attempting to understand the diversity and richness of human needs [5].

What the human needs? Are individual needs different from social needs? Do modern environments satisfy basic needs? How far are architects and planners responsible for these environments? Do buildings or the lay-out of cities influence people living needs and habits? Or is it merely a question of the environment inhibiting or facilitating some of people routine behaviour until, after some time, the human capacity to adapt enables people to reestablish control of the situation. Perhaps environments only provide the context in which the more important influence of social and economic conditioning determine people behaviour argue that to consider that environment determines people behaviour is anathema, an insult to people intelligence.

2. The role of places in creation of human architecture

Places are all around people, form alcoves, bars, churches, yards, zoos and etc. Places are not only rooms, buildings or out-door spaces, but total environments made up of physical spaces together with people, furnishing, machines and actions. Places form the settings for all the significant and insignificant events of people live. To understand places architects must become actively involved together with the people in definition of places [6].

People have strong feelings about places. Some places make them feel good: glad to be there, relaxed, excited and warm. People are drawn to these places and return to them as often as possible. Other places make people feel bad: uncomfortable, insignificant, unhappy. People avoid these places and suffer if they have to be in them.

People feelings about places are a combination of reactions to the physical nature of the place and to what is happening or has happened to somebody [7]. While the promise or memory of an enjoyable time can make a natural or even miserable environment attractive, an unpleasant event can transform a nice place into one without feeling returning to. On the other hand, physical properties can themselves make places pleasant or unpleasant. It can be very difficult to separate these aspects, since places are complex wholes which combine physical and human qualities.

People react differently to the same place, not only in the intensity of their reactions, but even in the basic direction of their feelings. One person might love a place which another hates, or each may love it for different reasons. Although people share their feelings about places with other people, variation in reactions results from differences in personality, cultural values, or previous experience. Relatively few places are universally acclaimed as wonderful or horrendous.

In people memories, places are often transformed; their size, shape, colour and décor [8]. Places offer the opportunity for solitude, comfort, privacy, retreat, separation between ourselves and others. It may be a real place, or may exist in fantasy only. From time to time the most of people need some space in which they feel more alone; space for collecting and defining them, and for dealing with their personal problems and joys. Seeking retreat, people can be able to find secret places, which vary according to where they live. In the city a secret place might be a rooftop, while in the suburbs it might be a tree house or car. For some people living in crowded conditions or lack of mobility make it difficult to have a secret place. Sometimes the only secret place people can find is deep inside themselves.

A pleasure dome is a place for enjoyment, fantasy, and delight if can be public or private, indoors or out, any size, shape, or style. Through using places people develop and expand their understanding of them [8].

Homes, work places, and the paths that connect them comprise the environments people use most in their daily lives. In these places people satisfy their needs and achieve a variety of objectives, from washing the dishes or growing vegetables to typing or talking on the telephone. Since people can't do everything in the same place, they move around to where they can find the people, space or facilities they need to do what they want.

People interact continually with the places where they live and work, altering them but also adapting themselves lives to their potentials and limitations. People feeling about space are reflected by their choice of a place to live. For most adults, buying a house is the single largest investment they ever make, with the greatest impact on their life-style. Choosing an apartment can be equally important in terms of the potential impact of its size, arrangement or location.

Many houses are specifically design to appeal to a particular style of living. On the other hand the places people live may also limit their activities, e.g. by not having north light for painting.

Using places, people alter them to suit their needs. To enable people to do the

things they wish and to show their selves to others, they distinguish their territories from those of other people and customize them to express their individuality. There are three types of changes: small-scale changes, such as hanging a pictures, larger scale changes, such as reorganizing the office and permanent changes, such as remodelling the waiting room. Many times, it is easier to move to a new place than to make extensive changes to an existing one.

People express individuality in their immediate surroundings of homes, in their work places, and in the objects and image they choose. People need opportunities to express their selves in the places, often feeling frustrated and alienated if they cannot personalize them. These limitations on personalization of places are sometimes codified, as in prison regulations or rental agreements.

People occupy a certain amount of space depending how important they are and what they are doing. Different activities require different amounts of space; visualize two similar activities which might occur on a farm sorting watermelons and sorting walnuts. The area required for performing an activity depends on several factors, including how big people are, how many of them are involved, what they are doing, and what they are using. Two different people may require different amount of space to perform the same activity, depending on how they move or feel [9].

People spend a lot of time moving around between buildings and within them; from school to home, from work to shopping, from lunch to the office. People go from the desk to the water cooler, from the bedroom to the bathroom, from the garage to the living room. Travel may take a significant proportion of their time.

Some people have little choice in moving around within the environment and so have limited opportunity to use a variety of places. Architects and planners have designed neighbourhoods, cities, and transportation systems which attempt to achieve the maximum accessibility to places and facilities for all people who live there. Sometimes these designs involve separating the routes of pedestrians, bicycles, cars, and buses. Other proposals have pedestrian systems linking clusters of houses, shops, schools and work places. Architects design for movement within buildings, with circulation often one of the major factors affecting the form and organization of a building. Corridors can become interior streets and spaces designed for shaping the quality of the experience as one moves through them.

Many people cannot use places easily. Even without a permanent disability, most of people at some time in their lives, will experience some difficulty in making use of the environment. Although the individual have many degrees off restricted mobility. A pregnant woman, a person on crunches due to a skiing accident, a child who is too small to see over countertops, a person pushing an infant in a stroller, someone with poor eyesight and any one with bad physical condition encounters some difficulty using places. Most places are design as if every individual were a healthy adult, but it has been estimated that about 25 % of the population have some characteristics which impairs mobility. Because removing architectural barriers makes the use of places easier for so many of people, barrier free design is likely to become the standard rather

than the exception.

As people use places, they consume energy and resources doing work, moving from one place to another and changing things. Energy changes cold places into warm ones, hot places into cool one, dark places into light ones. Different type of places and different live-styles use different amounts of energy for heating, cooling, lighting, cooking and movement in high-rise buildings.

Concern about limitations on the natural resources available for energy production has been growing in recent years [10]. The way buildings are constructed, the materials they are made from and how people use them determine how much energy they consume. To obtain such results new construction standards and stress thermal insulation and limitations of window areas should be applied.

People spend time in a wide variety of places, choosing them, modifying them and adapting to them. In some places people feel uncomfortable, realizing that they are not suitable for the activities they attempt to do in them. Some places, however, feel right to people, enhance they activities and enrich their lives.

How places work for people depend on how these assumptions compare with people actual preferences. The way people organize and arrange places reflects people systems of classification. Some places tell people a lot about themselves, almost as if they were speaking. They tell people about what happens there and about the people who live there.

Places are defined by boundaries. A boundary marks the edge of the place, physically separating and distinguishing it from its surroundings. The marking of inside and outside is one of the basic physical and symbolic aspects of the built environment [11]. Boundaries enable people to distinguish between places and to associate message, meanings, and rules with them.

There is a great range of physical elements which can act as boundaries. Any change that allows distinction can be a boundary, even a small one such as a difference of materials or a line on the ground. The edge where the sidewalk meets the grass marks a boundary between the public and a private places. A change of level, a row of chairs, a fence, a hedge or a solid wall can separate places. Large-scale boundaries include rivers, mountains, railway tracks and highways.

Boundaries are never total or absolute separations. There are always connections which allow passage from one side to the other. Places can be connected by bridge, a corridor, a gate, a door, a window or a gap in a hedge. Boundaries and connections influence people understanding and use of places, symbolically marking the edges and the transitions between them, likes a door. A door is a place made for an act that is repeated millions of times in a lifetime between the first entry and the last exit. The boundaries and connections act as filters which regulate the flow of information, people, and things from one side to the other.

Places are frequently very different in the front than they are in the back. Images of front bring to mind porches, stoops, portions, front doors, mailboxes, lawns and planters. Image of back bring to mind garages, service entrances, hanging laundry and trash

cans.

The kinds of things placed at front or back are defined by the dominant culture. In some cultures the most important symbol for the front might be the family car, while in other cultures–for example, traditional Spanish or Moslem ones–the back become absorbed into a courtyard where family and female-oriented activities are hidden from public view. Most Western cultures see front yards and entries as faces of places, greeting visitors and acting as a transition zone between the public and the private place.

Places can be shared or private. Shared places are those where people meet others–strangers, friends or family members, while private places are those where people do things alone or have sole control over what happens. Both places are needed for the variety of activities in people lives. Although places may be claimed as the exclusive territory of one individual or group, they may also be shared by many people. Sharing places can take many forms some places are always shared, like a bus station, others are exclusive for a short period of time, like a motel room; while still others may be shared in one situation and exclusive in another, such as a room in a restaurant which can be reserved for a special party.

Places work in many ways, supporting or hindering people in their activities. As people develop characteristic ways of carrying out these activities, they often adapt their actions to the places.

People want their homes to be safe and secure from intruders [12]. Physical features such as locks, chains, fences and symbols such as neighbourhood patrol notices, electronic alarms or large dogs provide security. But by keeping their eyes open, people themselves play an important role in protecting their places [13]. Places where it is easy to watch out for unusual activity often have lower crime rates and residents who feel more secure and safe [14].

The identification of an area as belonging to a family or group of families contributes to its defensibility. If an area is small, clearly defined by boundaries, visible from inside the house, and limited in access that defend it. Outsiders can be more easily noticed or challenged, children can be allowed to play without supervision, and resident may be willing to take responsibility for the upkeep of the area [15].

But the most important and almost inescapable element of the public places is the automobile [16]. Widespread use of the car has had greater impact on the planning, design, shape and functioning of cities and towns than any other single invention. By increasing travel range and decreasing travel time, cars are of tremendous benefit to their owner. But cars use scarce energy resources and create noise, pollution, and danger. They also require large amount of space to the stored, used, sold, and maintained.

The dominance of the car has transformed building and neighbourhoods. A comparison of early suburb with those planned for the automobile shows that as suburbs developed and extra space was added for the car, everything moved further apart, making walking more difficult. Driving to places became necessary and stored clustered together behind giant parking lots. Neighbourhood shopping streets and corner

groceries disappeared.

In residential areas the nature of street and traffic directly affect the people's live-styles. A family living at a busy four-lane street has to take difficult decisions about the use of inside and outside spaces for children's play, quiet or active living, the same family might be able to behave quite differently. Planning streets for both cars and people is an important and difficult challenge.

Zoning limits building. By regulating how areas can be used, zoning laws establish and maintaining identifiable patterns of development. The location of factories, theatres, schools and shops is often determined by zoning.

Each space is a complex but unique whole; each room, building street and neighbourhood has its own highly particular character. Over time, people understand its nature as a cluster of natural forces, built elements, patterns of use, concepts, meanings and impressions. When people experience a places, they evaluate, sort and structure these features into an identifiable image. Often, people end up with a feeling about some place without realizing what specific components contribute to its character. Expressing its individuality and complexity, a portrait of place is composed of the elements which make unique.

People vary in as many ways as places vary. Differences in race, sex, age, education, size, shape and ability all contribute to people diversity. While each of us is unique, people can belong to many groups with whom they share one or more characteristics. Groups of people many use places in similar ways or be found in the same part of town or building.

Historically, competition for available space and disagreement about joint use of places has been frequent sources of discord. Often, these disagreements over places express more about people relationship with others than about the actual space or its use. Status, rather then need or convenience, may determine which worker is assigned an available office.

When a place is design and constructed, certain assumptions are made about its share use. Some places are designated for exclusive use of a specific person or group, but in order for certain activities to occur, many environments must be shared for large number of people, but cannot function for just one individual. While sharing places and facilities makes sense in terms of energy savings, cost, efficient functioning, and social interaction, it is a problem for people who consider control of space as a symbol of status and power. Lack of exclusive control over placers not always is a negative situation; sharing places with others can often be a delight.

In order to judge a place, architects need standards and/or criteria to measure it. Problems can only be identified if there are some basis for comparison. Locking for trouble in places architects and planners should involve a systematic analysis, with specific ideas in mind about what to look for and where to look [17].

References

[1] Mikellides B.: *Architecture for People, explorations in a new humane environment*, Studio Vista London, 1980.

[2] Gronostajska B., Zamasz J., Danyub T., Folta M., Grudniok K., Kolonko A., Paśko A.: *Sobótki przebudzenie*, Konferencja i Warsztaty architektoniczne pt.: *Psychologia organizacji przestrzeni środowiska mieszkaniowego*, Oficyna Wydawnicza Politechniki Wrocławskiej, Wrocław, 2003, pp. 279.

[3] Bać Z.: Habitaty III Fali 2002. W: Habitat trzeciej fali. EXPO 2010 – Wrocław, Habitat 2002, XV Międzynarodowe Seminarium i Warsztaty Architektoniczne Szkoły Naukowej, w Prace Naukowe Wydziału Architektury Politechniki Wrocławskiej, 2002, pp. 13–16.

[4] Broady M.: *Planning for People*, National Counsil of Social Service, London, 1968.

[5] Gronostajska B.: *Zrównoważony rozwój wybranych struktur w architekturze mieszkaniowej*, Materiały Konferencji pt. „*Oblicza równowagi*", Wrocław, 2005, pp. 54.

[6] Farbstein J. and Kantrowitz M.: *People in places*, Prentice-Hall Int. Inc., London, 1978.

[7] Gronostajska B.: *Architektura dla ludzi*, Materiały Konferencji Definiowanie Przestrzeni Architektonicznej, pt.: *Co to jest ARCHITEKTURA*, Kraków, 2005, Czasopismo Techniczne Architektura, 102, z. 11-A/2005, pp. 255.

[8] Bagiński E.: *Teoretyczne postawy przyczynkowych rozważań nad przestrzenią w aspekcie społeczno-kulturowym*, w Planowanie przestrzenne, zarys metod i technik badawczych. Praca zbiorowa pod red. E. Bagińskiego, Wrocław, 1991.

[9] Bagiński E.: *Atrakcyjne przestrzenie miejskie zaplanowane i urządzone oraz miejsca żywiołowo powstające,* w Problemy miejskie a zjawiska planowania i żywiołowości, Praca zbiorowa pod red. K. Wódz, Katowice, 1990.

[10] Gronostajska B.: *Kolor jako tworzywo architektoniczne*, Kraków, 2006, Czasopismo Techniczne Architektura, 102, z. 11-A/2005, pp. 255.

[11] Gronostajska B.: *Architektura a nauka w świetle stosowania niekonwencjonalnych źródeł energii*, Materiały VII Sympozjum pt.: *Teoria a praktyka w architekturze współczesnej* pt.: *Architektura a Nauka*, Rybna, 2002, pp. 284.

[12] Gronostajska B.: *Kształtowanie bezpiecznego środowiska mieszkaniowego*, Materiały Konferencji pt.: *Architektura i Technika a Zdrowie*, Gliwice, 2006, 105.

[13] Gronostajska B.: *Bezpieczna przestrzeń zamieszkiwania*, Materiały Konferencji pt.: *Przestrzeń bezpieczna*, Kraków, 2005.

[14] Gronostajska B.: *Kreacja i modernizacja przestrzeni mieszkalnej – teoria i praktyka, na przykładzie wybranych realizacji wrocławskich z lat 1970–1990*, Monografia, Oficyna Wydawnicza Politechniki Wrocławskiej, 2007.

[15] Gronostajska, B., Zamasz J., Halej J., Kokot M., Krzemińska M., Mulawa P., Różalska D., Tracz K., Wojtasik M.: *Spokojna Przystań*, Konferencja i Warsztaty architektoniczne pt.: *Habitaty bezpieczne*, Wrocław, 2006, pp. 279.

[16] Gronostajska B.: *Samochód w osiedlu mieszkaniowym XXI-go wieku. Tendencje w kształtowaniu zabudowy mieszkaniowej współczesnych miast*, Dział Wydawnictw i Poligrafii Politechniki Białostockiej, Białystok, 2006, pp. 196.

[17] Gronostajska B.: *Współczesne trendy w rozwiązywaniu architektury mieszkaniowej w połączeniu z natura*, Materiały Konferencji Metamorfozy II pt.: *Architektura współczesna wobec natury*, Gdańsk, 2002, pp. 312.

Wpływ ludzkich uczuć na kreowanie budownictwa

W pracy omówiono współzależności pomiędzy kreowaniem budownictwa przez architektów a potrzebami mieszkańców oraz wpływem szeroko rozumianych miejsc na to budownictwo. Wykazano, że, gdy na podstawie obserwacji większość zależności staje się oczywista to jednak konieczne są drogie badania eksperymentalne, aby znaleźć poprawne zależności pomiędzy architektami, ludźmi i otoczeniem. Na ile badania rozwiązujące ten problem są istotne jest bardzo ważne dla architektów i urbanistów. Uzyskanie poprawnej odpowiedzi jest niezwykle trudne ponieważ architektura obejmuje różne powiązania, które są rozważane na różnych poziomach. Architekci i urbaniści projektują otoczenie, miasta, system transportowy, które ułatwiają osiągnięcie maksymalnej akceptacji miejsc i udogodnień ludziom tam żyjącym. Niektórzy ludzie mają ograniczone możliwości w swobodnym poruszaniu się, dlatego też nie maja swobody w wyborze miejsc. Gdy miejsca są projektowane i tworzone należy zwrócić również uwagę na możliwości ich powszechnego użytkowania. Niektóre miejsca są przeznaczone do wyłącznego użytkowania przez szczególne osoby lub grupy osób, lecz dla umożliwienia ludziom pewnych aktynowości środowisko musi być udostępniona dla większej liczby ludzi i nie może funkcjonować tylko dla pojedynczych osób. Do oceny miejsc konieczne są normy i kryteria dokładnej ich identyfikacji. Problem ten może być rozwiązany jedynie wtedy, gdy ludzie będą mieli podstawy do porównania miejsc.

ARCHIVES OF CIVIL AND MECHANICAL ENGINEERING

Vol. VIII 2008 No. 1

Information about PhD thesis at the Civil Engineering Faculty and the Mechanical Engineering Faculty of Wrocław University of Technology

Title: ***Identification of modal parameters of bridge structures applying exciters*** **(in Polish)**
Wyznaczanie cech dynamicznych konstrukcji mostowych za pomocą wzbudników drgań

Author: dr inż. Jarosław Zwolski
Supervisor: dr hab. inż. Jan Bień, Wrocław University and Technology
Promoting Council: Institute of Civil Engineering, Wrocław University of Technology
Reviewers:
Professor Wojciech Radomski, Warsaw University of Technology,
Professor Wojciech Glabisz, Wrocław University of Technology
Date of PhD thesis presentation: October 10th, 2007
PhD dissertation is available in Main Library and Scientific Information Centre of Wrocław University of Technology
The monograph contains: 313 pages, 161 colorful figures, 32 tables and 202 references in bibliography
Keywords: *bridge, tests, vibration exciter, experimental modal analysis*

Abstract: In the dissertation a proposal of methodology for modal testing of bridge structures by means of exciters is described. The employed method enables identification of resonance frequencies, mode shapes and damping ratios of the structure with higher accuracy and precision than traditionally used techniques e.g. excitation by means of road or railway traffic.

In dynamic tests of bridge structures the vibrations recorded during passage of vehicle are often analyzed, what leads to identification of characteristic of vibrating system "moving vehicle-structure" instead of modal parameters of structure itself. Using the free vibrations recorded after the vehicle has passed the bridge a spectra with low resolution in frequency domain are often obtained. It is due to damping which, in a broad class of bridge structures, causes fast decaying vibration down to the noise level and the time of the valuable signal acquisition is short.

In advanced analyses as FEM models updating or damage detection based on tracking changes of modal properties the accurate and precise results of Experimental Modal Analysis are required. In course of the work tests of 2 structures in laboratory were performed as well as tests of 15 full-scale bridge structures. The obtained results were successfully used in updating of the structure FEM model and in detection of a damage introduced into the structure. The analyses were carried out employing methods and software tools created by the author.

Information for Authors

Send to: *Archives of Civil and Mechanical Engineering*
Polish Academy of Sciences, Wrocław Branch
Podwale 75, 50-449 Wrocław, Poland

Archives of Civil and Mechanical Engineering (ACME) publishes both theoretical and experimental papers which explore or exploit new ideas and techniques in the following areas: structural engineering (structures, machines and mechanical systems), mechanics of materials (elasticity, plasticity, rheology, fatigue, fracture mechanics), materials science (metals, composites, ceramics, plastics, wood, concrete, etc., their structures and properties, methods of evaluation), manufacturing engineering (process design, simulation, diagnostics, maintenance, durability, reliability). In addition to research papers, the Editorial Board welcome: state-of-the-art reviews of specialized topics, letters to the Editor for quick publication, brief work-in-progress reports, brief accounts of completed doctoral thesis (one page is maximum), and bibliographical note on habilitation theses (maximum 250 words). All papers are subject to a referee procedure, except for letters, work-in-progress reports and doctoral and habilitation theses, which are briefly reviewed by the Editorial Board.

The papers submitted have to be unpublished works and should not be considered for publication elsewhere.

The Editorial Board would be grateful for all comments on the idea of the journal.

Detailed information about the Journal on web:
http://www.pan.wroc.pl
www.ib.pwr.wroc.pl/wydzial/czasopismoACME.html
http://www.acme.pwr.wroc.pl
http://www.wmech.pwr.wroc.pl

The papers should be submitted through the webside
http://www.acme.pwr.wroc.pl

Price 15 zł
(0% VAT)

Subscription orders should be addressed to:

Oficyna Wydawnicza Politechniki Wrocławskiej
Wybrzeże Wyspiańskiego 27
50-370 Wrocław